MEMBRANE POTENTIAL EFFECTS ON THE INTESTINAL TRANSPORT OF SALICYLATE

by

Suzanne Frank Adair
B.S., University of Wisconsin, 1963

DISSERTATION

Submitted in partial satisfaction of the requirements for the degree of

DOCTOR OF PHILOSOPHY

in

PHARMACEUTICAL CHEMISTRY

in the

GRADUATE DIVISION

(San Francisco)

Date Librarian

Degree Conferred: . . . . . .

ABSTRACT

A sensitive method of studying in vitro drug absorption has been developed, utilizing the short-circuit technique of Ussing with modifications by Schultz and Zalusky for use with mammalian small intestine. The method allows the continuous monitoring of the electrical properties of the tissue during drug absorption and also permits the adjustment of some of these properties. Thus, it is possible to observe the effect of the drug on the electrical parameters of the tissue as well as the effect of the electrical properties on the intestinal absorption of the drug.

The transmural flux of ^{14}C-salicylate across the epithelia of stripped rat jejunum was studied initially to demonstrate the contribution of the ionized species of drugs to the intestinal absorption process. The transmural potential difference (PD) was varied using the experimental instrumentation designed for this purpose. Salicylate responded to this change in potential in a similar manner as sodium and chloride ions, rather than as a neutral compound such as antipyrine. Double isotope techniques were employed in this study, with ^{14}C-salicylate and ^{3}H-antipyrine fluxes being determined simultaneously across the same tissue. Mathematical expressions were employed which related the transmural PD with transcellular absorption routes (via the cell membrane) and paracellular absorption routes (via the transmural shunt pathway). These experiments demonstrated that salicylate flux was, indeed, influenced by the transmural PD, whereas, the flux of antipyrine, a neutral compound, was essentially constant under various transmural PDs.

The transmural flux of ^{14}C-salicylate at short-circuit current (I_{sc}) was studied before and after the addition of agents affecting

cellular metabolism to further elucidate the mechanisms responsible for intestinal drug absorption. Each tissue segment served as its own control, and absorption rates were measured under both control and experimental conditions.

The addition of 1 mM ouabain, a selective inhibitor of active sodium-transport, to the buffer solution perfusing the serosal side of the tissue profoundly changed the electrical parameters of the tissue. The mucosal to serosal (M-to-S) flux of ^{14}C-salicylate was inhibited following serosal ouabain addition, and this change was apparent after a twenty-to-thirty minute interval. A similar delay was seen for the increase in transepithelial resistance (R). Ouabain was also added in the absence of sodium ions, insuring that the previous observations were due to the inhibition of sodium-transport rather than to other ouabain activities. Under these conditions, ouabain caused only a small change in the salicylate absorption rate; however, the initial ^{14}C-salicylate transport rate was much lower in the sodium-free choline buffer.

The addition of 25 mM glucose increased the transmural PD and I_{sc}, but no change in the ^{14}C-salicylate flux or transmural R was observed. This suggests that the transport of salicylate is not affected by a change in cellular metabolism which does not also affect the transmural R.

The addition of various concentrations of mucosal salicylate (a known uncoupler of oxidative-phosphorylation) decreased the transmural PD and I_{sc} while increasing the transmural R. The changes in these parameters appeared to show a saturable effect with respect to salicylate concentration. The M-to-S flux of ^{14}C-salicylate was also inhibited by the addition of mucosal salicylate. The decrease in the flux varied with the salicylate concentration, but not in a linear fashion. This indicated a

dose-dependent absorption of *in vitro* ^{14}C-salicylate.

This study has shown that changes in the permeability of the membrane (i.e., functional state), as reflected in the electrical parameters of the tissue, can be caused by various agents and, in turn, can affect *in vitro* salicylate ion transport, probably via the transmural shunt pathway.

In Memoriam

Louis A. Strait, Ph.D.

To Dennis

My partner in pharmacy, science,
and love...My partner in life.

ACKNOWLEDGEMENTS

I would first like to thank the faculty of the University of California School of Pharmacy for their intellectual and moral support during my stay there. I value the friendships that have developed during this association. Being so fortunate in this respect, they are too numerous to mention; but, I would like to single out Dr. Louis A. Strait and Dr. Roger G. Ketcham. The former graduate students from the University of California School of Pharmacy have also served to enrich my professional and social life.

Gratitude is expressed to Dr. I.S. Edelman for his suggestions and advice on this research.

I owe special thanks to Dean Jere E. Goyan for his help and support during my initial years in graduate school as well as his assistance with my research project.

I wish especially to acknowledge the excellent guidance of my research director, Dr. Leslie Z. Benet, who encouraged me, supported me, and tried to understand me during this research project. The respect and admiration that developed from this relationship has been important in my learning process. I thank Les for being a special friend as well.

I wish to thank Mr. Robert Vreeland for his expert technical assistance, Ms. Linda Kiefer for her overall aid and cheerfulness, and Mrs. Joan Ann Nathan for the excellent typing of this thesis.

Appreciation is extended to my parents, Arthur and Rebecca Frank, for their support and encouragement of my goals of higher education.

I thank my son, Kevin, for the sacrifices and inconveniences he doesn't yet realize he's endured during my quest for this degree.

To my husband, Dennis, I am especially appreciative for his support, encouragement, help, and his many sacrifices necessary to enable me to earn this degree. He is a source of inspiration and knowledge for me.

Finally, I am most thankful that my teachers, supporters, and friends were not male chauvinists -- at least not to me.

TABLE OF CONTENTS

Page

LIST OF TABLES

LIST OF FIGURES

Figure Page

Figure Page

INTRODUCTION

Historical Background

The intestinal absorption of drugs is an important area of research since most medication in this country is taken by the oral route. If the drug is poorly absorbed from the gastrointestinal (g.i.) tract or not absorbed at all (and the site of action for the drug is other than the g.i. tract) then no biological or pharmacological effect will be seen. Extensive research on the g.i. absorption of drugs has been carried out during this century and many reviews and chapters have appeared in the literature on this vital area. A wide variety of *in vivo* and *in vitro* methods have been used to study intestinal drug absorption. Multi-lumen catheters in human and animal subjects have been frequently used in isolating portions of the g.i. tract during *in vivo* absorption studies (1-5). Another *in vivo* model employs the unanesthetized rhesus monkey, surgically prepared with permanent cannulae (6, 7). Several methods of measuring *in vivo* intestinal drug absorption in experimental animals (predominantly rats and dogs) have also been described (8-10). An intact blood supply is maintained although the animal is anesthetized, surgically prepared and supine during the experiment. These studies are often termed *in situ* experiments rather than *in vivo* since the animals used are not in their normal environment during the course of the experiment.

Because of all the variables involved in studying the absorption of a drug administered orally (e.g., volume, composition, and pH of contents of the g.i. tract, rate of gastric emptying, degree of intestinal motility, dosage form of drug,

and amount of drug in solution), many investigators studying mechanisms of gastrointestinal absorption often use surgically prepared laboratory animals or in vitro preparations so that one portion of the g.i. tract can be studied. In these experiments the nature of the g.i. contents is controlled, and the investigator is assured that the drug is definitely in solution.

While all theories of drug absorption must eventually be corroborated by in vivo experimentation and clinical data, there are many advantages in using an in vitro system. It permits the use of automatic instrumentation for monitoring data from relatively inaccessible sites and allows much greater control of the experimental design and the experimental conditions. Another advantage of in vitro studies is that the effects of a drug can be directly observed and in many cases terminated by washing out the drug. Analysis of dose-response relationships may be carried out more precisely on the in vitro preparation.

In the past, the common in vitro techniques for studying intestinal drug absorption have included the everted sac (11), the Crane-Wilson modification (12), and a perfusion apparatus system (13). These techniques have been adequately described by various reviewers (14, 15). These conventional methods had been used previously by Benet and coworkers to study the effects of various buffer constituents on drug transfer across the in vitro rat intestine (16) as well as the apparent directional permeability coefficients for drug transport (17). Work had been directed towards explaining a possible difference in absorption of ionizable drugs vs neutral compounds. For the present investigation, a method generally used by physiologists in studying ion fluxes across epithelial tissues has been

applied to the study of intestinal drug fluxes in vitro. The short-circuit technique of Ussing and Zerahn (18) was originally employed in the study of sodium ion transport across the frog skin. This approach revolutionized the study of transmembrane ionic movements and associated phenomena in biological systems. The voltage clamp procedure was modified by Schultz and Zalusky (19) for use with mammalian small intestine in order to study ion fluxes, transmural potential differences (PD), and short-circuit currents (I_{sc}). The method allows the continuous monitoring of the electrical properties of the tissue during drug absorption and also permits the adjustment of some of these properties. Thus, it is possible to observe the effect of the drug on the electrical parameters of the tissue as well as the effect of the electrical properties on the intestinal absorption of the drug.

The voltage clamp procedure provides a more controlled system than other in vitro methods, since: the tissue chamber maintains a constant and known surface area of tissue exposed to drug; the apparatus permits the tissue to be well perfused and oxygenated so that tissue viability is less of a problem; the perfusing solutions are accessible and can be easily sampled repeatedly without disturbing the tissue; and, of course, the electrical parameters of the tissue and solution are known and can be adjusted.

Intestinal tissue has an inherent potential difference that can be measured. This is due primarily to active ion transport across the tissue. The I_{sc} is equal to the net active ion transport. Both I_{sc} and ion transport are fluxes and can be expressed in units of either amperes or equivalents/time. At short-circuit current, the potential difference across the tissue is zero. This is accomplished by imposing

across the tissue a voltage (essentially a bucking voltage) which is equal and opposite to that due to active ion transport. In some tissues (such as frog skin, for which the short-circuit system was originally developed), the only ion transported actively is sodium. Mammalian intestine was at first thought to be similar to frog skin in this respect (19). However, more recent work indicates that chloride ion is also subject to an active transport process (20, 21). There has also been speculation that active transport of bicarbonate ion may occur, but this has not been conclusively proved (20). Thus, the I_{sc} value for mammalian intestinal tissue is a resultant of all the active processes occurring across the tissue and no "blanket" statements should be made about changes in I_{sc} being definitely due to changes in sodium transport without first investigating and proving that sodium transport has indeed changed. Yet, a change in the I_{sc} does definitely imply a change in net active ion transport across that tissue.

Mammalian intestine is an exceedingly low resistance tissue (averaging 22Ω-cm^2 in these experiments). In comparison, stomach tissue shows a relatively higher resistance, 500Ω-cm^2 (22), as does the submandibular salivary duct, 400Ω-cm^2 (23), while some examples of high resistance tissues include toad urinary bladder, 800Ω-cm^2 (24) and frog skin, 2,000Ω-cm^2 (25). Epithelia from the gall bladder and renal proximal tubule show a low resistance, similar to that of the small intestine and are considered "leaky" (26, 27). This may account for the large number of compounds that are reabsorbed across these organs. A transmural shunt pathway across the tight junction (zonula occludens), through which certain ions

and small organic molecules diffuse, has been proposed by Fromter and Diamond (26) to explain passive ion transport across a number of tissues.

Transcellular Transport

Modern theories of absorption were developed from the unit membrane model of Davson and Danielli (28) which conceptualized a membrane as a bimolecular lipid leaflet containing only small pores. All transport, active and passive, was assumed to occur across the membrane of the cell, i.e., transcellularly. This has been the basic assumption for drug molecules as well as various ions, such as sodium, potassium, and chloride and nonelectrolytes, such as water, urea, glucose, and the smaller amino acids. The pores in the cell membrane were calculated to be from 4 to 7 Å in diameter, and it was hypothesized that the above ions and small water-soluble molecules may be absorbed via these water-filled channels or pores. Further, since most drug molecules are larger than the proposed diameter of these cellular pores, it was assumed that drugs did not diffuse through these pores, but rather were absorbed by crossing the cell membrane. The pH partition theory (or theory of nonionic diffusion) of Hogben, Brodie, Schanker, and coworkers (10, 29-32) is based on the assumption that only the nonionized molecule moves across the cell membrane by a process similar to solution in the membrane; hence, these workers suggested that the partition coefficient of the drug molecule was critical in predicting which compound would be absorbed. Similarly, the pK_a of the drug would also be important in

determining the "absorbability" of the compound since only the nonionized fraction could partition into the membrane. The "virtual pH" hypothesis (30) was developed to explain data that did not fit the pH-partition theory; e.g., salicylic acid was still well absorbed from the intestine at pH 7.4 while being >99.9% ionized. A microclimate of pH 5.3 at the surface of the intestine was proposed to account for the greater acid absorption observed at higher pH's than expected from the theory.

The "virtual pH" hypothesis had previously been criticized by Barry et al. (33) and Benet (34, 35), as discussed by Wagner (36). The possibility of a membrane-bounded virtual pH phase was questioned by Benet since interposition of a pH 5.3 microclimate between two bulk solutions that are in equilibrium should have no effect in changing the concentration of nonionized drug next to the absorption surface. Smolen (37) has also shown that the virtual pH hypothesis is thermodynamically untenable. Smolen demonstrated that the equilibrium ratio of total solute concentrations in the bulk phases on each side of the membrane is identical and independent of whether or not the barrier is permeant to the ionized species. The ratio depends only upon the magnitude of the pH gradient across the membrane and the ionization constant of the solute. The ratio is also entirely independent of the existence of any "virtual pH" at the surfaces of the barrier which may differ in pH from the values measured in the respective bulk phases.

The fact that ionized drug molecules are absorbed across the intestine has been accepted by many workers (16, 37-41). A new theory by Jackson et al. (42) has recently been proposed

regarding intestinal weak electrolyte transport. A three-compartment model system is proposed where the pH of the intermediate compartment is greater than that of the bulk phases. This theory also contains the assumption that only the uncharged species is absorbed from the mucosal solution; i.e., the mucosal barrier is impermeable to the ionized molecule.

It is now widely accepted that small inorganic ions (sodium, potassium, chloride, bicarbonate, etc.) are absorbed across certain tissues by two routes -- transcellular and paracellular. For example, over 80% of the passive sodium transport has been shown to occur via a transmural shunt pathway in rabbit ileum (43). However, organic drug ions have been assumed to traverse biological membranes at very slow rates and only to a limited extent due to their low partition coefficients; and several investigators still believe that only the uncharged drug molecules pass the gastrointestinal barrier (44-46).

Paracellular Transport

Fromter and Diamond (26) and Schultz and Frizzell (21) have suggested that solute molecules do not necessarily have to pass through tissue by a transcellular route exclusively. They suggest that a paracellular pathway may exist via the so-called tight junctions and that this intercellular space may be more accessible than had previously been hypothesized on the basis of electron micrographs. The nature of these tight junctions (also termed zonula occludens or junctional complexes) and the intercellular channels has been the subject of much research. Ultrastructural studies have revealed long

intercellular spaces between the cells of transporting epithelia (47, 48). Recent anatomical work (49-52) has shown that the tight junction consists of a series of barriers where cell membranes from adjacent cells come in very close proximity. The barriers, known as punctate contacts or "kisses," apparently represent fibrils as seen in cross sections (53). Diamond (53) has visualized an epithelium (a sheet of cells surrounding a cavity held together at the luminal surface by tight junctions) as a six-pack of beer, with the cells represented by the beer cans and the plastic frame of the six pack signifying the tight junctions. A series of papers by Barry, Diamond, and Wright (54-56) contain a detailed theoretical treatment of ion permeation through neutral pores and an extensive analysis of conductances and diffusion potentials across rabbit gall bladder. These authors concluded that ion permeation takes place through neutral water-filled pores lined with fixed dipoles oriented such that the electronegative groups determine cation selectivity. It has been demonstrated that the tight junctions of rabbit ileal mucosa are permeable to lanthanum ion (57), as are those of the proximal tubules of the toad kidney (58). Electronmicroscopy has shown that lanthanum ion moves through the zonulae occludens of several low resistance epithelia, but not through high resistance epithelia such as frog skin (59). The permeability of the shunt pathway appears to be determined by factors that influence the width of the lateral interspaces and the "tightness" of the junctional complexes (60). Factors that bring about cell swelling, such as perfusion with hypotonic solutions (61, 62) or metabolic

inhibition (63-65) increase transepithelial resistance, whereas shrinking of cells by exposure to hypertonic solutions has the opposite effect (61, 62).

Benet et al. (16) and Mayersohn and Gibaldi (66) have found that replacing sodium ion with potassium ion in the perfusing buffer caused a decrease in the rate of absorption of various drugs, especially if they were ionized. Since increased potassium ion concentration has been shown to cause swelling of the intestinal epithelial tissue via water uptake (67), it has been proposed that the swelling caused by the increased potassium ion closes off the tight junctions between columnar cells in the mucosal epithelium. This phenomenon would affect transport of compounds that were absorbed via the paracellular route and should have a minimal effect on those compounds absorbed transcellularly. Mayersohn et al. (68) proposed that polar molecules penetrate the isolated intestine by movement along intercellular channels existing between adjacent mucosal cells. They found that inhibition of passive transfer of polar solutes across the everted rat intestine occurred when the intestine was immersed in buffer solutions which resulted in tissue fluid uptake. They proposed that the tissue fluid uptake caused swelling of the cells, and that this increase in cell volume led to a narrowing of the intercellular channels. The agents causing an inhibition of passive drug transfer in their studies included a high concentration potassium buffer (66, 69), an ammonium buffer (66), glucose and xylose buffers (70), and a general hypotonic buffer solution (71). They found no inhibition of drug transport in the presence of ouabain (66).

Mathematical expressions describing the transcellular and paracellular routes of ion absorption have been developed by Schultz and coworkers (43). These equations indicate that both pathways may be important in the passive transport of an ion across a biological tissue barrier, and not just the transcellular path as had previously been assumed. The mucosal to serosal flux ($J_{m \rightarrow s}$) of an ion has been related to the transmural PD according to the following theoretical equations:

$$J_{m \rightarrow s} = J_m + J_d \qquad \text{(Eq. 1)}$$

$$J_{m \rightarrow s} = J_m + {}_oJ_d \, \xi^{-1/2} \qquad \text{(Eq. 2)}$$

$$J_d = {}_oJ_d \, \xi^{-1/2} \qquad \text{(Eq. 3)}$$

where

$\xi^{-1/2} = [\exp (z F PD/R T)]^{-1/2}$

z = ionic charge

F = Faraday constant

PD = potential difference across the tissue

R = gas constant

T = absolute temperature

J_m = unidirectional flux (m→s) via the mucosal membrane

J_d = unidirectional flux (m→s) via the shunt pathway at any PD

${}_oJ_d$ = unidirectional flux (m→s) via the shunt pathway at short-circuit current (PD = 0)

Equation 1 states that the total unidirectional flux of a compound from mucosa to serosa is composed of the flux of

that compound across the mucosal membrane (via the cell) and the flux through the transmural shunt pathway (via intercellular water). When a charged species is involved, Equation 3 comes into play. This equation relates the flux via the shunt pathway to the imposed potential difference across the tissue. Frizzell and Schultz (43) have demonstrated that if the unidirectional flux of an ion is attributable to simple ionic diffusion and if the partial ionic conductance is independent of the imposed transmural PD, there should be a linear relation between that flux and $\xi^{-1/2}$. The equations were derived assuming that the flux via the cells (J_m) will change negligibly compared to the change in the flux via the shunt pathway (J_d) caused by the transmural PD changes.

Note that in Equation 2 there is a linear relation between the mucosal to serosal flux, $J_{m\rightarrow s}$, and a function of the potential difference, $\xi^{-1/2}$. This equation states that a plot of $J_{m\rightarrow s}$ versus $\xi^{-1/2}$ (the PD function) will have an intercept related to the flux via the cell, J_m, and a slope equal to the flux via the transmural shunt pathway at short-circuit current, ${}_oJ_d$. The relationship between $J_{m\rightarrow s}$ and $\xi^{-1/2}$ (the PD function) has been shown for sodium under various conditions such as: [a] varying sodium concentration, the presence of [b] choline, [c] lithium (43), [d] theophylline (43, 72), and [e] glucose (73). This relationship has also been demonstrated for chloride, potassium, and rubidium ions (43, 73). Ionic diffusion has thus been shown to be affected by a change in imposed PD.

Automatic Voltage Clamp

Electrical monitoring has long been an important tool in elucidating information concerning the physiological characteristics and responses of tissues. The short-circuit current device introduced by Ussing and Zerahn (18) revolutionized the study of transmembrane ionic movements and associated phenomena in biological systems. Modifications of this voltage clamp technique for use in studying the mammalian small intestine were made by Schultz and Zalusky in 1964 (19). Mammalian small intestine creates a special problem when adapting this procedure for study because of the low electrical resistance of the membrane. Since the agar bridges for measuring the potential difference across the tissue are a finite distance from the tissue, the resistance of the solution between the bridges and the tissue, which may be in the range of 15-25 ohms, can become significant. If high resistance tissues are used, such as frog skin or toad bladder, the resistance contribution from the solution gap is negligible compared to the 1000 to 2000 ohm resistance of this type of tissue. However, if the solution resistance were to be ignored with stripped mammalian small intestine, an error of up to 50% might occur. Clarkson and Toole (74) first pointed out the necessity of correcting for this potential drop in the bathing solution when setting the short-circuit current of the tissue. The correction procedure can be carried out manually with just a microammeter and a millivoltmeter connected to the source and sensing electrodes, but this manual procedure is an extremely cumbersome and time-consuming task. In addition, rapid

changes of the transmural potential difference across the tissue (due to the addition of various test agents) may cause errors in the calculation of the new I_{sc} value due to the time required for recording the reading of two points on the E vs I curve and graphically determining the new I_{sc} value. This, in turn, could cause errors in the value calculated for the tissue resistance. The time spent in determining the new I_{sc} values and changing the setting to maintain zero potential difference across the tissue would cause problems in trying to take samples of the bathing solutions to determine drug transport during this interval. For these reasons, an automatic voltage clamp with an IR compensator was designed and used in this work.

A number of automatic voltage clamps have been reported in the literature, but, for the most part, they were not designed for low resistance mammalian tissue; and, therefore, do not include the capacity for correction of the solution resistance. Mullins (75) designed an automatic voltage clamp to use in studying anion flux in frog skin. In Mullins' clamp, the potential of the sensing electrodes were fed to a Brown-Honeywell chopper-amplifier. The amplifier's output drove a servometer connected to a ten-turn helical potentiometer which controlled the potential supplied to the source electrodes and completed the negative feedback loop. A clamp utilized by Menninger et al. (76) for isolated frog skin and toad bladder also made use of a negative feedback system using a pair of high gain operational amplifiers. A secondary loop was included which limited the effects of transients caused by switching and other high frequency noise in the

system. The use of an amplifier to monitor each of the sensing electrodes allowed the amplifiers and the clamped region to be maintained at virtual ground potential. This decreased the errors which could arise from stray leakage to ground.

A device described by Wright (77) utilized the 100 Hertz output of an electrometer attached to the sensing electrodes. This signal was amplified and rectified and used to power the source electrodes, and thus close the feedback loop. These three systems, while using various methods to produce a closed negative feedback loop, still fail to provide IR compensation to correct for the solution resistance. The automatic clamp of La Force (78) employed operational amplifiers in a considerably more sophisticated system which was capable of clamping the voltage across the frog skin or clamping the current passing through the tissue. It also featured a special alternating current clamp and detector to follow tissue resistance in a time span which may be considered short compared to the time for ion redistribution. Barry et al. (79) and Isaacson et al. (80) have described similar instrumentation for the automatic measurement of potentials and short-circuit currents of amphibian epithelia. These clamps also had no provision for the correction of the IR drop in the circuit due to the resistance of the solution. The lack of this capability restricts the use of these instruments, without incurring significant error in the estimation of the I_{sc}, to those tissues demonstrating high resistance as compared to the solution resistance.

Candia (81) constructed an automatic clamp using the servomotor system of a recorder to clamp the voltage of the

membrane, correct for solution resistance, and record the short-circuit current. The system used a ten-turn potentiometer coupled to the servomotor and pen of the recorder. The correction for solution resistance was made by using the recorder's feedback potentiometer to correct the null point as a function of current. However, this approach is based on large tissue resistances and potentials such that the sensitivity is limited, and the response time is tied to the mechanical servomotor system.

The automatic voltage clamp described by Quay and coworkers (82, 83) was intended for use with tissues of resistance similar to that of the solution. This system utilized operational amplifiers to control the feedback loop and to amplify the signal which drives the current source electrodes. This system contained the desirable features of an offset circuit to correct imbalance in the electrodes, as well as an IR compensation network to account for the resistance of the solution. A distinct disadvantage of all the automatic voltage clamps that have been discussed here is the direct electrical coupling of the sensing portion of the clamp circuit with the current supply system. Thus, there is incomplete isolation of the low potential difference seen at the sensing electrodes from the relatively high potential required to pass the short-circuit current through the connecting agar bridges and solutions. An automatic voltage clamp was designed for this investigation. The clamp, built by Mr. R. Vreeland, Research and Development Laboratories, University of California - San Francisco, incorporates IR compensation and virtual isolation through the use of photo-optical isolators. The

details of this clamp will be discussed in the Experimental section.

Electrical Effects of Salicylate

Salicylic acid was chosen as the model compound for the experiments designed to investigate the transport of ionized compounds across the intestinal barrier. Salicylic acid is virtually 100% ionized at blood pH, 7.4. The g.i. absorption of salicylate has been studied extensively, *in vivo* and *in vitro*. Mayersohn and Gibaldi (66, 68, 71) measured salicylate flux in the presence of various ions, drugs, and metabolic inhibitors. In their work, they had observed that ouabain had no effect on the intestinal flux of salicylate. However, in their studies, salicylate was present in concentrations of 2 mg/ml. Salicylic acid is known to be an uncoupler of oxidative-phosphorylation, and thus, poses the possibility that salicylate itself could affect the tissue in a manner which would, in turn, affect the flux of salicylate. The possibility of nonlinear behavior was based on clinical and physiological studies, which abound in the literature, involving aspirin-induced damage to the g.i. mucosa of man and laboratory animals. Furthermore, salicylic acid is also a keratolytic agent and might directly attack the tissue. Clinically, the damage is manifest in man by visible, bleeding erosions of the epithelial lining of the stomach and may persist for hours or days after aspirin ingestion (84-97). Hingson and Ito (88) recently carried out extensive morphological studies of the gastric mucosa following a few minutes of exposure to aspirin and other weakly acidic carboxylic acids in the presence of various concentrations of hydrochloric

acid. Their observations suggest an extensive damage and death of surface mucus cells not solely directed at cell secretory activity. Because of the observed injury to the gastric mucosa following oral ingestion of aspirin, several enteric coated preparations of aspirin are on the market to avoid gastric upset and damage. This means that the drug would then dissolve lower in the g.i. tract and come in contact with the small intestinal mucosa. Therefore, one reason for studying the effects of various concentrations of sodium salicylate added to the mucosal side of the stripped jejunum is to see the effects of salicylate on the electrical parameters of the tissue.

Little is known of the mechanism of action of analgesics. Certain discrepancies occur regarding the analgesic potency of several compounds and also disagreement concerning their site of action (89-93). Some theories as to the mechanism of action of salicylate have been suggested. Ferreira (94) has observed that pain receptors are sensitized by prostaglandins, which strongly supports his suggestion that aspirin-like drugs induce analgesia by blocking the synthesis of prostaglandins. Additional evidence supporting this theory of analgesia has been reported by Hamberg (95), who found that the excretion rate of the major urinary metabolite of prostaglandins E_1 and E_2 in man was strongly suppressed following oral administration of therapeutic doses of indomethacin, aspirin, and sodium salicylate. It has been further suggested that the analgesic actions of the salicylates could be due to a membrane related phenomenon. Barker and Levitan (89, 96-99) have found that salicylates produce an increase in the permeability of a

molluscan neuron to potassium ion and a decrease in the permeability of the neuron to chloride ion. Salicylate caused the permeability to change in a reversible, dose-dependent manner, producing a concomitant increase in membrane potential and a decrease in membrane resistance (96). These changes reduced the output from a particular neuron, as well as the effectiveness of synaptic input to a neuron. Because of the time element involved (seconds), their results indicate changes in membrane permeability rather than alterations in metabolic processes. Analogs of salicylate and benzoate also reversibly increased the membrane potential and the conductance of the molluscan neuron by increasing potassium ion conductance and decreasing chloride ion conductance (98). The relative potencies of these analogs were closely correlated with their octanol-water partition coefficients and their pK_a values. Thus, the solubility of an aromatic acid in the membrane and the relative concentration of aromatic anions present were the primary factors which these workers found to change the membrane conductance and permeability (98). Salicylate was also found to cause a reversible dose-dependent decrease in the permeability of rubidium, cesium, sodium, and lithium ions relative to that of potassium ions (99). These results suggest that the changes in cation selectivity result from the adsorption of salicylate anions to the membrane with a subsequent increase in the density and field strength of anionic sites in the membrane.

McLaughlin (100) hypothesized that the "receptor site" of the neuronal membrane for salicylate is the phospholipid bilayer. An adsorption of salicylate anions to the bilayer

would produce a negative electrostatic surface potential which would modify the interfacial ion concentrations, and thus give rise to the observed changes in permeability. This was found to be the case for the artificial phospholipid bilayer membranes that McLaughlin used (100). All of the effects of salicylates observed to date on phospholipid bilayers and mollusk neurons can be accounted for in terms of a simple molecular mechanism: the hydrophobic adsorption of the salicylate to the insulating bilayer and the concomitant production of a negative surface potential. This action is not unique to salicylates, as the uncoupler, 2,4-dinitrophenol (101), the fluorescent probe 1-anilino-8-naphthalene sulfonate (102), and the indicator dye bromthymol blue (100) also are adsorbed to the membrane.

Kasbekar (84) studied the effects of salicylate on in vitro preparations of isolated bullfrog gastric mucosa. The hydrogen ion secretory rate, transmural PD, and resistance were the three parameters measured. When 20 mM salicylate was added to the serosal perfusing medium, the hydrogen ion secretory rate and the transmural PD both decreased, while the tissue resistance increased. All three parameters showed near-complete reversal following salicylate washout. The addition of 20 mM salicylate to the mucosal bathing solution also resulted in decreases in the hydrogen ion secretory rate, transmural PD, and resistance. In this case, however, there was only a partial recovery of the secretory and electrical parameters following repeated washouts of salicylate, indicating the irreversible nature of the changes induced by mucosal instillation of the drug (84). The effects of

salicylate on the gastric mucosa are probably due to interference with energy metabolism, since salicylic acid may facilitate backdiffusion of hydrogen ion and bring about lysis of the epithelial cell. Kasbekar (84) further concludes that "the inhibition of mucosal energy metabolism may lower the threshold of the gastric mucosal barrier to H^+ in some unknown manner. More likely, however, salicylate-induced increase of anionic field strength in the epithelial cell membrane may increase its proton selectivity. The resulting permissive intracellular diffusion of luminal H^+ may be responsible for the observed reversible cellular damage."

Statement of the Problem

The purpose of this investigation was to demonstrate that some ionic species contribute significantly to the intestinal absorption of drugs. The transmural flux of sodium salicylate across stripped rat jejunal epithelia was studied initially to show that salicylate anion was contributing to the absorption process. Experimental instrumentation designed to allow the potential difference across the intestinal tissue to be varied was utilized to demonstrate the existence and contribution of the ionized species. If salicylate responds to this change in potential in a similar manner to that seen for sodium and chloride ions, rather than as for a neutral compound such as antipyrine, then the ionic species should be contributing to the absorption of salicylate. Salicylic acid was chosen as the model drug in this study because at pH 7.4 (the pH of plasma and the pH of the perfusing solutions used in these experiments) the drug is greater than

99.9% ionized. Thus, salicylic acid should be a prime candidate for proving the existence of drug ion transport. Antipyrine was used as a model for a nonionized drug. Double isotope techniques were employed in this study. The g.i. absorption of these two drugs have been investigated extensively (9, 10, 16, 32, 62) , and the results of these studies were used as the basis for many drug absorption theories.

The intracellular pH of the rat jejunal tissue was determined at various imposed transmural potential differences. This parameter, the intracellular pH, was examined to see if a change resulted from the various imposed transmural potential differences. If the intracellular pH were altered under these conditions, then the percent of nonionized salicylic acid present would also be changed, and this, in turn, would affect the rate of salicylate absorption across the tissue.

Much past work has focused on the passive transfer of drug molecules across an inert membrane which acts simply as a semipermeable barrier. However, it is possible that interference or changes in the normal cellular metabolism of the <u>in vitro</u> mammalian intestine may affect the intestinal absorption of passively transported drug solutes. To study this, the transmural flux of ^{14}C-salicylate across the epithelia of stripped rat jejunum at I_{sc} was determined in the presence of various agents affecting cellular metabolism. The perturbing agents examined included ouabain, a selective inhibitor of active sodium-transport; a choline-containing buffer devoid of sodium ion; glucose, an actively transported sugar which is also metabolized; and sodium salicylate itself. Various concentrations of sodium salicylate were investigated as to their

effects on the mucosal to serosal flux of ^{14}C-salicylate across the intestinal tissue. These experiments were performed to determine if a dose-dependent relationship exists for the *in vitro* absorption of ^{14}C-salicylate.

EXPERIMENTAL

Short-Circuting Apparatus

Short circuiting was achieved with a special voltage clamp designed in conjunction with the Research and Development Laboratories, University of California - San Francisco. Several performance characteristics were specified for the clamp in order to overcome the problems described in the Introduction:

- a circuit for automatic IR compensation
- a circuit for compensation of voltage offset
- a manual mode, as well as the automatic circuitry
- the capability of reversing the polarity of the current source and, thus, the transmural potential
- the ability to clamp the transmural electrical potentials at preselected values (up to $\pm$ 20 mv. in the automatic mode or up to $\pm$ 100 mv. in the manual mode)
- the ability to run up to four different tissues simultaneously with one voltage clamp

The automatic voltage clamp utilizes inexpensive and readily available operational amplifiers to achieve both accuracy and a rapid response. Additional features which make this instrument unique include the use of photo-optical isolators giving virtually complete electrical isolation and an adjustable offset circuit for balancing at other than zero voltage.

A schematic diagram of the electrical circuit is shown in Figure 1. The tissue chamber is depicted in the figure with the tissue represented as a voltage, E_m, and resistance, R_m, (analogous to a battery). The sensing agar bridges, represented by resistances R_a and R_b, contact the perfusing solution at

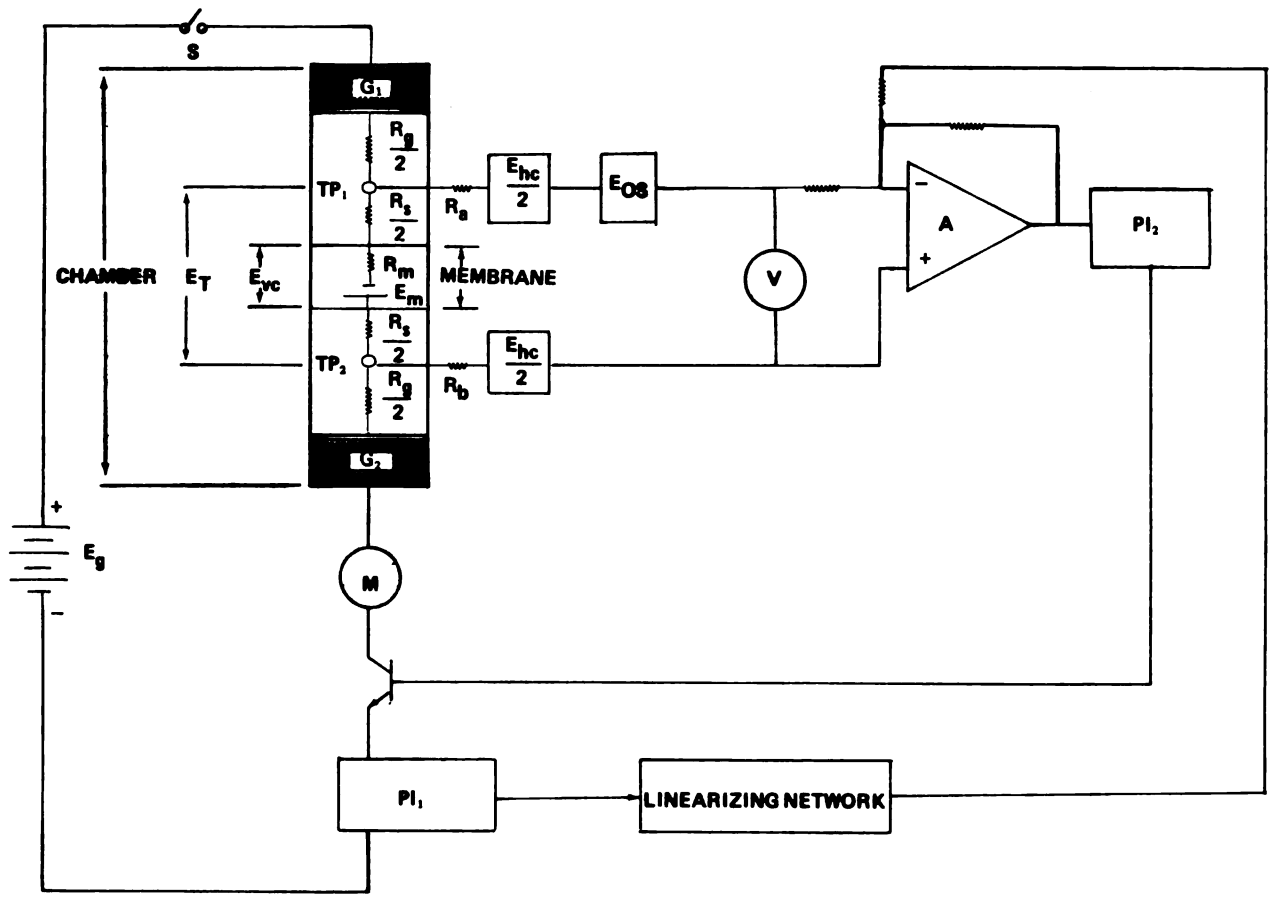

Figure 1. Schematic diagram of electrical circuit of automatic voltage clamp emphasizing resistances.

R_a and R_b:	Resistances representing the sensing agar bridges
R_m:	Resistance of the tissue
R_s:	Resistance of the solution
R_g:	Total resistance of the current source elements
E_m:	The transmural tissue potential difference at zero current
E_T:	Potential difference at the sensing electrodes
E_{vc}:	Potential difference across the tissue
E_{hc}:	The electrode error potential at zero current (due to the small mismatching of the electrodes)
E_{OS}:	The offset voltage
E_g:	The source potential
S:	Switch
M:	Ammeter (microammeter)
V:	Voltmeter (millivoltmeter)
A:	Amplifier
PI_1 and PI_2:	Photo-optical isolators
TP_1 and TP_2:	Points at which the sensing agar bridges contact the perfusing solution
G_1 and G_2:	Source agar bridges and electrodes

points TP_1 and TP_2, respectively, and lead to a pair of small fiber junction calomel reference electrodes (Beckman #41239). Even well matched electrodes will show a small difference in potential, and this is represented in Figure 1 as the half-cell potentials, $E_{HC}/2$. G_1 and G_2 represent the silver-silver chloride electrodes used for supplying current to the tissue chamber. These electrodes were made by plating coiled silver wire with AgCl by passing a current of 2.5 mA for four hours through 0.1 N HCl solution. The resistance of these electrodes due to polarization is not of concern in this apparatus because a large voltage source is used (180 volts). The resistance from the point of attachment of the source electrodes to the tips of the sensing agar bridges, TP_1 and TP_2, include the source electrode resistance, source agar bridges and the resistance of the solution separating the tips of the sensing and source agar bridges. The resistance of these two systems carrying current across the tissue chambers are represented in Figure 1 as $R_g/2$. The output to the voltmeter, V, is the potential difference, PD, between the two sensing agar bridges and includes the IR drop across the solution, as well as the potential of the tissue. When the tissue is short circuited ($I R_m = E_m$), the PD across the tissue is zero, but the potential, E_T, read on the voltmeter is not zero. This is due to the drop in electrical potential due to solution resistance. (As discussed previously, this is a problem with low resistance tissues, such as mammalian small intestine, but can be neglected with high resistance tissues, such as frog skin.) To maintain the PD across the tissue at 0 mv, current is supplied by a negative feedback loop using an operational amplifier, A.

By definition

$$E_T = E_{IR} + E_{vc} \qquad \text{(Eq. 4)}$$

where

E_T = the measured potential at the sensing electrodes read on the millivoltmeter

E_{IR} = the potential drop due to the passage of current through the solution resistance on each side of the membrane

E_{vc} = the potential across the tissue itself.

Under short-circuit conditions, E_{vc} is set equal to zero and then $E_T = E_{IR}$. Also, the following relationship is true

$$E_{vc} = I R_m + E_m \qquad \text{(Eq. 5)}$$

where

I = current flow through the tissue

R_m = the electrical tissue resistance

E_m = the transmural tissue potential difference at zero current

In the short-circuited state, where $E_{vc} = 0$, then $E_m = I R_m$.

At balance, the sum of the input to the operational amplifier's positive and negative terminals will always be nearly zero. This is a well established property of all negative feedback closed loop servo systems. It follows then, when no IR drop compensation is used, that

$$E_T + E_{HC} + E_{OS} = 0 \qquad \text{(Eq. 6)}$$

where

E_{HC} = the electrode error potential at zero current (due to the small mismatching of the electrodes)

E_{OS} = the offset voltage

In order to cancel out E_{HC}, the value of E_{OS} is set equal to $-E_{HC}$, thus giving $E_T = 0$. The system will now balance with zero potential at the sensing electrodes, but not at the membrane.

To assure that the potential across the membrane will be zero ($E_{vc} = 0$), the IR drop due to the bathing solution must next be compensated for. The linearizing network on the circuit diagram (Figure 1) is the IR compensation system which has been built in to correct for the solution resistance between the sensing agar bridges. Recalling Eq. 4, the value of $-E_{IR}$ is added at the operational amplifier summing junction. The output of the operational amplifier is now E_{vc} multiplied by the gain of the amplifier. Since this is a null balance servo system, the current, I, will be adjusted so that $E_{vc} = 0$. This is accomplished by increasing I until $I R_m = E_m$.

This apparatus employs photo-optical isolators, PI_1 and PI_2 in Figure 1, to separate the 180 volt battery supply (used as the current source) from the potential sensing electrodes. Other systems rely on the common mode rejection of the operational amplifier for isolation. Thus, this system is unique due to the use of the photo-optical isolators which give virtually complete isolation from the current source. The photo-optical isolation may be observed in the complete circuit diagram depicted as Figure 2, or even more easily in a second schematic, Figure 3, which depicts the circuitry for one channel of the apparatus. In Figure 3, E_{IR} represents the voltage drop between the sensing agar bridge and the membrane, which was not specifically identified in Figure 1, but was rather represented as resistances ($R_s/2$) on each side of the tissue. The IR drop compensator employs a Monsanto MCT2 photoisolator to send the

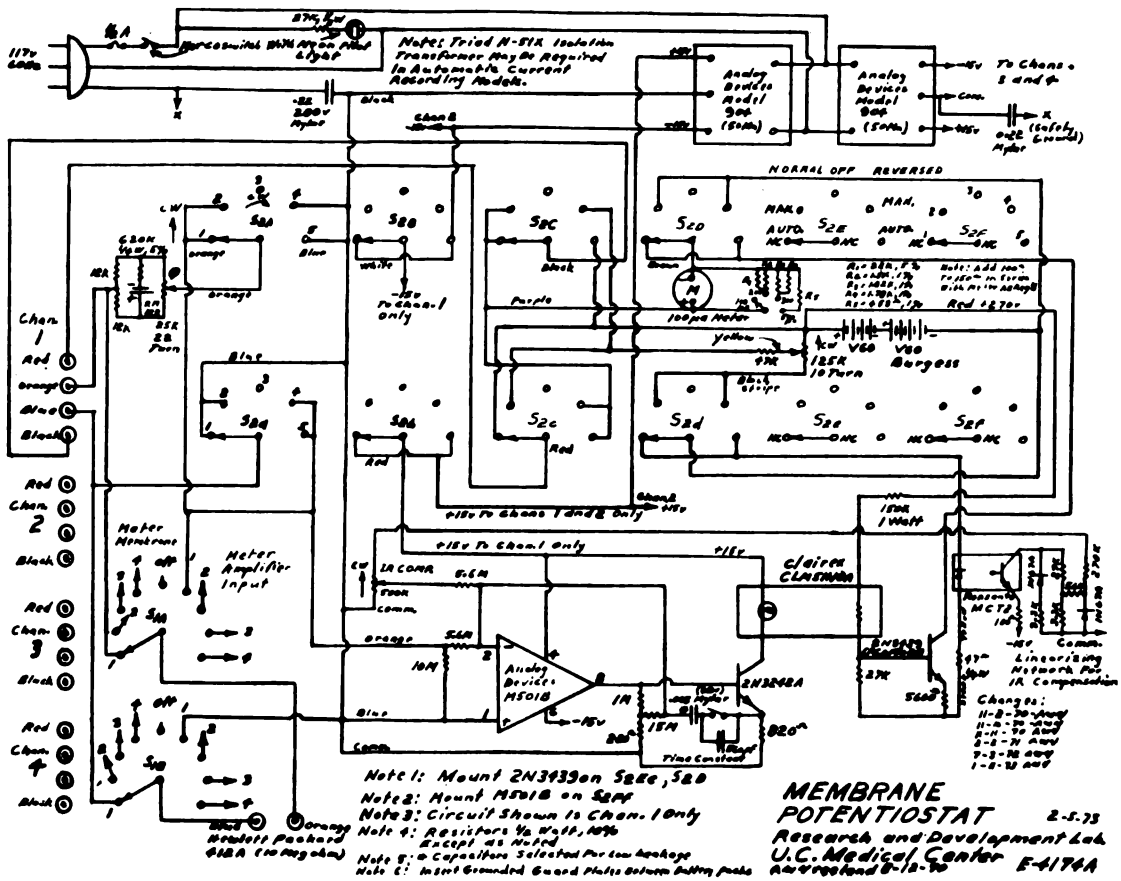

Figure 2. Schematic diagram of electrical circuit of automatic voltage clamp emphasizing photo-optical isolation.

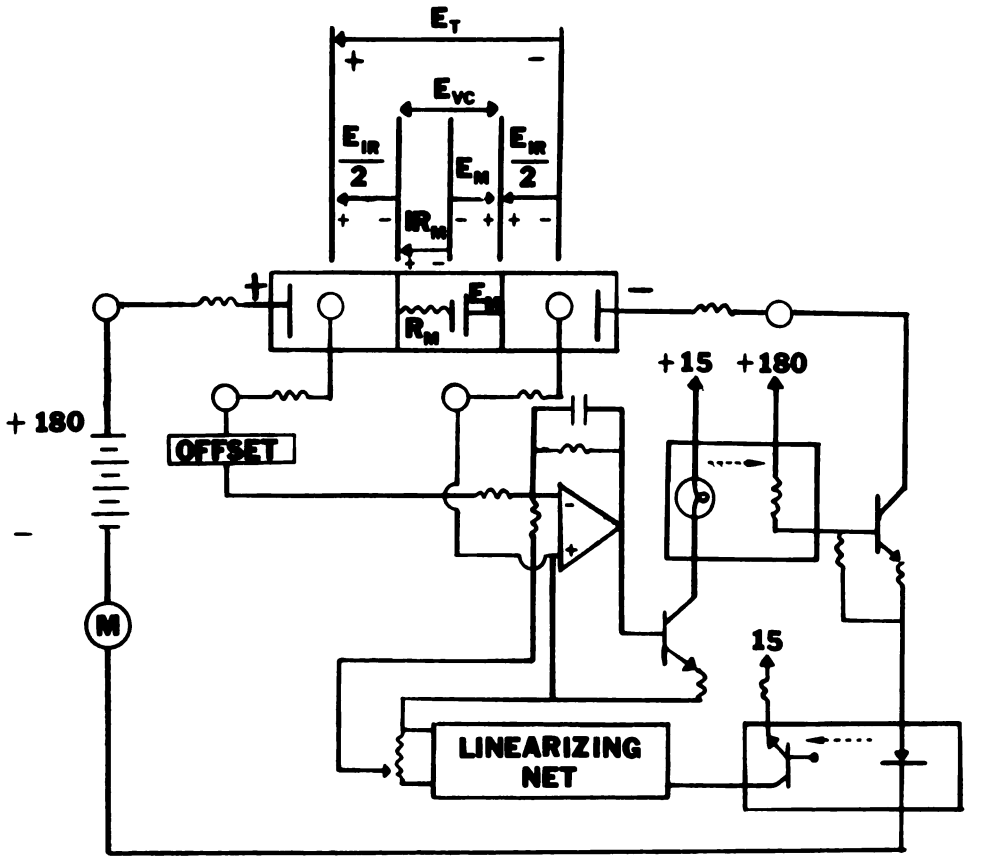

Figure 3. Electrical circuitry for one channel of automatic voltage clamp. (See text and Figure 1 for legend.)

current through the tissue chamber and develop an output voltage that is a function of this current. This particular photoisolator is designed to be used with considerably higher currents in the milliampere range. It was found, however, that it could be used in the low microampere range, although its output was not linear. In order to obtain a linear output, a linearizing network employing two diodes was used. These diodes are Germanium diodes which are operating with the current in the forward direction so that they function as nonlinear resistances. In combination with the other resistors shown, these nonlinear resistors produce a linear input-output characteristic as shown by the curve in Figure 4.

Four separate microammeters, M, were incorporated into the clamp, as seen in Figure 5 which is a photograph of the automatic voltage clamp. A switch under each meter changes the sensitivity to one of the four ranges: 0-100 μA, 0-200 μA, 0-300 μA, or 0-500 μA. The potential differences were measured with a Hewlett-Packard Model 412A millivoltmeter, which has a 10 megohm input impedance. A high meter resistance is necessary in order to avoid loading the potential sensing agar bridges. This millivoltmeter has 40 DB of 60 cycle rejection at full scale which is important in an unshielded system.

Chambers and Towers

A schematic diagram of the chamber set up is shown in Figure 6, which consisted of three parts: A - the perfusion tower; B - the lucite tissue chamber, front view; and C - a view of the open chamber. The glass perfusion tower (available from MRA, Inc., Boston, Massachusetts) (Figure 6, A) is water-jacketed and

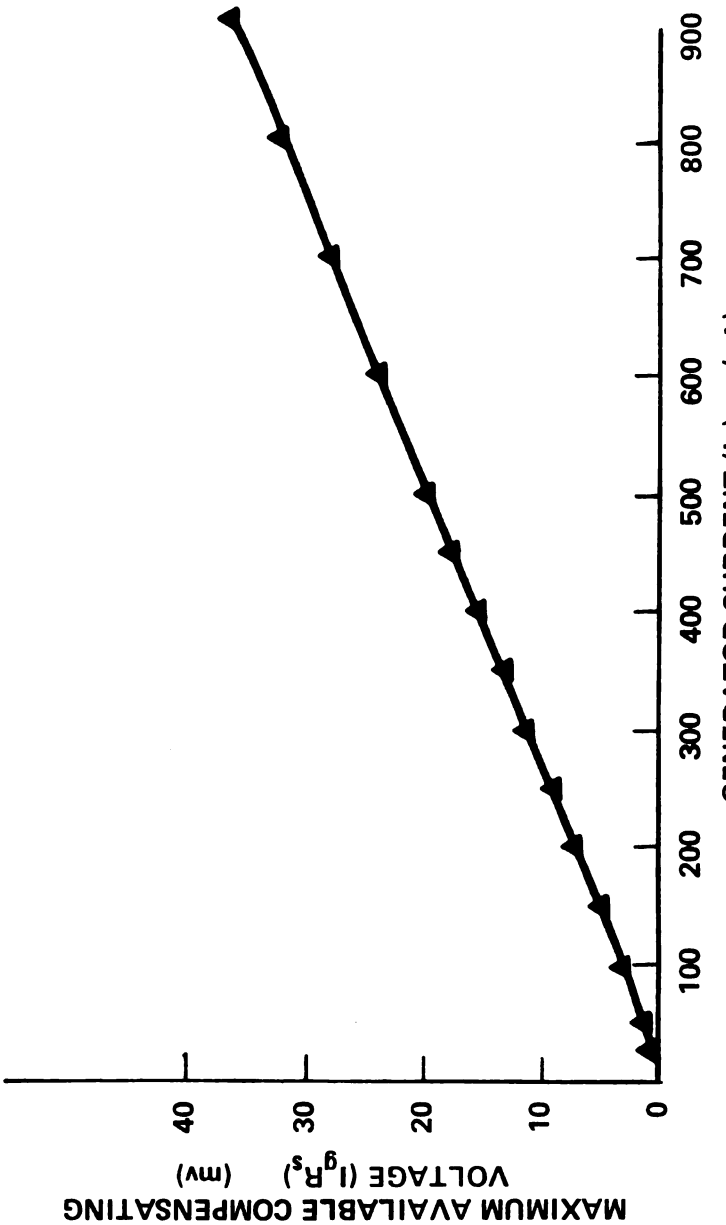

Figure 4. Linear input-output characteristic of linearizing network of automatic voltage clamp.

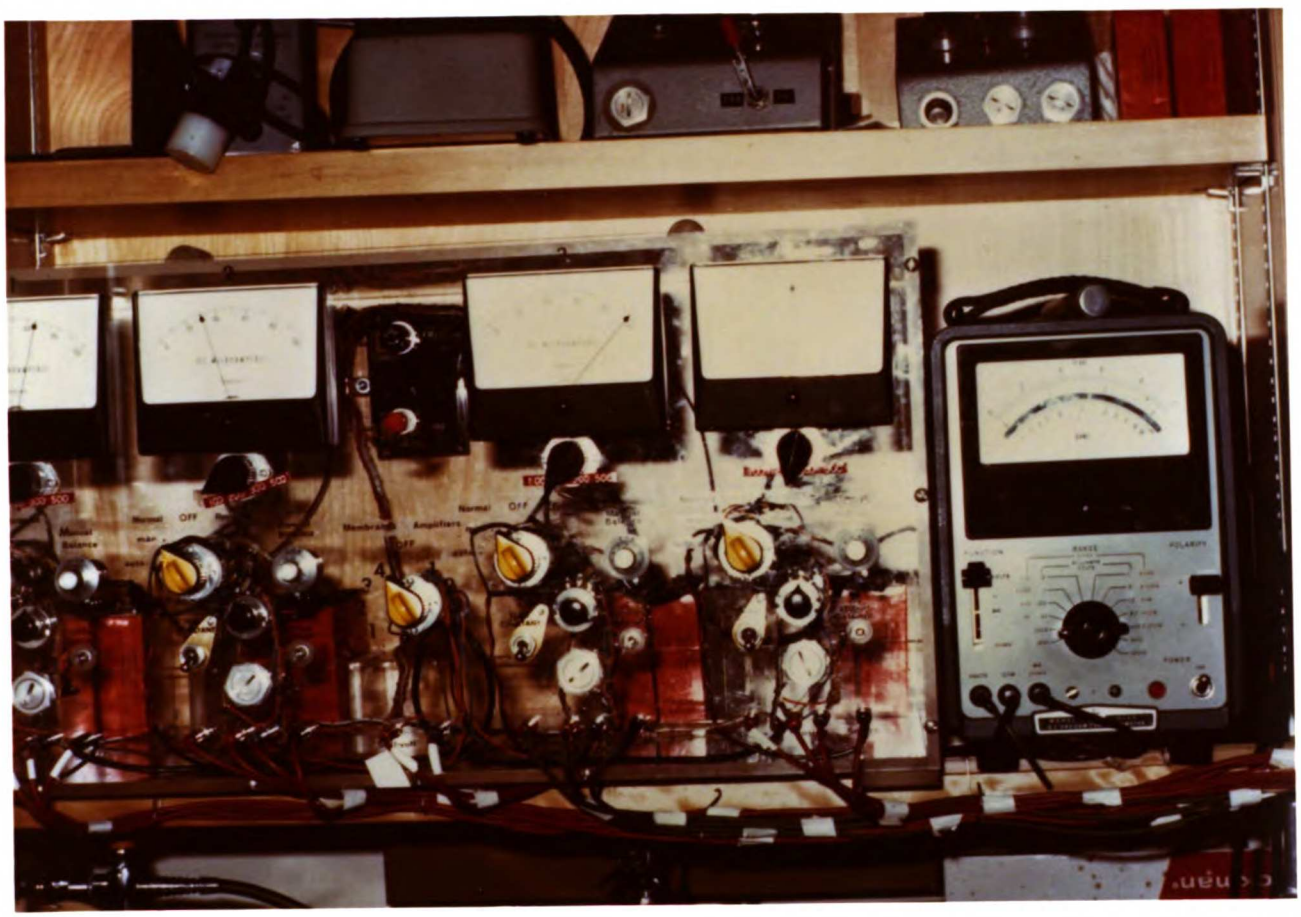

Figure 5. Photograph of automatic voltage clamp and voltmeter.

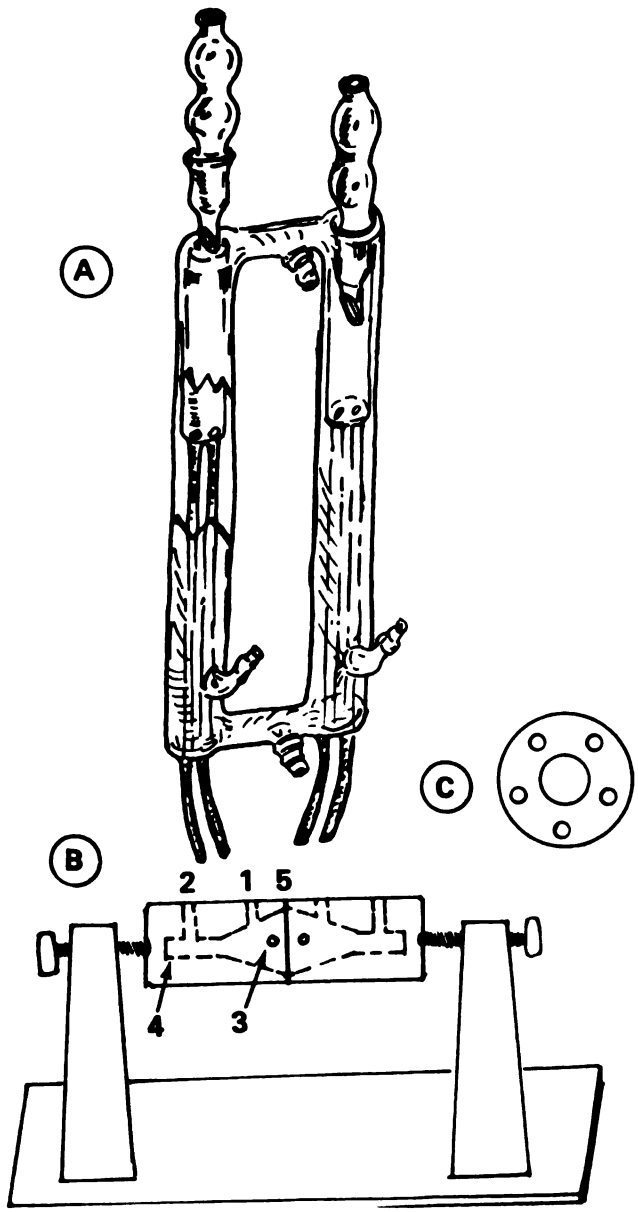

Figure 6. Schematic diagram of perfusion tower and tissue chamber.

- **A. Perfusion tower**
- **B. Tissue chamber**
  1. **Influx – opening for connection to perfusion tower**
  2. **Efflux – opening for connection to perfusion tower**
  3. **Port for agar bridge to sensing electrode (opens to front of chamber)**
  4. **Port for agar bridge to source electrode (opens to back of chamber)**
  5. **Position of tissue**
- **C. Open view of tissue half chamber (shows positioning of 5 pins over which tissue is mounted).**

was maintained at 37° C by a constant temperature circulating water bath (Neslab Instruments, Durham, New Hampshire). The solution reservoirs were capped with glass condensors in order to minimize evaporative losses. A gas-lift circulating system was used for perfusing the mucosal and serosal faces of the tissue separately with 10 ml of buffer solution. The gas employed (95% O_2, 5% CO_2) was first bubbled through distilled water in a scrub tower to minimize evaporation. Figure 6, B, shows the tissue chamber (Model C-25-12, E. W. Wright, Co., New Haven, Connecticut). The openings at the top of each chamber (B: 1 = influx, 2 = efflux) were connected via three-way stopcocks and tygon tubing to the perfusion tower. The ports in front (B:3) allowed access for the agar bridges from the sensing electrodes. The rear ports (B:4) connected the agar bridges to the source Ag-AgCl electrodes to maintain full contact with the perfusing solution. The tissue was positioned at point 5 in Figure 6, B, after being mounted over the pins of one half chamber, as seen in Figure 6, C. This half chamber was taken and clamped together with its corresponding mate. The exposed surface area of the tissue is 1.12 cm^2. The sensing agar bridges were positioned 1.5-2 mm from the tissue. The source agar bridges were approximately 20 mm from the tissue. Figure 7 is a photograph showing the entire experimental setup: the automatic voltage clamp, the four towers and chambers, and the voltmeter.

Buffers

Krebs-Henseleit buffer (103) was the primary solution used as the perfusing medium. The composition of this buffer is

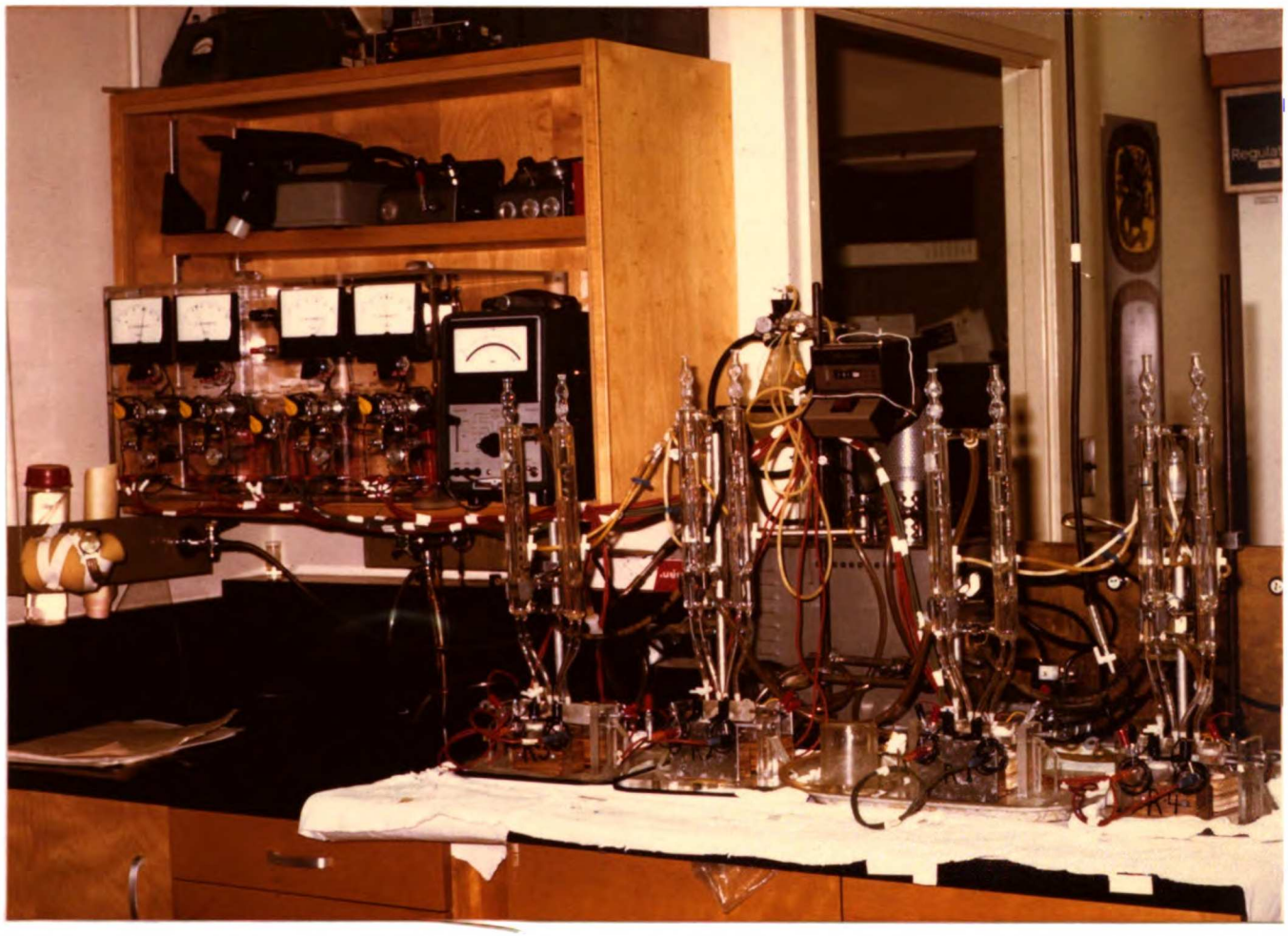

Figure 7. Photograph of entire experimental setup.

listed in Table I. A 10 ml volume of buffer solution was introduced into each side of the glass perfusion tower. In most experiments, 25 mM d-glucose was added to the buffer solution prior to instillation in the perfusion tower, except in those studies where the effect of glucose was specifically studied. The solutions used to treat the tissue prior to mounting did not contain any added sugar. In all cases, the solutions used on the mucosal and serosal sides of the tissue were equal in osmolarity. Another buffer solution that was used was termed Partial K-H or Partial Krebs-Henseleit buffer. The composition of this solution is also shown in Table I. This solution was made in quantity and was used to make the Krebs-Henseleit buffer. It was also used in the preparation of the agar bridges as discussed subsequently.

A sodium-free buffer was used in some experiments, where choline salts replaced the sodium salts. The composition of this buffer is given in Table I as choline-I buffer. At first, this solution was put only on the mucosal side of the tissue with the normal Krebs-Henseleit buffer on the serosal side; but, due to the nature of the "leakiness" of this tissue preparation, it was necessary to use sodium-free media on both sides of the tissue. In these cases, it was necessary to alter the potassium ion concentration in the buffer (choline-II buffer in Table I) in order to prevent excess leaking of intracellular potassium ion (104). The addition of sodium salicylate to the bathing media on the mucosal side of the tissue was investigated for various effects. Concentrations of 1.0, 2.5, and 5.0 mg/ml sodium salicylate were used. The salicylate solutions were added to the mucosal bathing media approximately 40 to 60

Table I

Composition of Perfusate Buffers

A. Krebs-Henseleit Buffer (or K-H Buffer)

$[Na^+]$	= 143	mM
$[K^+]$	= 6	
$[Ca^{++}]$	= 2.5	
$[Mg^{++}]$	= 1.2	
$[Cl^-]$	= 128	
$[H_2PO_4^-]$	= 1.2	
$[SO_4^=]$	= 1.2	
$[HCO_3^-]$	= 25	

or

0.9%	NaCl	118	m moles	769.2 ml
1.15%	KCl	4.8		30.8
0.11 M	$CaCl_2$	2.5		23.1
2.11%	KH_2PO_4	1.2		7.7
3.82%	$MgSO_4 \cdot 7H_2O$	1.2		7.7
1.3%	$NaHCO_3$	25		161.5
				1000.0 ml

(all of above ingredients are 0.154 M, except $CaCl_2$)

B. Partial Krebs-Henseleit Buffer (or Partial K-H Buffer)

0.9%	NaCl	100	parts	80 ml
1.15%	KCl	4		3.2
1.3%	$NaHCO_3$	21		16.8
				100.0 ml

Table I (continued)

C. Choline-I Buffer

	choline Cl	118	m moles	16.476 gm
1.15%	KCl	4.8		30.8 ml
0.11 M	$CaCl_2$	2.5		23.1 ml
2.11%	KH_2PO_4	1.2		7.7 ml
3.82%	$MgSO_4$	1.2		7.7 ml
44%	choline HCO_3	25		9.38 gm

distilled H_2O q.s. ad. 1000.0 ml.

D. Choline-II Buffer

	choline Cl	118	m moles	16.476 gm
1.15%	KCl	4.8		30.8 ml
0.11 M	$CaCl_2$	2.5		23.1 ml
2.11%	KH_2PO_4	1.2		7.7 ml
3.82%	$MgSO_4$	1.2		7.7 ml
	$KHCO_3$	14		1.402 gm
44%	choline HCO_3	11		4.13 gm

distilled H_2O q.s. ad. 1000.1 ml.

minutes after the start of radioactive flux experiments. The activity of the radioisotopes and the sodium ion concentration of the mucosal solutions were maintained constant before and after the addition of the unlabelled sodium salicylate. The composition of the sodium salicylate replacement solution is given in Table II.

All chemicals used in the preparation of these buffers were of reagent grade. (KCl, KH_2PO_4, $MgSO_4$, and NaCl were purchased from Mallinckrodt; $CaCl_2$ and $NaHCO_3$ were purchased from Matheson, Coleman and Bell, while choline bicarbonate was purchased from Baker Chemical Co. and dextrose was purchased from Fisher Scientific.

Agar Bridges

The agar bridges were constructed using PE 280 tubing (Intramedic polyethylene tubing, I.D. = .085" x O.D. = .128", Clay Adams Co., Parsippany, New Jersey) filled with 4% w/v agar (Bacto-Agar, Difco Laboratories, Detroit, Michigan). Originally, 1 M KCl solution was used as the solvent in this preparation; subsequently, Partial K-H buffer (see Table I, B) was used resulting in a solution containing 123.2 mM NaCl, 25.9 mM $NaHCO_3$, and 4.9 mM KCl. The powdered agar and the buffer solution (50 ml) were placed in a small Erlenmeyer flask with a magnetic stirrer and boiled for approximately one hour (with a loose fitting condensor type top on the flask to prevent evaporization). To prevent decomposition of the agar at elevated temperatures, the Erlenmeyer flask was placed in a boiling water bath during this heating period. When the agar solution appeared clear with a slight tannish color, the bridge

Table II

Sodium Salicylate Replacement Solution

	Na Salicylate	582.5	mg
1.15%	KCl	0.92	ml
0.11 M	$CaCl_2$	0.69	ml
2.11%	KH_2PO_4	0.23	ml
3.82%	$MgSO_4 \cdot 7H_2O$	0.23	ml
1.3%	$NaHCO_3$	4.85	ml
		6.92	ml

distilled H_2O q.s. ad. 30.0 ml.

add 0.135 gm glucose and 0.3 ml ^{14}C-salicylate solution

(0.1 ml of ^{14}C-salicylate solution normally added to 10 ml)

could be made successfully. A plastic disposable tuberculin syringe fitted with a piece of latex tubing was attached to the PE tubing and the agar solution was drawn into the tubing. The PE tubing was disconnected, briefly held horizontal and then placed on paper toweling to cool. The agar bridges were subsequently stored submerged in the Partial K-H solution.

The agar bridges which were to be placed closest to the tissue, the sensing bridges, were cut at a slant to expose more of the agar toward the tissue. These bridges were fit into the ports of the chamber with a small piece of rubber cut from surgical gloves, which served as a gasket (sealer) to prevent leakage of the perfusing solution. Each rubber gasket was slit with a scalpel or razor once the bridge was in place to allow the agar to be exposed to the buffer solution. A 1/4" length of latex tubing (I.D. = 1/16" and O.D. = 1/8") was used as a sleeve for sealing the agar bridges placed in the rear ports and connected to the source electrodes. Care was taken in inserting the bridges so that the ends were positioned in the middle of the chambers and not touching the sides, so that the bridges would be in full contact with the perfusing solution.

Drug Solutions

A solution of ouabain (catalogue #14, 193-3, Aldrich Chemical Co., Milwaukee, Wisconsin), a cardiac glycoside which is a specific inhibitor of sodium-transport, was made in Partial K-H buffer such that 1 ml of this solution, when added to 9 ml of the perfusing serosal fluid, contained the appropriate amount of ouabain resulting in a final serosal concentration of 1×10^{-3} M. This concentration of ouabain was maintained in the

serosal bathing solution for the remainder of the experiment following the initial addition of ouabain.

Unlabelled antipyrine (Aldrich Chemical Co.) solutions were used in some experiments. Antipyrine was dissolved in Partial K-H buffer and these solutions were made to be equal in concentration to the ^{14}C-salicylate solution.

Unlabelled sodium salicylate (Eastman Organic Chemicals) was dissolved in a special buffer as listed in Table II for the sodium salicylate replacement solution. This solution was used for experiments in which salicylate was added to the mucosal perfusing solution to determine the effect of mucosal salicylate on the ^{14}C-salicylate transport rate. This sodium salicylate solution was prepared such that the sodium ion concentration as well as the sodium ion/potassium ion ratio and the radioactive isotope concentration would remain constant. This salicylate solution was made such that when a certain concentration of sodium salicylate was desired, a predetermined volume of the mucosal solution was removed and an equal volume of the sodium salicylate replacement solution was added. Thus, to attain a final mucosal concentration of 1 mg/ml of sodium salicylate, 0.6 ml of the sodium salicylate replacement solution was added. For a 2.5 mg/ml final concentration, the volume change of the mucosal solution was 1.5 ml, whereas, a final 5 mg/ml concentration of sodium salicylate in the mucosal perfusing solution necessitated a 3.0 ml volume change.

Radioisotopes

All flux measurements were made using drug compounds isotopically labelled with ^{14}C or ^{3}H. ^{14}C-salicylate was obtained

from New England Nuclear (activity 1 mCi/28.7 mg, lot #506-076) and from ICN (activity 500 μCi/28.9 mg, lot #553662 and activity 500 μCi/36.1 mg, lot #551972). The isotope was received as solid crystals and was made up in stock solutions with the addition of Partial K-H buffer. These solutions had an activity of 55-90 μCi/ml. A sample of 100 μl of this solution was added to the mucosal perfusing media for the flux experiments. Other radioactive isotopes used in these studies include: ^{3}H-antipyrine (obtained from New England Nuclear, specific activity 170 mCi/m mole, lot #297-015-001); ^{14}C-DMO, chemical name 5,5-dimethyl-oxazolidine-2, 4-dione (obtained from New England Nuclear, specific activity 1 mCi/14 mg, lot #252-125), ^{3}H-inulin (obtained from ICN, specific activity 43 mCi/gm, lot #7327-64), and ^{14}C-butanol (obtained from New England Nuclear, specific activity 250 μCi/1.5 mg, lot #729-087). All isotopes used were checked for identity and radioactive purity by thin layer or paper chromatographic methods, as listed in Table III. The chromatograms were scanned with a Varian-Berthold Radioscanner (Model LB 2722) in order to determine the location of radioactive spots. Cold reference material was also chromatographed and developed to determine the R_f value for comparison with the radioactive chromatogram. In all cases, only a single radioactive spot was seen having a R_f value corresponding to that seen in the chromatogram of the authentic non-radioactive compound.

Surgical Procedures

Male Sprague-Dawley rats weighing 300-400 grams were allowed free access to food (standard rat chow) and water prior to the experiment. The rats were decapitated with a guillotine. The small intestine was rapidly exposed by a midline abdominal

Table III

Chromatographic Methods for the Determination of Radiopurity

Compound	Method	Solvent
Antipyrine	TLC (silagel F)	cyclohexane/acetone 40:50
DMO	TLC (silica gel G)	chloroform/methanol 9:1
Inulin	ascending paper (Whatman #1)	butanol/ethanol/water 52:18:30
Salicylic acid	TLC (silagel F)	ethanol/ammonium hydroxide 30:1

incision. The intestine was severed at the pylorus and gently pulled up and out of the rat. The first 25 cm of small intestine was discarded. A 20 cm section was then excised and flushed with pH 7.4 K-H buffer (see Table I) at room temperature. This rinsed jejunal section was drawn over a wetted glass rod of appropriate diameter and placed in a chilled buffer solution kept in an ice bath. The serosa and muscularis externa were removed by blunt dissection as in the procedure reported by Wolfe et al. (105). The fat and mesentery were pulled loose along the mesentery reflection, and the external layers gently teased off along the whole length of the tissue. A lighted magnifying lens was used as an aid in performing this stripping technique. Figure 8 is a diagrammatic representation of the small intestine in cross section. The tissue layers removed, serosa and muscularis externa, are readily visible in this diagram. The tissue was slit with a scalpel along the mesentery. Four successive 2 cm. sections, not containing any Peyer's patches because of possible problems with electrical interference, were mounted, mucosal side up, on four lucite half chambers with the use of fine tissue forceps. Each half chamber was clamped together with its corresponding half and attached to the perfusion tower.

Calibration of Apparatus

A few hours prior to the actual transport measurements, the voltmeter, the automatic voltage clamp, and the circulating constant temperature bath were turned on and allowed time to "warm up." The glass towers were well rinsed first with distilled water and then with the buffer solution. The tygon tubing connecting the tower to the chamber was clamped with large

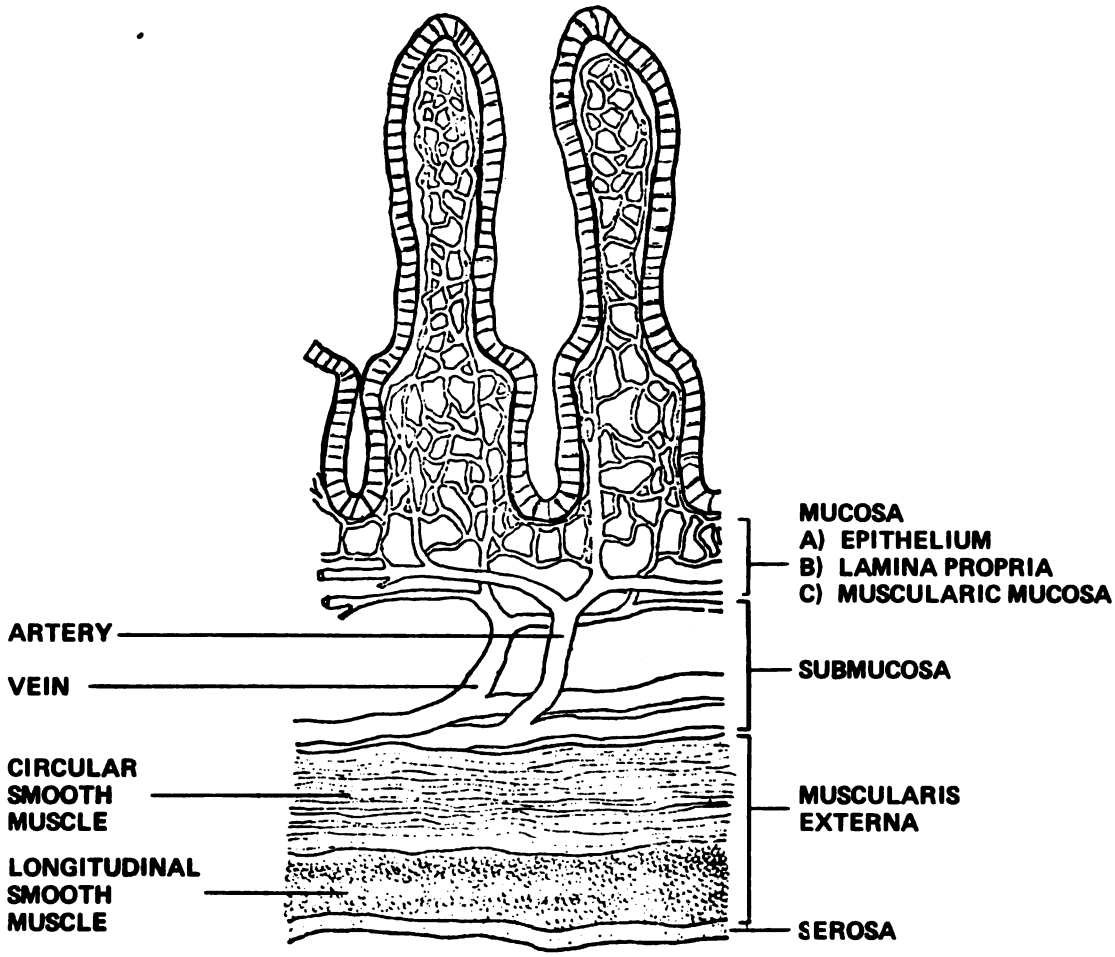

Figure 8. Diagrammatic representation of the small intestine in cross section.

hemostats and then the buffer was added to each tower. The chambers, which were stored submerged in a beaker of distilled water, were rinsed and dried. A parafilm gasket was placed over the holding pins of the half chambers on which the stripped membranes would be later placed. The agar bridges, with their appropriate gaskets, were inserted into each half chamber. The half chambers were then put together, noting the engraved letters on each so that they were always in the same sets. The chambers were then mounted in the stands and the tygon inlet and outlet tubings, fitted with 3-way stocpcocks, were inserted into the openings on the tops of the chambers. The tubing was then unclamped and the buffer allowed to enter the chambers. The other ends of the agar bridges were inserted into the proper electrodes. The gas (95% O_2, 5% CO_2) was turned on and the gas lines were attached to the glass towers and bubbling was started. The setup was checked to determine that there were no air pockets in the tower or chamber which might prevent the buffer solution from perfusing adequately.

After the system had equilibrated (approximately 30 minutes after the addition of the buffer) and shortly before sacrificing the rat, a standard curve of voltage-current data was made. A standard voltage-current curve must be made for each set of chambers and bridges before the tissue was mounted. The potential differences produced across the agar bridges connecting the sensing electrodes were read at five current values: 0, 100, 200, 300, and 500 μA. The PD read on the voltmeter at the 0 μA setting (E_{HC}) indicated the small mismatching of the electrodes, which was nulled out by an offset circuit (Figure 1). The voltage-current points were plotted as described by Clarkson and Toole (74) and

Field et al. (20) and were used to correct the observed potential for the IR voltage drop occurring in the solution between the tissue and the tips of the sensing bridges. The voltage drop is due to the current passing through the resistance of this small portion of solution. Figure 9 indicates the graphical method used to determine this correction. The five voltage vs current data points were plotted (shown as line 1 in Figure 9). The slope of line 1, voltage vs current data determined without tissue, is the resistance, R_s, due to the solution between the bridges and the tissue. After line 1 was plotted, the inlet-outlet tygon tubes were clamped shut and the chambers dismounted and drained. The parafilm gaskets were removed from the chambers and stored. The glass towers were next unclamped and drained completely. They were then re-clamped and 10 ml of warmed buffer was introduced into each side of each tower. After the tissues had been mounted on the pins of the half chambers, the chambers were again mated, mounted in the stands, and reattached to the glass towers. The agar bridges were reconnected to the electrodes. The inlet-outlet tubes were unclamped and the buffer allowed to circulate and perfuse the tissue. Transmural potential differences were read immediately to make sure that the tissue was viable and that the bridges and electrodes were working properly and not shorted.

When all four tissues have been mounted, the transmural potential difference (the voltage reading across the tissue at open circuit, E_m), which is point B on line 2 in Figure 9, and the current needed for a zero potential difference reading on the voltmeter, point C on line 2 in Figure 9, were quickly determined and plotted. The short circuit current value, I_{sc},

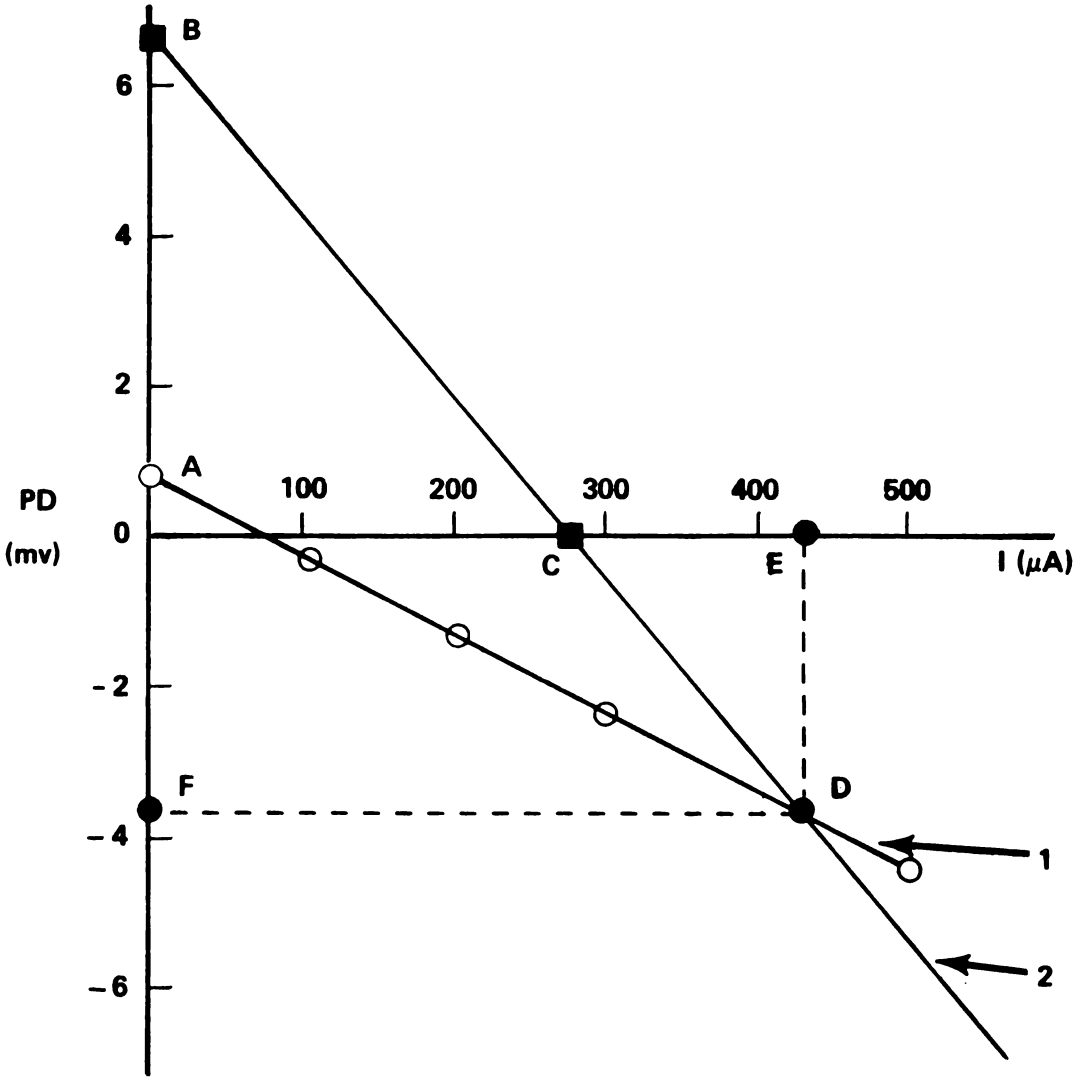

Figure 9. Graphical determination of short-circuit current.

Line 1: Current-voltage data determined without tissue.
Line 2: Current-voltage data determined with tissue.

A: Potential reading without tissue present, showing mismatch of electrodes.

B: Potential reading with tissue present (transmural PD = B – A) at open circuit.

C: Current necessary for zero potential reading between agar bridges (reading on voltmeter.

D: Point where two straight lines intersect – short-circuit conditions.

E: Short-circuit current, I_{sc}.

F: Potential reading across agar bridges when tissue is at short-circuit conditions.

(point E in Figure 9) was determined graphically from the point where the two lines intersect and this was then recorded. The slope of line 2 is the total resistance of the system, R_T, and is equal to the sum of the solution resistance and the tissue resistance, R_m. If R_s were ignored using stripped mammalian small intestine, an error of up to 50% is possible. When the tissues had stabilized, as indicated by constant values for the I_{sc}'s, the instrument was switched to the automatic mode using the following procedure. The IR drop compensator was turned completely counter clockwise. When the ammeter needle stopped oscillating, the offset voltage was adjusted so that the balance point on the voltmeter corresponded to the zero current electrode potential (point A in Figure 9). The IR-drop compensator potentiometer was then adjusted clockwise until the short-circuit condition values (as previously determined graphically) were read on their respective meters (point E on the ammeter and point F on the voltmeter). Once in the automatic mode, it was not necessary to graphically determine I_{sc} again. The I_{sc}, the potential difference reading at the shorted condition, PD_{sc}, and the open circuit transmural PD were recorded every five to ten minutes during the normal run of the experiment. If electrical changes were induced by added agents, then the frequency of the readings were increased to make sure that enough points were obtained for an accurate graphical representation of the data.

Calculation of Tissue Resistance

The electrical properties of the tissues were monitored throughout the experiments. The transmural PD and the I_{sc} were read directly from the appropriate meters and recorded on a

worksheet as shown in the Appendix, Figure A-1. The ohmic tissue resistance, however, was calculated from the other electrical parameters and then recorded as in Figure A-1. The slope of line 2 in Figure 9 is equal to the total resistance of the system, R_T, which in turn is equal to the solution resistance, R_s, plus the tissue resistance, R_m, ($R_T = R_s + R_m$). The resistance of the tissue could be calculated in different ways, depending on the data available.

(1) $$R_m = \frac{PD_{\text{(at zero current)}}}{I_{\text{(at } E_T = 0)}} - R_s \qquad \text{(Eq. 7)}$$

where

$PD_{\text{(at zero current)}}$ = point B in Figure 9

$I_{\text{(at } E_T = 0)}$ = point C in Figure 9

R_s = slope of line 1 in Figure 9

or

(2) $$R_m = \frac{PD_{\text{(at zero current)}} - PD_{sc}}{I_{sc}} - R_s \qquad \text{(Eq. 8)}$$

where

PD_{sc} = point F in Figure 9

I_{sc} = point E in Figure 9

or, more generally

(3) $$R_m = \frac{PD_{\text{(at } I_1)} - PD_{\text{(at } I_2)}}{I_1 - I_2} - R_s \qquad \text{(Eq. 9)}$$

where

I_1 and I_2 are different currents imposed across the tissue

and $PD_{(at\ I_1)}$ and $PD_{(at\ I_2)}$ are the potentials read directly on the voltmeter at these currents. R_m was monitored and observed during the experiments along with the other electrical parameters which could be read directly from the meters.

Maintenance of Fixed Potential Across Membrane

In some experiments, the PD across the tissue (E_{VC}) was maintained at finite values other than zero. The potential difference across the tissue could be adjusted both in the manual and automatic modes. In the automatic circuit, the transmural PD range was limited to $\pm$ 20 mv, while a range of $\pm$ 100 mv was possible with the manual mode. During these offset experiments, it was not always possible to monitor the corresponding current at the limits of the voltage range because the current often exceeded 500 μA, the highest value which could be read on the ammeters. Open circuit transmural potential differences were monitored before and after the different PD settings so as to not interfere with the drug flux during the experiments where a constant transmural PD was maintained. Therefore, it was not possible to determine tissue resistance during these potential difference experiments.

Intracellular pH Determination

Experiments were undertaken to determine the intracellular pH (pH_i) of the rat jejunal tissue at $\Delta PD = 0$ and at maximal positive and negative imposed PDs. This was done to see if the effect on ionic drug transport caused by the imposed PDs was, in fact, due to changes in pH_i's related to PD changes. The pH_i of the jejunal tissue was determined following the method of Waddell and Butler

(106). This method is based on the cellular to solution distribution of the weak acid, 5-5-dimethyl-2, 4-oxazolidinedione (DMO), the chief metabolic product of the antiepileptic drug trimethadione (Tridione®)

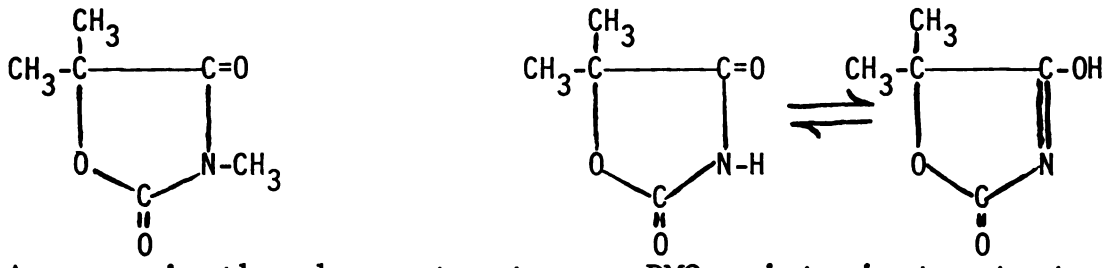

As seen in the above structures, DMO exists in two tautomeric forms; the form on the right is capable of forming stable ionized water-soluble salts with various cations (107).

Certain assumptions must be made in order to use DMO for the calculation of intracellular pH. These assumptions are:

(1) The undissociated form of the acid diffuses through the cellular membrane and reaches the same concentration in the aqueous medium on both sides of the membrane;

(2) Neither tautomeric species of DMO is bound to any cellular constituent;

(3) The apparent dissociation constant of the indicator is the same in the cell water as that determined in the extracellular water;

(4) Neither tautomeric species enter fat; and

(5) The compound is not metabolized.

Under these assumptions and with the knowledge of the concentration of total indicator in extracellular and cellular water, as well as the pH of the extracellular water, the pH_i can be calculated (108).

Inulin was used to determine the extracellular volume of

the tissue, a value which must be known before the pH_i can be calculated. Unfortunately, because the tissue could not be blotted completely to remove excess bathing medium, a true tissue extracellular volume could not be determined. The value that has been calculated as the extracellular volume in this experiment also includes this adhering solution. Thus, this value cannot be used as a true parameter of the tissue (since it is much too large) and cannot be compared with other literature values of extracellular space in rat jejunum. However, its use is justified here since there is an artificially larger extracellular space that is being measured. Using this value for the volume of the extracellular space does not affect the calculation of the true pH_i, since the concentration of DMO in this extracellular volume will be consistent with its size. The pH_i was calculated using the following equation:

(Eq. 10)

$$pH_i = pK_a + \log \left\{ [C_r(1 + V_r) - V_r] \; [10^{(pH_o - pK_a)} + 1] - 1 \right\}$$

where

pH_i = intracellular pH

pK_a = $-\log K_a$ (K_a = acid dissociation constant of DMO)

pH_o = extracellular pH (the pH of the external solution)

$$Cr = \frac{C_T}{C_e} \qquad \text{(Eq. 11)}$$

$$C_T = \frac{\text{total DMO in tissue}}{\text{total water of tissue } (V_r)}$$

or

$$C_T = \frac{\text{cpm's due to DMO in tissue sample}}{\text{weight of wet tissue} - \text{weight of dry tissue}}$$

C_e = concentration of DMO in the extracellular space (or in the external solution)

$$V_r = \frac{V_e}{V_i} \qquad \text{(Eq. 12)}$$

V_e = extracellular water volume of tissue

or

$$V_e = \frac{\text{cpm's due to } {}^3\text{H-inulin in tissue sample}}{\text{concentration of } {}^3\text{H-inulin in external solution}}$$

V_i = intracellular water volume of tissue

or

$$V_i = V_T - V_e$$

The value of the pK_a of DMO was taken as 6.13 at 37° C (106). Equation 10 was first described by Waddell and Butler (106) and its derivation is given by Irving et al. (107). Figure A-2 in the Appendix is an example of a worksheet used in the calculation of pH_i. From this sheet, how the pH_i was determined can be seen.

The preparation of tissues and the methods for monitoring the electrical apparatus in the pH_i experiments were identical to those previously described. Samples of 100 µl of ^{14}C-DMO and ^{3}H-inulin were added to the mucosal and serosal bathing solutions. Gulyassy (109) has pointed out that a large error in the calculation of pH_i may be made if tracers are added to the bathing medium of only one side of the tissue (unilateral labelling) due to the continuous loss of tracer into the other solution. The DMO method for determining pH_i is based on the assumption that the activity of the nonionized form of DMO is

the same inside and outside the cell. This would not be the case with unilateral labelling, because distribution equilibrium of DMO would not be reached. Therefore, bilateral labelling was carried out in all experiments in this work.

Samples (0.1 ml) of the bathing solutions were taken and placed on pellets of filter paper and allowed to dry. These samples were later combusted in the Packard Tri-Carb Oxidizer Model 305. The tissues, after being maintained at fixed PDs for over 60 minutes, were gently blotted while still mounted on the half chamber. However, they were not blotted sufficiently to remove all excess and adhering solution because of the fear of removing some of the mucosal tissue. The tissue area exposed to the blotting solutions was carefully cut away from the rest of the tissue and placed in tared drying vials. The tissues were weighed, dried to constant weight, and then combusted in the oxidizer to determine the amount of both isotopes in the tissue. The scintillation cocktails used in experiments with the oxidizer were a mixture of 3 ml ethanolamine, 9 ml methanol, and 7 ml of scintillator (4 gm Omniflor to 1 liter scintillation grade toluene) for use with ^{14}C-samples and Aquasol (obtained from New England Nuclear) for use with ^{3}H-samples. The samples were read and analyzed in the Packard Tri-Carb liquid scintillation counter as will be discussed subsequently.

Flux Measurements

Transmural fluxes of salicylate, antipyrine, and butanol were determined by the use of radioisotopes. Tracer quantities of ^{14}C-sodium salicylate, ^{3}H-antipyrine, or ^{14}C-butanol were introduced into the perfusion solution bathing the mucosal side

of the tissue after the electrical parameters were stable and I_{sc} conditions were being maintained in the automatic mode. In some experiments, ^{14}C-salicylate and ^{3}H-antipyrine were both added to the mucosal perfusion solution and double isotope counting techniques were used. The serosal solutions were sampled at five and ten minute intervals to determine the transport rates of the isotopes. A few samples (0.1 ml) of the mucosal solutions were taken at different times during the experiment to insure that the mucosal concentration was essentially constant. (The mucosal concentrations of the ^{14}C-butanol experiments were monitored closely because of problems of suspected evaporation.) Because the serosal samples were 1 ml and the total serosal volumes were 10 ml, buffer solution was added back to the serosal side to maintain constant volume. Thus, all components of the serosal solution were maintained constant except for the isotope concentration. Corrections were made for the amount of tracer removed by this sampling technique, as will be shown later. This procedure also helps to maintain the system at sink conditions during these experiments. Since the concentration of the radioisotopes on the mucosal side was essentially constant, the counts per minute (cpm's) of the mucosal samples were averaged and this value arbitrarily set equal to 1000 μ units/ml. The cpm's of the serosal samples were then related to the mucosal concentrations by this factor. Thus, the cumulative amount transported (from mucosa to serosa) was essentially a percentage of the constant amount on the mucosal side.

Serosal samples were placed in glass scintillation vials containing 10 ml of Aquasol. Mucosal samples were treated similarly except 0.9 ml of buffer was added to each vial, so

that all sample vials had the same solution composition (except for isotopes). Blank samples were taken of all solutions before introduction of the radioisotope. Figure A-3 in the Appendix is an example of a worksheet used to monitor the serosal and mucosal samples taken to determine drug fluxes.

A Packard Tri-Carb Model 3375 liquid scintillation counter was used to measure the radioactivity. The factory pre-set window settings were used for all but the DMO-inulin experiments. When ^{14}C- or ^{3}H- isotopes were used singly, the wider window settings were used. However, in the experiments with double isotopes, narrower window settings were used. Automatic external standardization (AES) was used in the assay of these samples to determine counting efficiency. Since the volume and buffer composition of the samples were constant, all samples showed the same efficiency within the experimental error of the scintillation counter. Also, the method of calculations was such that the concentration of the serosal side was related to that of the mucosal side, and since the samples were all uniform and showed the same efficiency, there was no need to calculate the activity of the samples since the counts per minute (cpm's) gave just as much information as the disintegrations per minute (dpm's) or microcuries. Each sample was counted at least twice and to at least 10,000 counts.

Flux Calculations

Due to the removal of relatively large volume serosal samples and the add back of buffer solution which resulted in dilution of the trace compound in question, calculations were necessary in order to determine the rate of transport of the

isotope. Worksheets were set up to aid in the calculations, as shown in Figures A-4 and A-5 in the Appendix. The worksheet shown in Figure A-4 was used to calculate a transport rate for a drug when a single isotope was used (either ^{14}C or ^{3}H in these experiments) or for a ^{14}C-labelled drug when the two isotopes were used. Figure A-5 shows the worksheet employed in calculating the transport rate for a ^{3}H-labelled drug in the presence of a ^{14}C-labelled drug. The net cpm's of the mucosal samples were averaged and this value set equal to 1000 μ units per ml, as shown in the upper portion of Figures A-4 and A5. The concentrations calcuated for the serosal samples are related to the mucosal samples by this factor and are essentially percentages of the mucosal concentration.

When two isotopes were run in these experiments, there was a slight modification in the calculation of transport of the ^{3}H-labelled drug. The techniques for double isotope counting are such that the tritium activity can be essentially excluded from the ^{14}C-channel. However, the low energy or tritium channel will register counts due to both isotopes. If a sample containing only ^{14}C-labelled material (no tritium present) is read in both the low and high energy channels, then the cpm's due to the ^{3}H-sample can be calculated by the following relationships:

$$N_1 = C_1 + H_1 \qquad \text{(Eq. 13)}$$

$$N_2 = C_2 \qquad \text{(Eq. 14)}$$

$$H_1 = N_1 - \frac{N_2}{b} \qquad \text{(Eq. 15)}$$

$$b = \frac{C_2}{C_1} \qquad \text{(Eq. 16)}$$

where

N_1 = net cpm in channel 1 (tritium channel)

N_2 = net cpm in channel 2 (^{14}C-channel)

C_1 = net cpm due to ^{14}C in channel 1

C_2 = net cpm due to ^{14}C in channel 2

H_1 = net cpm due to ^{3}H in channel 1

Once the values for H_1 have been calculated, then the procedure for the rest of the calculations for determining the transport rate of the tritium isotope follow the same format as for the ^{14}C-isotope.

In order to calculate the amount transported per ml in each time interval as shown in both worksheets, the dilution due to sampling must be taken into account. In the first interval, the calculated concentration of the sample is equal to the amount/ml transported in that interval. However, the concentration of this first sample must now be corrected for the added buffer by multiplying by 0.9 which is the fraction of the volume remaining after a sample is taken. This new concentration is then subtracted from the concentration of the second interval and this is the amount/ml transported for the second interval. This procedure continues as such for all the intervals, and since there is a volume of 10 ml, multiplying by 10 and summing the intervals gives the cumulative amount transported. If

C_1 = concentration of serosal sample 1 (in μ units/ml for time interval 1)

C_2 = concentration of serosal sample 2 (in μ units/ml for time interval 2)

C_3 = concentration of serosal sample 3 (in μ units/ml for time interval 3)

C_i = concentration of serosal sample i (in μ units/ml for time interval i)

then

A_i = cumulative amount transported from zero time to the i^{th} interval (in μ units).

It follows that

$$A_i = 10\,C_1 + 10\,(C_2 - .9C_1) + 10\,(C_3 - .9C_2) + \cdots + 10\,(C_{i+1} - .9C_i) \qquad \text{(Eq. 17)}$$

and

$$A_n = 10\,C_1 + 10 \sum_{i=2}^{n} (C_i - .9C_{i-1}) \qquad \text{(Eq. 18)}$$

and the general equation can be stated as

$$A_n = V\,C_1 + V \sum_{i=2}^{n} \left(C_i - \frac{V_r}{V}\,C_{i-1}\right) \qquad \text{(Eq. 19)}$$

where

V = volume of medium perfusing the serosal surface (in ml)

V_r = volume of perfusion medium remaining after a sample is taken.

A plot was then made for the cumulative amount transported vs time. The slope of this graph is the rate of flux of the isotope from mucosa to serosa. The 20 minute sample for ^{14}C-salicylate flux studies was the earliest time point taken in the slope calculations since there is a lag period in the transport of salicylate and steady state transport must be reached.

In these experiments, $J_{m \rightarrow s}$ is the slope of this graph and is the unidirectional flux of isotope from mucosa to serosa (in $\frac{\mu \text{ units}}{\text{hr. cm}^2}$). This flux constant can be expressed as follows:

$$J_{m \rightarrow s} = \frac{\Delta A_n}{\Delta t_n} \frac{1}{S} \qquad \text{(Eq. 20)}$$

where

S = surface area of tissue exposed to transport (1.12 cm^2).

The flux rates for all experiments were determined using a weighted linear least squares regression program. The weighting factor was taken as the inverse squared of the dependent variable, i.e., the cumulative amount transported. A nonweighted linear least squares regression was also run for each set of data and excellent agreement was found between the weighted and nonweighted results because of the good fit of the data.

Control and Experimental Conditions

In an attempt to eliminate tissue-to-tissue and animal-to-animal variation, each tissue segment served as its own control and transport rates were measured under both control and experimental conditions. Control conditions for the experiments reported here used tissue maintained at I_{sc} where no perturbers or inhibitors were added to either solution bathing the tissue. Experimental conditions included the addition of glucose (to both mucosal and serosal solutions, to maintain iso-osmolarity, although the addition of glucose to the mucosal side alone should have been sufficient to exert a response), the addition of serosal ouabain to buffer solutions with and without sodium ions, and the addition to the mucosal perfusion solution of various concentrations of unlabelled sodium salicylate. Control and experimental transport rates were calculated separately using the linear least squares regression program. The computed transport rates were then compared using a paired t-test which

indicated whether there were any significant differences in the rates of transport due to the addition of the various agents. The use of each tissue segment as its own control decreases the amount of variation often seen in biological preparations.

Similar analyses were run on the data from the potential difference experiments. The control condition in this case was again the determination of drug flux under the short circuit condition, while the experimental condition was the determination of drug flux when a large positive or negative potential was imposed across the tissue. The fluxes of salicylate, antipyrine, and butanol were determined at I_{sc} (PD = 0) and at various imposed PD's. Each of the transport rates was calculated separately with the linear least squares regression program. The computed transport rates from these experiments were then treated in a similar fashion as the control and experimental transport rates discussed above.

RESULTS

Control Conditions

Initial experiments were run with stripped and unstripped tissues. Only electrical parameters were monitored. As expected, it was noted that both the transmural PD and I_{sc} were higher in stripped tissue than in unstripped tissue. Calculated tissue resistance for the unstripped preparation ranged from 40 to 60 ohms while the stripped jejunum had an electrical resistance range of 15 to 25 ohms. It appeared that the stripped tissue was viable for a longer period of time, although no formal studies were run to corroborate this observation.

Tissues used for all subsequent experiments were stripped of serosa and muscularis externa. Stripped and unstripped rabbit ileum have been compared as to I_{sc}, ionic permeability, and rate of deterioration (20). Field *et al.* (20) found that the stripped preparation gave rise to a higher and more stable I_{sc}, and its response to the addition of glucose was substantially greater. They found that the electrical resistance of the stripped tissue was about half that of the full thickness ileum. The lowering of the electrical resistance was associated with an increase in the magnitudes of the unidirectional sodium ion and chloride ion fluxes as well as a more rapid approach of their fluxes to steady state. Wolfe *et al.* (105) found different rates of absorption for salicylate in everted sac preparations that had been stripped of serosa and muscularis externa as compared to the unstripped preparation. The initial experiments performed in this study showed trends similar to that of Field *et al.* (20) with respect to a higher I_{sc} for stripped tissue *vs* unstripped tissue (Field: 61 μA and 21 μA, respectively; this work: ~240 μA and 160 μA, respectively) and a lower transmural resistance for stripped tissue in comparison to unstripped rat jejunum (Field: 45 Ω-cm^2 and 89 Ω- cm^2, respectively; this work: 22 Ω- cm^2 and 56 Ω-cm^2,

respectively).

Figure 10 is a composite graph of the three electrical parameters for one tissue of rat jejunum monitored over time. Zero time is taken as the death of the animal. The transmural PD, or E_m, is plotted in Graph A with the serosal surface positive with respect to the mucosal surface. The I_{sc} and R_m values are shown in Graphs B and C, respectively. There is normally a slight decline in PD and I_{sc} with time due to slow tissue deterioration. However, on the whole, the three parameters are reasonably stable over the time course of the experiment.

A sample mucosa to serosa flux of ^{14}C-salicylate, $J^{SA}_{m\rightarrow s}$, (at ΔPD = 0) is shown in Figure 11. This is the result of a typical experiment run using the procedures described previously. Tracer was added to the mucosal reservoir and its appearance in the serosal compartment determined. There was an initial lag period for the transport of salicylate, but $J^{SA}_{m\rightarrow s}$ was independent of time after an initial period of less than 20 minutes. In this plot, time zero is taken at the introduction of the radioisotope into the buffer solution perfusing the mucosal side of the tissue. Constant electrical parameters were attained before the introduction of isotope. The cumulative amount transported is plotted in units of μ units/cm^2 as described in Experimental. The slope of this graph yields the transport rate constant. The 20 minute sample is the first time point taken in the calculation of the flux constant.

Potential Difference Changes

Changing the transmural PD changes the transport rate of

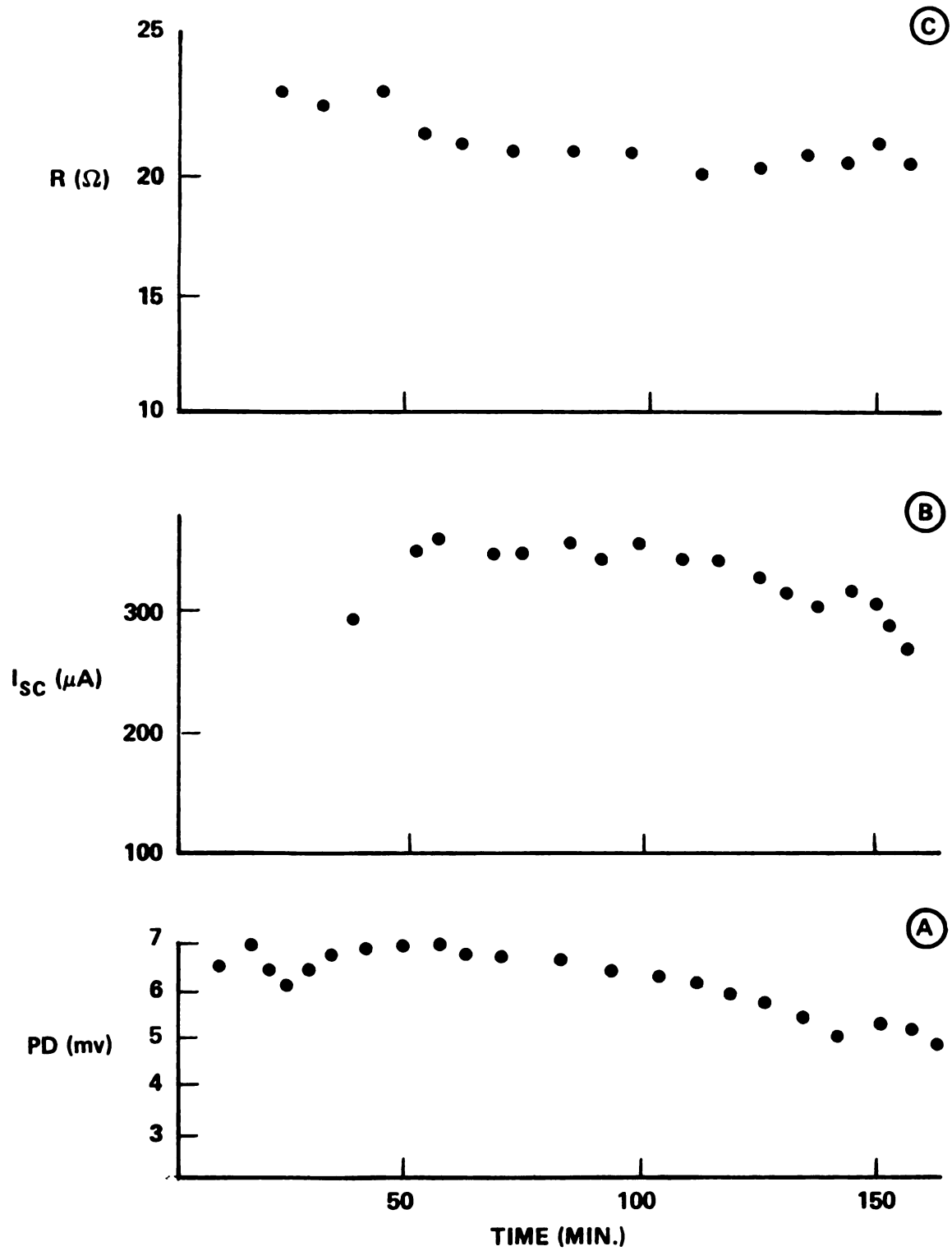

Figure 10. Composite graph of transmural electrical parameters of stripped rat jejunum.
The three parameters were monitored in one tissue
A: Transmural PD
B: Transmural I_{sc}
C: Transmural R

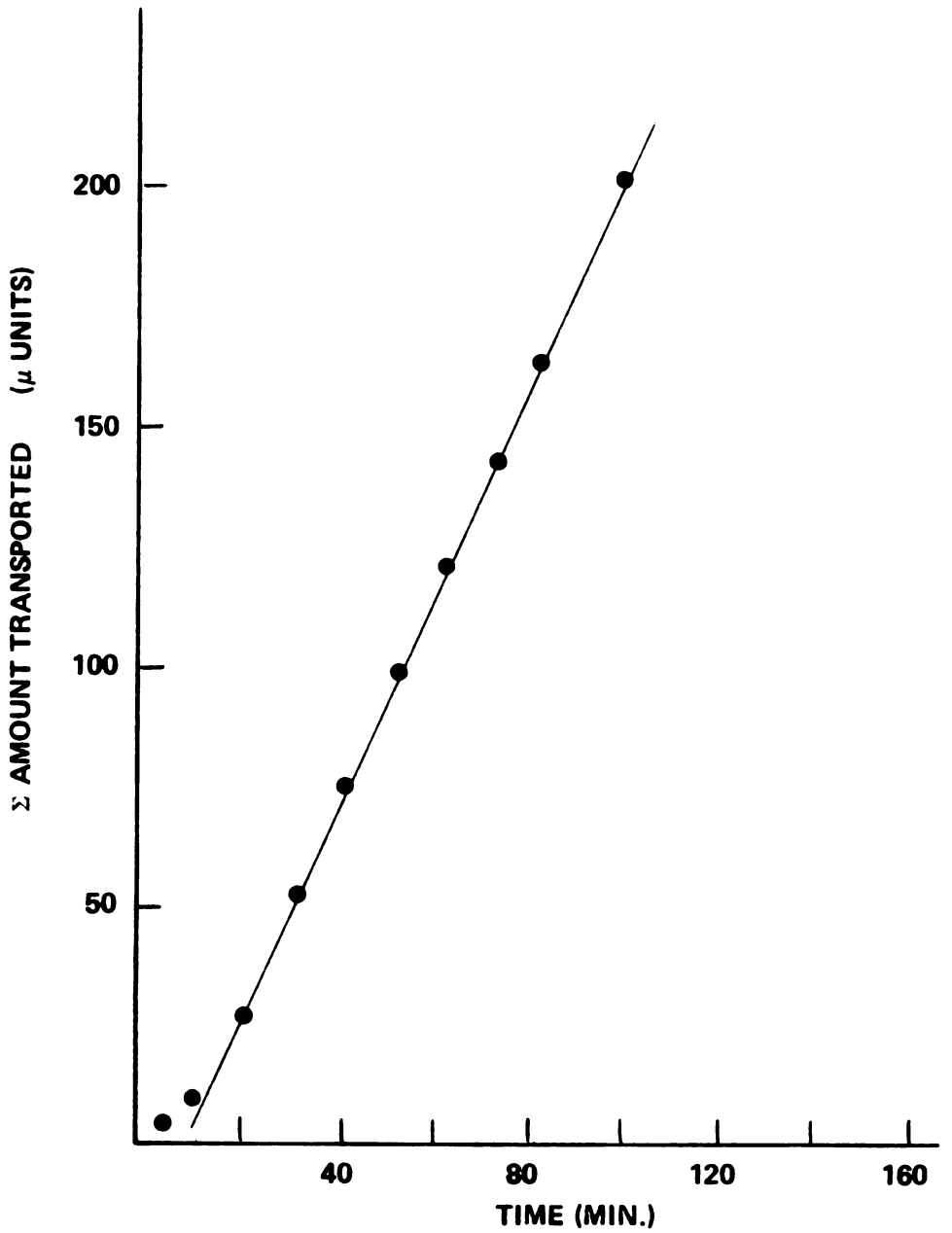

Figure 11. Plot of M-to-S flux of ^{14}C-salicylate under control conditions. The result of a typical experiment using procedures described in text.

salicylate. Cumulative transport of salicylate and antipyrine and the effect of a change in transmural PD are shown in Figure 12. This plot exemplifies an experiment where two drug fluxes across a single tissue are measured simultaneously. Initially the tissue was maintained at I_{sc} (Δ PD = 0 and E_{vc} = 0), then the imposed PD across the tissue was increased to +20 mv for 50 minutes. In the third stage of this experiment, the transmural PD was decreased to -45 mv for 50 minutes. Antipyrine, which exhibits a faster rate of transport than salicylate, was hardly affected by the changes in the imposed potential in this experiment; whereas, there were definite changes in salicylate flux, which corresponded with the transmural PD changes.

In some experiments, however, when the maximum positive PD was imposed across the tissue, antipyrine flux did change, but in the opposite direction to that of salicylate. Initial experiments were run to determine whether salicylate or antipyrine might affect the transport rate of the other compound. No interactive effects were found for the transport of salicylate at short circuit current (or at maximum positive and negative imposed transmural PDs) as seen in Table IV. Antipyrine flux was somewhat higher in the absence of salicylate than in the presence of equimolar salicylate. However, only five tissues were used and four of the tissues were from the same animal. The fluxes of ^{3}H-antipyrine from that one animal were higher than other ^{3}H-antipyrine fluxes observed, and it was assumed that the presence of salicylate did not cause any interactive effects on the transport of antipyrine.

Figure 13 depicts a study where the transport of ^{14}C-salicylate was investigated under four different experimental

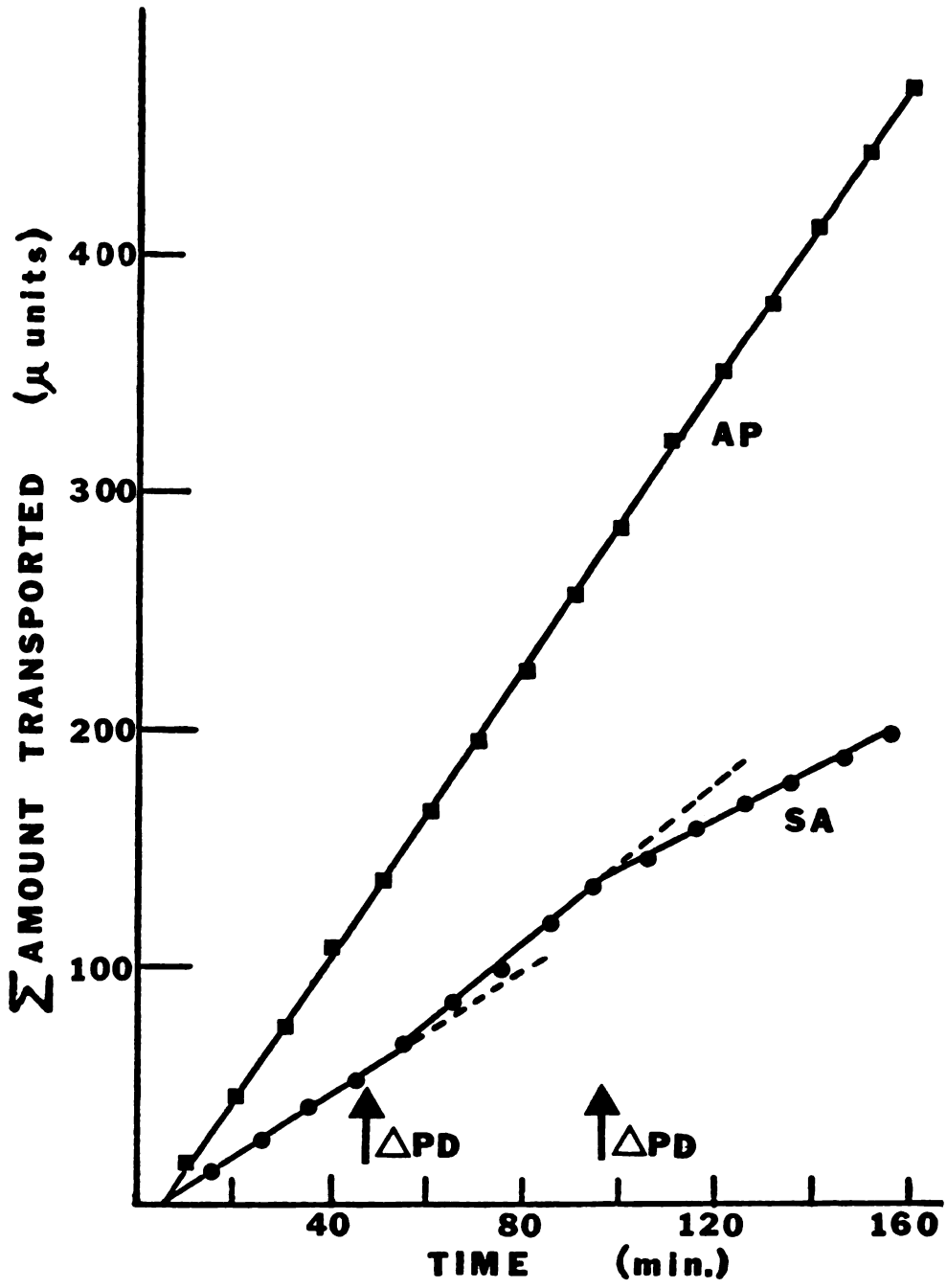

Figure 12. Effect of transmural PD on ^{14}C-salicylate flux and ^{3}H-antipyrine flux. The results of a typical experiment using one tissue with the two drug fluxes measured simultaneously. At the arrows the transmural PDs were changed.

Table IV

Effect of Antipyrine on ^{14}C-Salicylate Flux

and

Effect of Salicylate on ^{3}H-Antipyrine Flux

	- Antipyrine	+ Antipyrine
$J^{SA}_{m \rightarrow s}$	84.9* ± 2.6 (SEM) (n = 18)	84.8 ± 4.0 (n = 18)
unpaired t-test:	Not significant at 20% confidence interval $p > 0.8$	

	- Salicylate	+ Salicylate
$J^{AP}_{m \rightarrow s}$	190.3 ± 13.5 (n = 5)	153.4 ± 5.4 (n = 12)
unpaired t-test:	$.01 > p > .005$	

* units of flux = $\frac{\mu \text{ units}}{\text{hr. cm}^2}$ (where the mucosal concentration = 1000 μ units/ml)

conditions. Initially, the tissue was short circuited (ΔPD = 0), then the transmural PD was increased to +90 mv and a subsequent increase in the salicylate flux was observed. The imposed transmural PD was next set at -75 mv, and a concomitant decrease in salicylate flux occurred. It was noted that the ^{14}C-salicylate flux under a negative transmural PD was lower than the flux when the tissue was short circuited. In the fourth stage of the experiment, the tissue was returned to the initial conditions of ΔPD = 0, at the short-circuited state. The flux of ^{14}C-salicylate during this fourth condition was essentially the same as the flux determined during the initial measurement, where the tissue was under the short-circuit condition in each case. This similarity indicates that the tissue was not damaged by the imposed conditions, and that the different fluxes observed at positive and negative PDs were not artifacts of irreversible tissue damage.

It is possible that the permeability of the tissue may have been altered by the imposed PD. Studies on toad bladder (110) have shown a change in tissue resistance at higher PDs. Increasingly large hyperpolarizations resulted in the appearance of a transition point in the current-voltage relationship, beyond which the resistance (slope) abruptly increased. A similar effect was noted with frog skin by Mandel and Curran (111). By measuring the flux of urea during these PD changes and noting changes in urea flux, Mandel and Curran found that the permeability of frog skin was altered during the imposition of large positive and negative PDs. The effect of varying the current on the stripped jejunal tissue segment was checked in the present study. The transmural PD ranged from +80 mv to

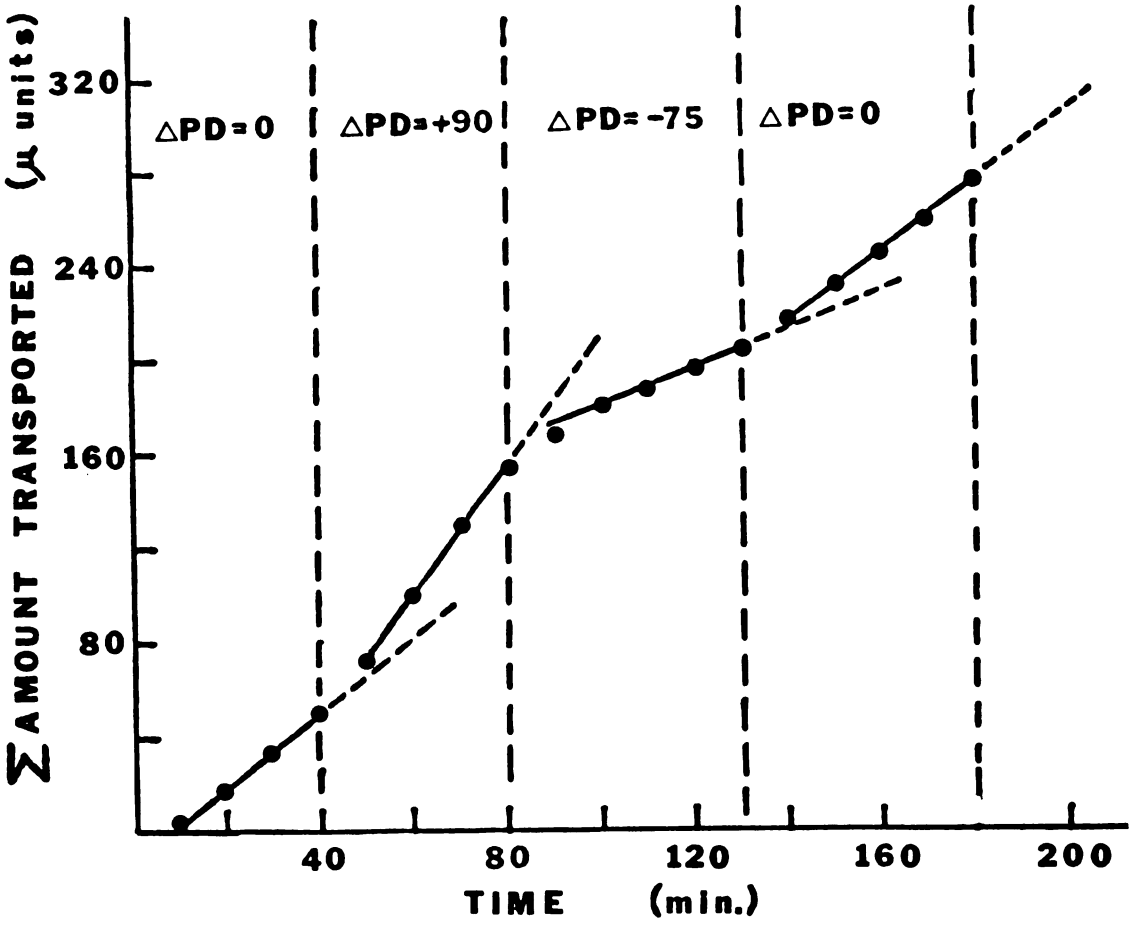

Figure 13. Effect of transmural PD on ^{14}C-salicylate flux (four conditions). The results of a typical experiment using one tissue.

-80 mv and the resistance of the tissue was constant over the entire range. This showed that the tissue acted as a linear resistor over the range studied and that there was no change in tissue resistance and, hence, in tissue permeability due to the imposed PD over the range studied. Other studies have also shown mammalian intestine to behave as a linear resistor (19, 20, 43).

Table V lists the ^{14}C-salicylate transport constants at the different transmural PDs of the four conditions of this experimental design, with averages and standard errors given. The transport rates from experiments run at all positive transmural PDs were lumped together, with similar average values presented for the experiments at all negative transmural PDs. The actual values of the transmural PDs covered a range of approximately 15-90 mv for each of the positive and negative changes. The individual ^{14}C-salicylate transport rates corresponding to specific imposed transmural PDs found in these experiments are subsequently treated in Discussion where various relationships and theories are presented. A paired t-test was used to indicate that the fluxes at the different negative and positive PDs were significantly different from each other and from the fluxes at I_{sc}. The flux under short-circuit conditions at the end of the experiment was not significantly different from the flux under the same conditions at the beginning of the experiment as shown by the level of significance determined from the paired t-test. Data from similar experiments, where only the first three conditions were imposed on the tissue, are shown in Table VI. The tissue was not returned to the final short circuited condition, since it was shown in the previous series of

Table V

Effect of Transmural Potential Difference on ^{14}C-Salicylate Flux
(Four Conditions)

$J_{I_{sc}}$ (initial)	88.7* ± 3.1 (SEM)
$J_{-\Delta PD}$	58.7 ± 2.8
$J_{+\Delta PD}$	150.5 ± 3.1
$J_{I_{sc}}$ (final)	91.3 ± 4.9

by paired t-test

$p < 0.001$

for all sets of pairs except $J_{I_{sc}}$ (initial) and $J_{I_{sc}}$ (final)

$0.2 > p > 0.1$

n = 10 tissues (three animals)

* $\frac{\mu \text{ units}}{\text{hr. cm}^2}$ (where the mucosal concentration = 1000 μ units/ml)

I_{sc} = at short-circuit current

$-\Delta PD$ = at negative imposed transmural potential difference

$+\Delta PD$ = at positive imposed transmural potential difference

Table VI

Effect of Transmural Potential Difference on ^{14}C-Salicylate Flux (Three Conditions)

$J_{I_{sc}}$	83.0* ± 3.5 (SEM)
$J_{-\Delta PD}$	58.6 ± 3.9
$J_{+\Delta PD}$	122.4 ± 7.2

$P < 0.001$ by paired t-test for all sets of pairs

n = 20 tissues (six animals)

* $\frac{\mu \text{ units}}{\text{hr. cm}^2}$ (where the mucosal concentration = 1000 μ units/ml)

I_{sc} = at short-circuit current

$-\Delta PD$ = at negative imposed transmural potential difference

$+\Delta PD$ = at positive imposed transmural potential difference

experiments that the tissue was still viable and responding as expected. Again, it is seen that the fluxes are all significantly different from each other. Table VII lists the antipyrine flux data under the various imposed PDs. A paired t-test showed there was some significant differences between the three transport rates, but the changes in the antipyrine flux were not as large as the salicylate flux alterations due to various imposed transmural PDs.

^{14}C-Butanol Flux

Because a small change in antipyrine flux was noted when the maximum positive transmural PD was imposed across the tissue, experiments were undertaken to determine the flux of ^{14}C-butanol at maximum positive and negative transmural PDs. Butanol was chosen because it is not ionized and because it is characteristic of high lipid - low water soluble compounds. During the first series of experiments, it was found that the mucosal concentration of ^{14}C-butanol did not stay constant, as the mucosal concentration of the radioisotopes did in all the other experiments. In the next set of experiments involving ^{14}C-butanol, the mucosal side was monitored more frequently than usual in order to try to characterize this change in the mucosal isotope concentration. Figure 14 shows the change in the mucosal concentration of ^{14}C-butanol with time. It appeared that ^{14}C-butanol was lost from the mucosal perfusing solution by a first order process.

A plot of the cumulative amount of ^{14}C-butanol transported vs time was not a linear function (as observed in the studies with ^{14}C-salicylate and ^{3}H-antipyrine), but rather appeared to approach an asymptotic value as can be seen in Figure 15. The

Table VII

Effect of Transmural Potential Difference on ^{3}H-Antipyrine Flux (Three Conditions)

$J_{I_{sc}}$	152.2* ± 5.1 (SEM)
$J_{+\Delta PD}$	138.5 ± 7.1
$J_{-\Delta PD}$	169.2 ± 5.8

n = 13 tissues

paired t-test

$J_{I_{sc}}$	&	$J_{+\Delta PD}$	$.05 > p > .02$
$J_{I_{sc}}$	&	$J_{-\Delta PD}$	$p < .001$
$J_{+\Delta PD}$	&	$J_{-\Delta PD}$	$p < .001$

* $\frac{\mu \text{ units}}{\text{hr. cm}^2}$ (where the mucosal concentration = 1000 μ units/ml)

I_{sc} = at short-circuit current

$-\Delta PD$ = at negative imposed transmural potential difference

$+\Delta PD$ = at positive imposed transmural potential difference

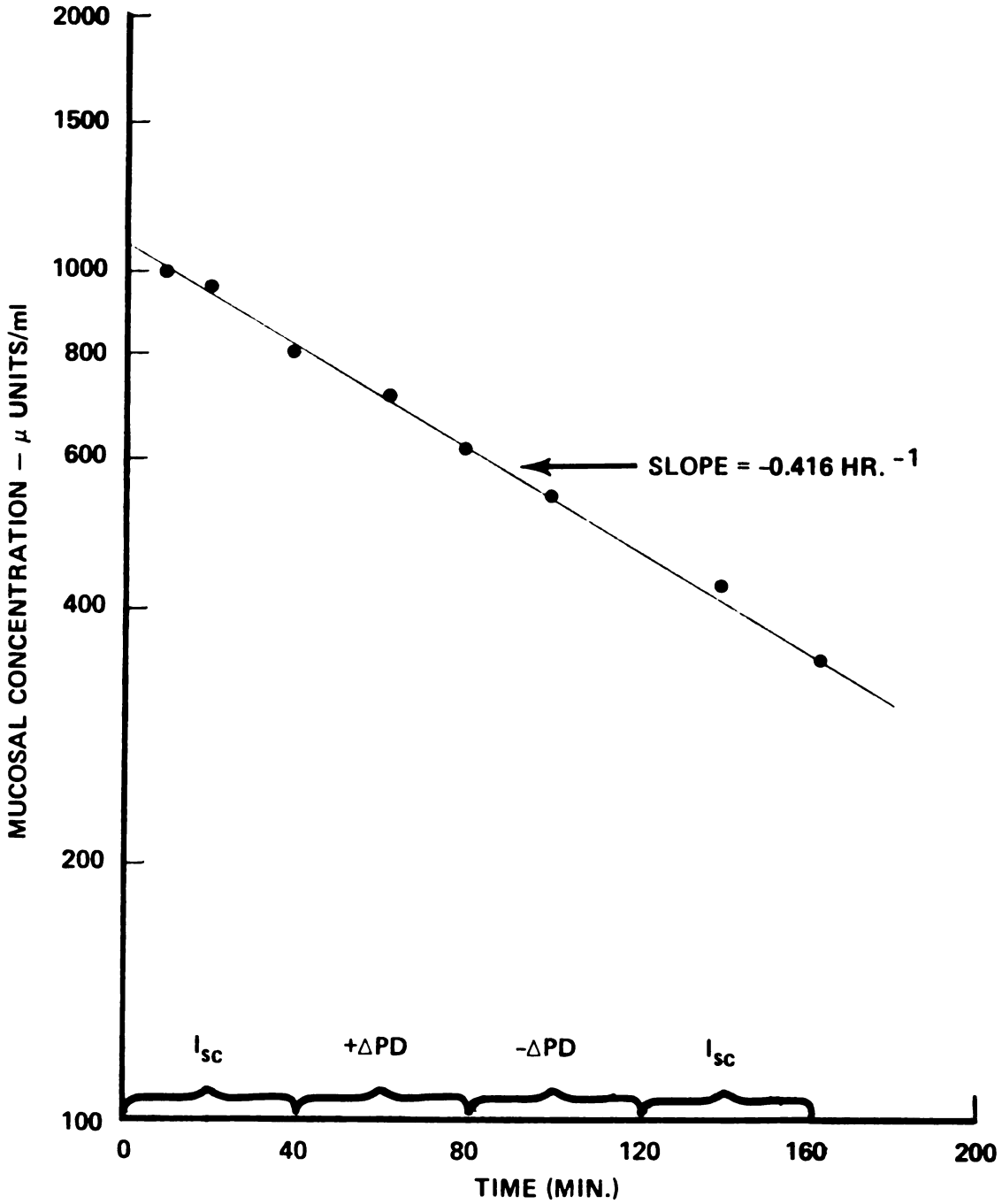

Figure 14. Change of mucosal concentration of ^{14}C-butanol with time during ΔPD experiments. The results of a typical experiment using one tissue maintained at various PDs: at ΔPD = 0 (I_{sc}); at maximum positive PD (+ΔPD); at maximum negative PD (-ΔPD).

serosal perfusion solution sampling scheme was maintained at ten minute intervals through these experiments. The tissue potential was maintained at the following four conditions: initially at I_{sc}, at maximum positive transmural PDs, at maximum negative transmural PDs, and finally again at I_{sc}. These conditions and their intervals are also shown in Figure 15.

Since the experiments were run at 37° C, the possibility of the ^{14}C-butanol vaporizing from the buffer solution in the water-jacketed glass towers was investigated. To further determine this change in isotope concentration, the glass towers were set up without the chambers or tissues present. The inlet and outlet tubing at the bottom of each tower were connected together to allow circulation of the buffer solution to occur. Various concentrations of ^{14}C-butanol were placed in each tower. Five samples were taken from each tower over a 90 minute interval. The first order rate constant describing the changes in concentration of ^{14}C-butanol varied from 0.22 hr.$^{-1}$ to 0.27 hr.$^{-1}$.

To interpret the results of the ^{14}C-butanol experiments, it was necessary to formulate the following model:

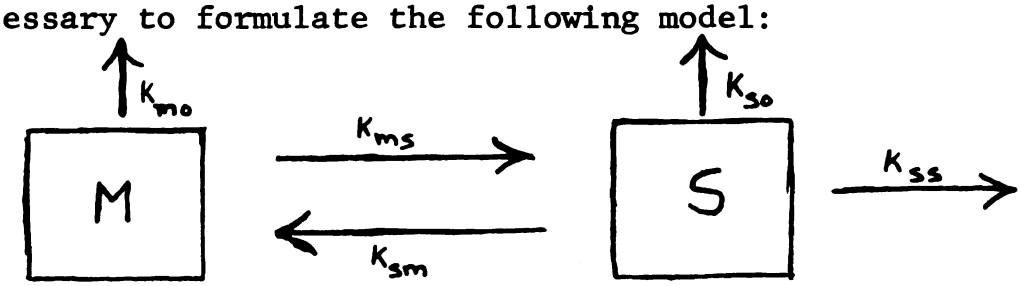

where

M = the mucosal compartment, with 10 ml volume

S = the serosal compartment with 10 ml volume

k_{mo} = the first-order rate constant due to evaporative loss from the mucosal compartment

k_{so} = the first-order rate constant due to evaporative loss from the serosal compartment

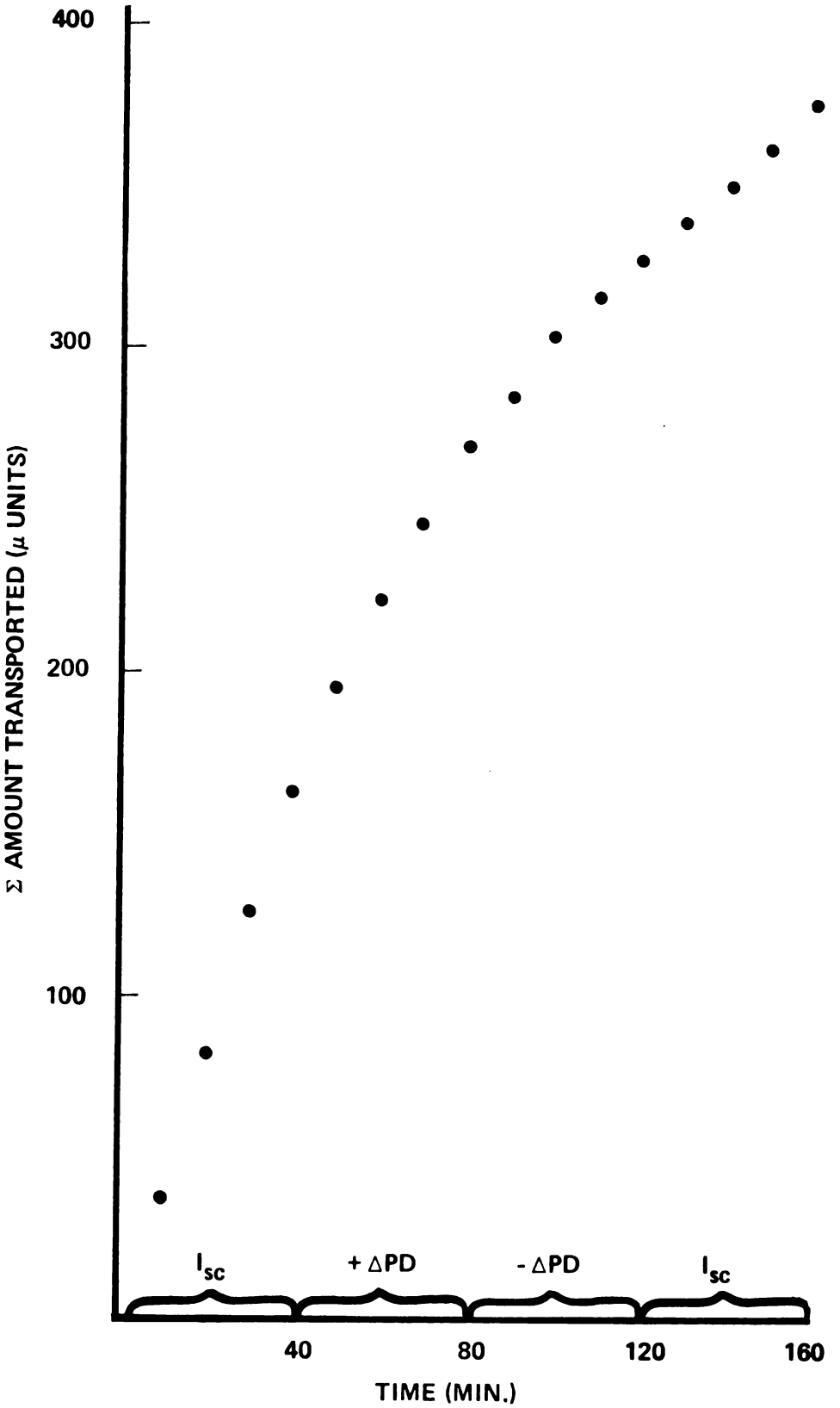

Figure 15. Cumulative amount of ^{14}C-butanol transported with time during ΔPD experiments. The results of a typical experiment using one tissue, maintained at various PDs: at ΔPD = 0 (I_{sc}), at maximum positive PD (+ΔPD), at maximum negative PD (- ΔPD).

k_{ms} = the first-order rate constant describing the mucosal to serosal flux

k_{sm} = the first-order rate constant describing the serosal to mucosal flux

k_{ss} = the first-order rate constant describing the loss from the serosal compartment due to sampling. (Although loss is actually discontinuous, it may be approximated by a log-linear function.)

It was assumed that the sampling from the mucosal compartment was insignificant, since the sample size was 0.1 ml and only nine samples were taken over the three hour period. Nothing was added back to the mucosal compartment; therefore, the concentration of this compartment was not affected by the sampling. On the other hand, the serosal samples were 1.0 ml, from a 10 ml volume, with samples taken every ten minutes.

What is of interest in this problem is determining if k_{ms} changed when the transmural PD was changed. Another way to determine the effect of the imposed transmural PD would be to plot the actual cumulative amount transported from M→S *vs* time, as in previous experiments as shown in Figures 12 and 13. The value for k_{mo} and k_{so}, which are equal, was determined by experiment and found to be 0.24 ± 0.01 hr.$^{-1}$. A value of 0.42 ± 0.05 hr.$^{-1}$ was found for the slope of the log-linear plot of the mucosal concentration of ^{14}C-butanol with time. The differential equation for the mucosal concentration changing with time is $\frac{d[M]}{dt} = -(k_{mo} + k_{ms})[M] + k_{sm}[S]$, or $\frac{d[M]}{dt} = -k_M[M] + k_{sm}[S]$, where $k_M = k_{mo} + k_{ms}$. Since the value of the slope is about twice the value of k_{ms} and [M] is always maintained much larger than [S], the product of $k_M[M] \gg k_{sm}[S]$, and thus the equation may be approximated as a monoexponential relationship, $\frac{d[M]}{dt} \cong -k_M[M]$. Thus, $k_{ms} = k_M - k_{mo}$, values that have been determined, and

k_{ms} = 0.18 $hr.^{-1}$. Furthermore, because the mucosal concentration *vs* time plot was a straight line, this suggested that k_{ms} did not change over the time interval investigated due to the imposed transmural PD.

Intracellular pH

For this series of experiments, 39 tissues from ten animals were used as shown in Table VIII. If the calculated values of the pH_i's of all 39 tissues are averaged, the pH_i equals 7.32 $\pm$ 0.04 (SEM). Six tissues from four animals were maintained at large positive imposed transmural PDs, and the pH_i's averaged 7.44 $\pm$ 0.03. Similarly, the calculated pH_i's of six tissues from four animals kept at maximum negative imposed transmural PDs averaged 7.39 $\pm$ 0.05. The average pH_i of the 27 remaining tissues all maintained at I_{sc} equalled 7.27 $\pm$ 0.05. Using only those experiments where among the four tissues all three conditions were imposed, that is positive and negative PDs as well as I_{sc} (Experiments B and C on October 22 and the Experiment on October 4), no significant difference between pH_i for the three treatments was observed. It was noted that a trend toward increasing pH_i values was seen over the two-month period during which these studies were conducted. No adequate explanation of this effect is apparent.

Ouabain Addition

The electrical properties of the rat jejunum before and after the addition of serosal ouabain are shown in Figure 16, which is a composite graph of the three monitored electrical parameters. In these plots, zero time is taken at the death

Table VIII

Results of Intracellular pH Experiments

Date	Chamber	pH_i	Avg.	Date	Chamber	pH_i	Avg.
8/31/73	2	6.86		10/3/73	1 (-ΔPD)	7.22	
	3	6.87	6.88		2 (-ΔPD)	7.34	7.34
	4	6.91			3 (+ΔPD)	7.46	
					4 (+ΔPD)	7.35	
9/1/73A	1	7.17		10/4/73	1 (-ΔPD)	7.29	
	2	7.27	7.12		2	7.38	7.36
	3	7.04			3 (+ΔPD)	7.37	
	4	7.00			4	7.39	
9/1/73B	1	7.27		10/22/73A	1	7.47	
	2	7.18	7.16		2	7.48	7.51
	3	7.18			3	7.58	
	4	7.01			4	7.51	
9/25/73	1	7.39		10/22/73B	1	7.56	
	2	7.34	7.40		2 (+ΔPD)	7.55	7.53
	3	7.02			3 (-ΔPD)	7.52	
	4	7.85			4 (-ΔPD)	7.50	
9/28/73	1	7.35		10/22/73C	1 (+ΔPD)	7.38	
	2	7.39	7.30		2 (-ΔPD)	7.49	7.46
	3	7.24			3	7.43	
	4	7.23			4 (+ΔPD)	7.52	

-ΔPD = negative imposed transmural potential difference

+ΔPD = positive imposed transmural potential difference

all other tissues maintained at I_{sc}

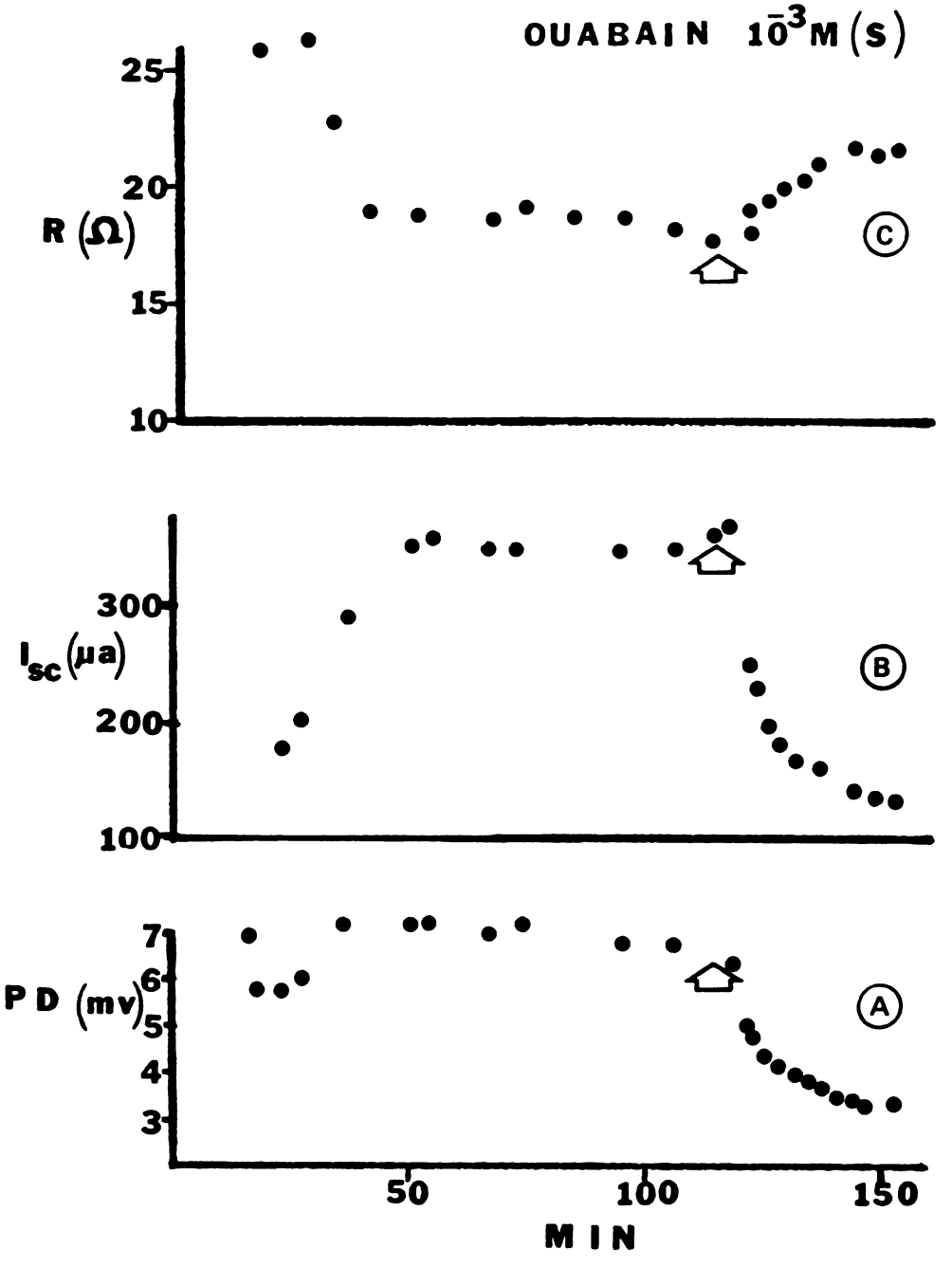

Figure 16. Effect of serosal ouabain addition on the transmural electrical parameters of stripped rat jejunum at I_{sc}. The three parameters were monitered in the same tissue. At the arrow ouabain (1×10^{-3}M) was added to the serosal solution.

A: transmural PD
B: transmural I_{sc}
C: transmural R

of the animal. The transmural PD, in millivolts, was plotted *vs* time in Graph A. At the arrow, ouabain ($1x10^{-3}M$) was added to the serosal perfusing solution. An immediate decrease in the potential was observed. In Graph B, I_{sc} was plotted in units of microamperes. After the introduction of ouabain, this parameter also showed an immediate and permanent (rather than transient) decrease. While the I_{sc} started to decrease immediately, it did take some time to reach a steady plateau level. This was the classical effect of ouabain on the transmural PD and I_{sc} of epithelial tissue. Graph C in Figure 16 shows the calculated ohmic resistance of the tissue plotted *vs* time. Again, there was a change in this parameter after the addition of ouabain; in this case an increase was observed. The peak of this increase occurs 25 to 30 minutes after the ouabain introduction.

Experiments were run to see the effect on the tissue of washing out the ouabain. Figures 17 and 18 are examples of the results of this study. Note that after the washout of ouabain, the transmural PD (Figure 17) and I_{sc} (Figure 18) reached a peak and then continued the slow decline normally seen with the aging of the preparation (as observed in Figure 10, A and B). Therefore, these parameters approached the values extrapolated previous to the ouabain addition. This indicated that the action of ouabain was reversible under the conditions of concentration used and the time period during which the tissue was exposed to ouabain.

The mucosa to serosa flux of ^{14}C-salicylate, $J^{SA}_{m \rightarrow s}$, was determined before and after the addition of serosal ouabain. The cumulative amount transported *vs* time was plotted in Figure 19, with the arrow indicating the time of serosal ouabain addition.

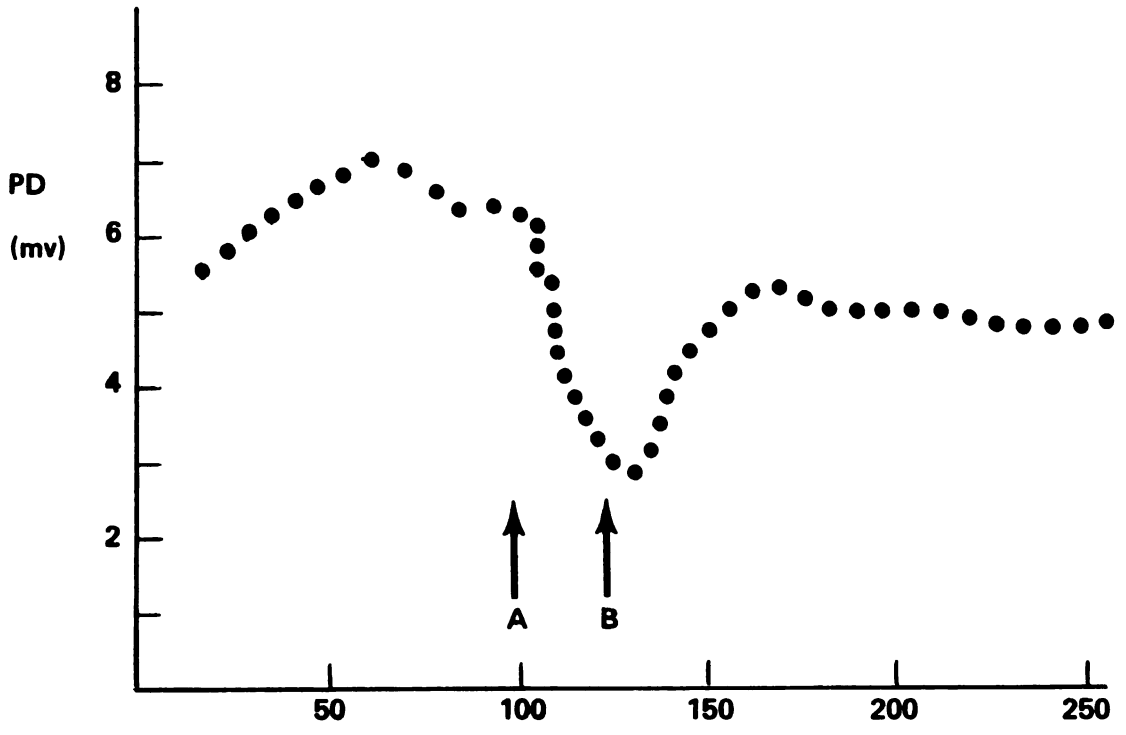

Figure 17. Effect of serosol ouabain addition and washout on transmural PD. The results of a typical experiment. At arrow A ouabain (1 x 10^{-3}M) was added to the serosal solution. At arrow B the serosal solution was drained, ouabain washed out and the serosal solution replaced with K-H buffer.

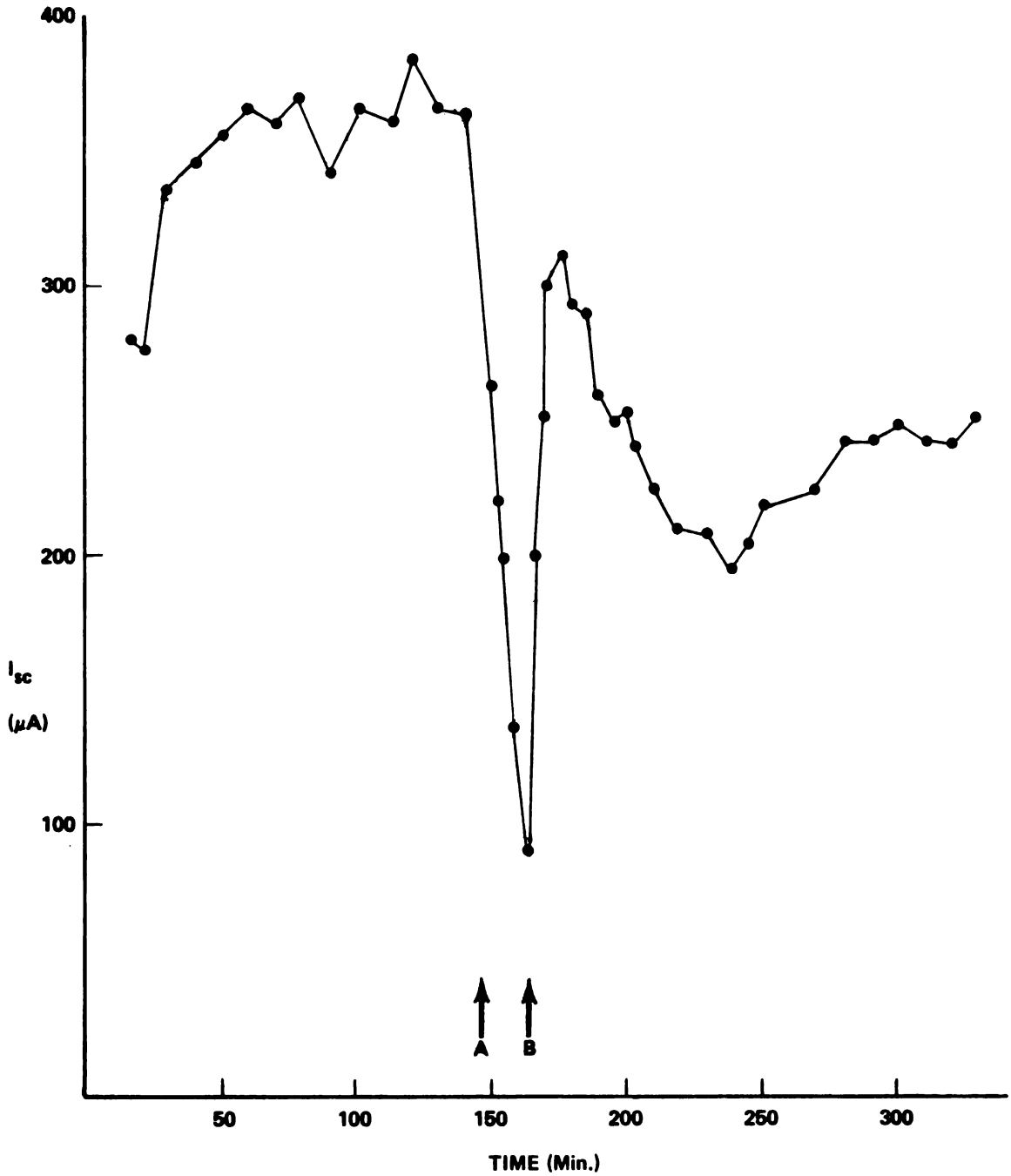

Figure 18. Effect of serosal ouabain addition and washout on transmural I_{sc}. The results of a typical experiment. At arrow A ouabain (1×10^{-3}M) was added to the serosal solution. At arrow B the serosal solution was drained, ouabain washed out and the serosal solution replaced with K-H buffer.

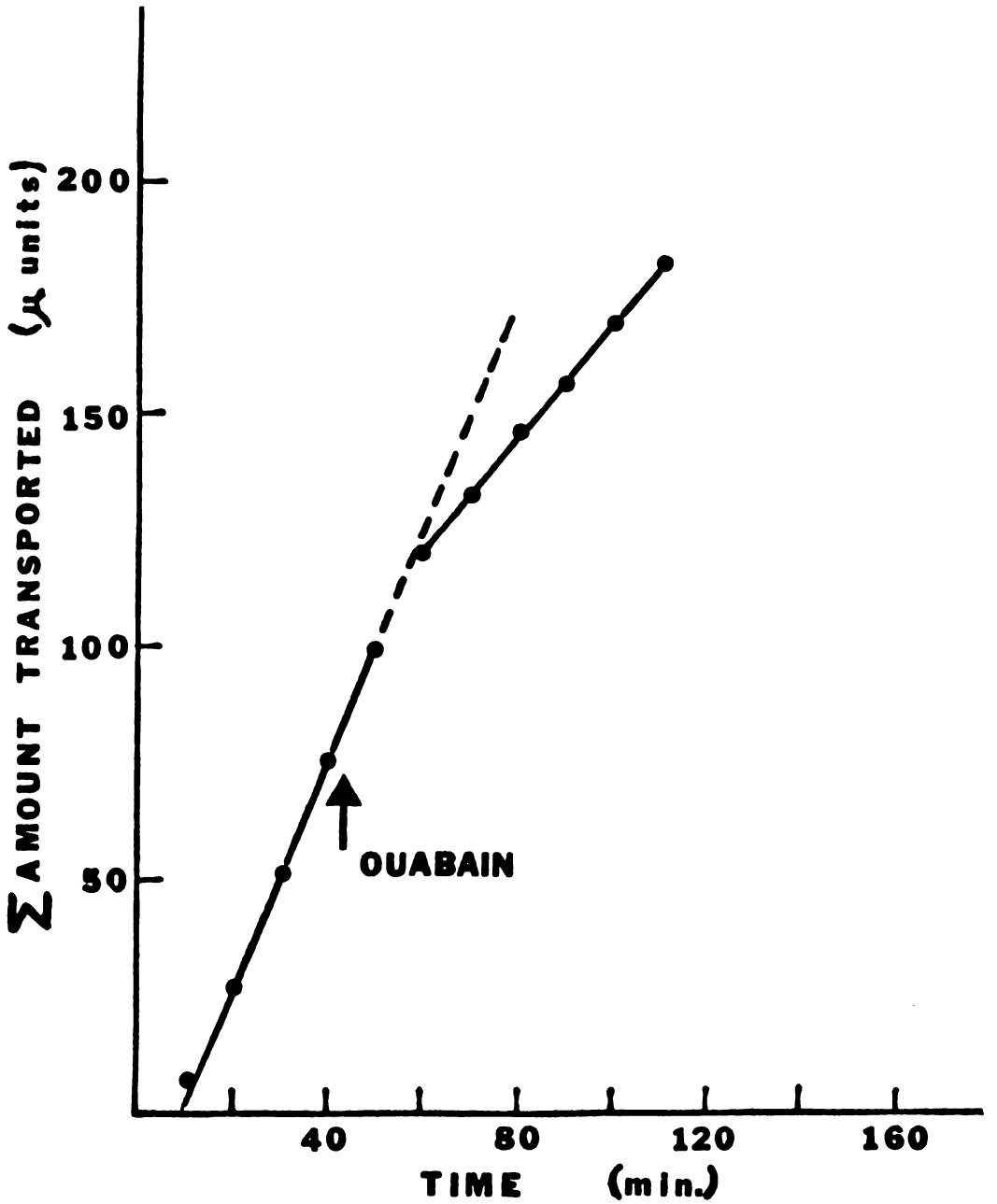

Figure 19. Effect of serosal ouabain addition on ^{14}C-salicylate flux at I_{sc}. The results of a typical experiment. At the arrow ouabain (x x 10^{-3}M) was added to the serosal solution.

The slopes of this graph yield the transport rate constants. In this plot, time zero is taken as the time of introduction of the radioisotope into the buffer solution perfusing the mucosal side of the tissue. Constant electrical parameters were attained before the introduction of the radioisotope. The addition of ouabain produced a definite change in the slope of this plot, and this change became apparent 20 to 40 minutes after the addition. Control experiments were run with tissues to which no ouabain had been added and there was no change in transport of salicylate, and, in fact, the flux followed the dotted line in the graph. This is well illustrated by the data in Table IX.

This experimental technique allows the use of each tissue as its own control. During this first part of the study, the tissue is run as control, in this case at I_{sc} with no additive compound, and then, after a sufficient period of time for the flux to stabilize, the experimental condition (in this case the addition of serosal ouabain) is imposed. This procedure decreases the amount of variation often seen in biological preparations.

The average rate constants for the ^{14}C-salicylate transport studies showing the effect of ouabain (with the tissue maintained at I_{sc}) are listed in Table X. A paired t-test indicated that the fluxes before and after serosal ouabain addition were significantly different. Also, the percent change in the transport rate constant caused by ouabain was significant. This study used 28 tissues from nine animals. It was expected that the percent change in the transport rate would be significant, since these were paired transports run on the same tissue. It might be possible that the percent change could be significant without

Table IX

Control Flux of ^{14}C-Salicylate

$J_{\overline{a}}$	110.7* ± 5.9 (SEM)	Not significant at $p < 0.5$ by paired t-test
$J_{\overline{p}}$	110.3 ± 6.2	
% change of flux	-0.03% ± 2.49%	

n = 14 tissues (seven animals)

* $\frac{\mu \text{ units}}{\text{hr. cm}^2}$ (where the mucosal concentration = 1000 μ units/ml)

(same time intervals as ouabain experiments)

Table X

Effect of Serosal Ouabain Addition on ^{14}C-Salicylate Flux at I_{sc}

$J_{\overline{a}}$	117.2* ± 6.0 (SEM)	$p < 0.001$ by paired t-test
$J_{\overline{p}}$	87.9 ± 4.5	
% change of flux	-23.6% ± 2.9%	$p < 0.001$

n = 28 tissues (nine animals)

* $\frac{\mu \text{ units}}{\text{hr. cm}^2}$ (where the mucosal concentration = 1000 μ units/ml)

there being a significant difference between the average fluxes before and after the serosal ouabain addition, due to normal biological variation. However, the difference between the average fluxes was significant even when these values were pooled.

Effect of Sodium-Free Buffer

To insure that the ouabain effect on the salicylate flux was due to its inhibition of sodium transport only, and not to some other inherent activity of ouabain, the same experiments were run again in sodium-free media. Choline salts replaced all sodium salts in the buffer solution, everything else remaining the same. This choline buffer solution (choline-I buffer solution in Table I) was added to the mucosal side of the tissue while the regular K-H buffer (with sodium ion) was used on the serosal side of the tissue. This procedure didn't work because the stripped rat jejunum is such a leaky tissue that sodium ions were passing from the serosal solution to the mucosal solution, and this was reflected in the I_{sc} values.

Therefore, sodium-free media was placed on both sides of the tissue, but this time the potassium ion concentration was raised to 20 mM from 6 mM in the regular K-H buffer (Choline-II buffer in Table I) as proposed by Asano et al. (104) to prevent excessive leaking of intracellular potassium ion. During the surgical preparation of the tissue, sodium-containing K-H buffer was routinely used, with sodium-free buffer used only in the perfusion apparatus. About 15 minutes after the tissue was mounted, the choline buffer was drained from the apparatus, the the tower and chamber rinsed, and new choline buffer solution added. This was done to remove any of the sodium ions that might

have been left adhering to the tissue. After the tissue had stabilized from the rinse, ^{14}C-salicylate was added to the mucosal solution and transport rates determined. Ouabain was later added to the serosal fluid, as in the previous experiments.

In the absence of sodium ion, the transmural potential was essentially zero, as was the I_{sc}. The tissue could not be maintained at I_{sc} because the instrumentation is incapable of automatic operation at such low potentials. The experiments were, therefore, run at open circuit. Calculation of the tissue resistance (accomplished by reading PDs at preset current values), however, showed a higher value with choline buffer than for the similar experiment run in the presence of sodium ion. In fact, the tissue resistance in choline buffer was almost twice that in sodium buffer (R in choline buffer averaged 36 Ω, while R in sodium buffer averaged 21 Ω). The introduction of ouabain did not appear to affect the transmural resistance of the stripped rat jejunum in choline buffer, as it did in regular sodium-containing buffer. However, a paired t-test showed a difference at the 95% confidence interval. Table XI lists the average transmural resistances determined in choline buffer before and after the addition of serosal ouabain. At the end of some of the experiments, the choline buffer was replaced with the regular sodium-buffer to see if there might be any effect on the electrical parameters of the tissue. The tissue resistance dropped to 20 ohms (as can be seen in Table XI), the average value of transmural resistance in the presence of sodium-containing buffer, while a 2.0 to 2.5 mv increase in transmural PD was noted, as shown for a typical experiment in Figure 20.

Table XI

Effect of Serosal Ouabain Addition on Transmural Resistance in Sodium-Free Buffer

$\bar{R}_a$ $36.7\Omega \pm 1.3\Omega$ (SEM)

$\bar{R}_p$ $34.3\Omega \pm 1.0\Omega$

$.05 > p > .02$ by paired t-test

n = 15 tissues (four animals)

Choline buffer washed out and K-H buffer (with Na^+) added

$\bar{R}_{p(Na^+)}$ $20.9\Omega \pm 1.2\Omega$

n = 6 tissues

$p < 0.001$ for $\bar{R}_a$ vs $\bar{R}_{p(Na^+)}$ by paired t-test

$\bar{R}_a$ = average calculated resistance before addition of ouabain

$\bar{R}_p$ = average calculated resistance after addition of ouabain

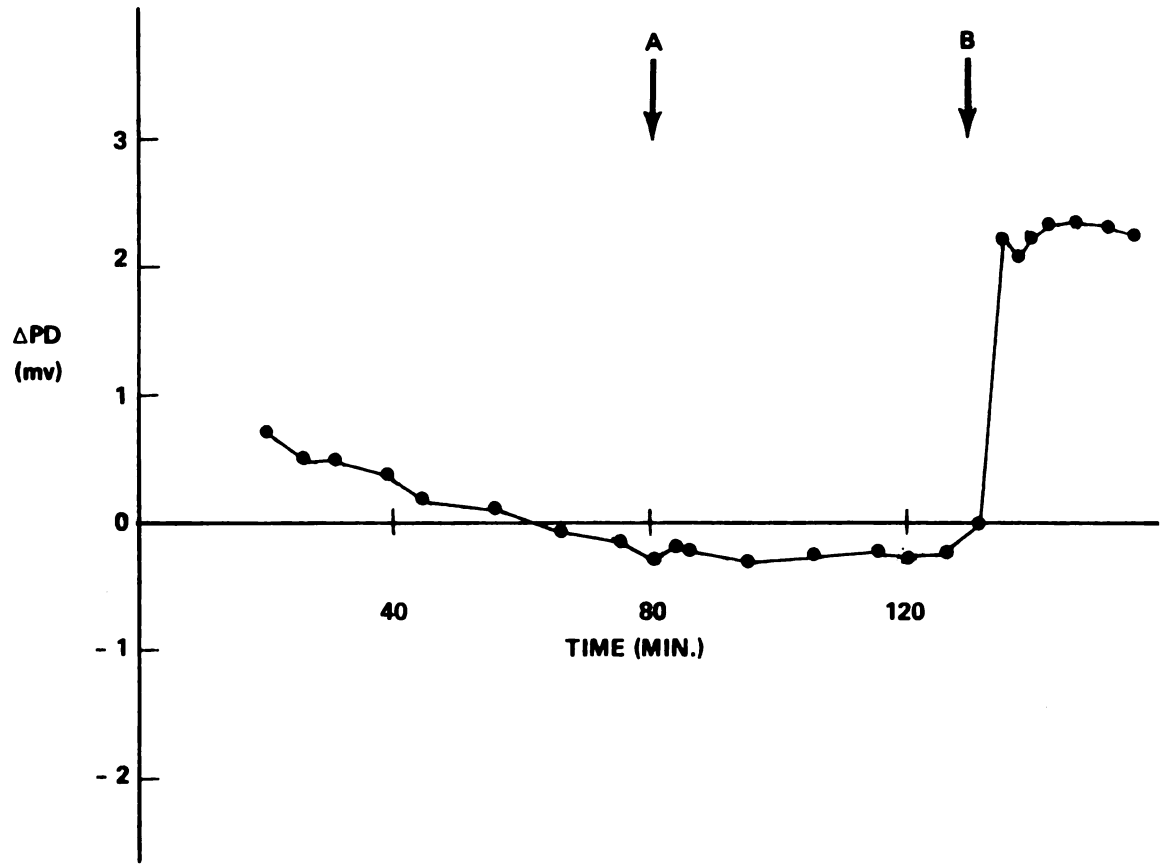

Figure 20. Effect of serosal ouabain addition on transmural PD in sodium-free buffer and sodium-containing buffer. The results of a typical experiment. At arrow A ouabain (1×10^{-3}M) was added to the serosal solution (choline-II buffer). At arrow B the serosal solution was drained, the tissue rinsed and replaced with sodium-containing K-H buffer.

The ^{14}C-salicylate flux in the absence of sodium ion and the effect of serosal ouabain addition is illustrated in Figure 21. It can be seen that the initial flux is much lower than that seen in sodium-containing buffers (see Tables IX and X), and there is only a small change in the flux due to ouabain addition when averages of all tissues are compared. The data from these experiments are shown in Table XII. Statistical treatment showed, however, that this slight increase in the transport rate constant after the introduction of ouabain was significant. This change in flux of ^{14}C-salicylate corresponds to the alteration observed in the transmural resistance.

Since in the sodium-free buffer there was only a small change in the transport rate of ^{14}C-salicylate and in the transmural resistance, and no change in the other tissue electrical parameters upon the introduction of serosal ouabain, it was thus concluded that the changes observed previously in the sodium-containing buffer were due to ouabain inhibition of the sodium-pump. The flux of ^{14}C-salicylate in choline-buffer is much lower than in the presence of sodium ion. Similar observations have been made for the flux of benzoic acid when sodium-buffer is replaced by a choline-buffer (112). The electrical parameters were also affected by the presence of choline in this present study. There was essentially no detectable transmural PD or I_{sc} and the transmural tissue resistance was approximately double the value observed in the presence of sodium-buffer. Nellans et al. (72) observed comparable findings using the in vitro stripped rabbit ileum. They also found that active chloride ion absorption was abolished in the absence of sodium ions. This was mainly due to a decrease in the M-to-S flux of

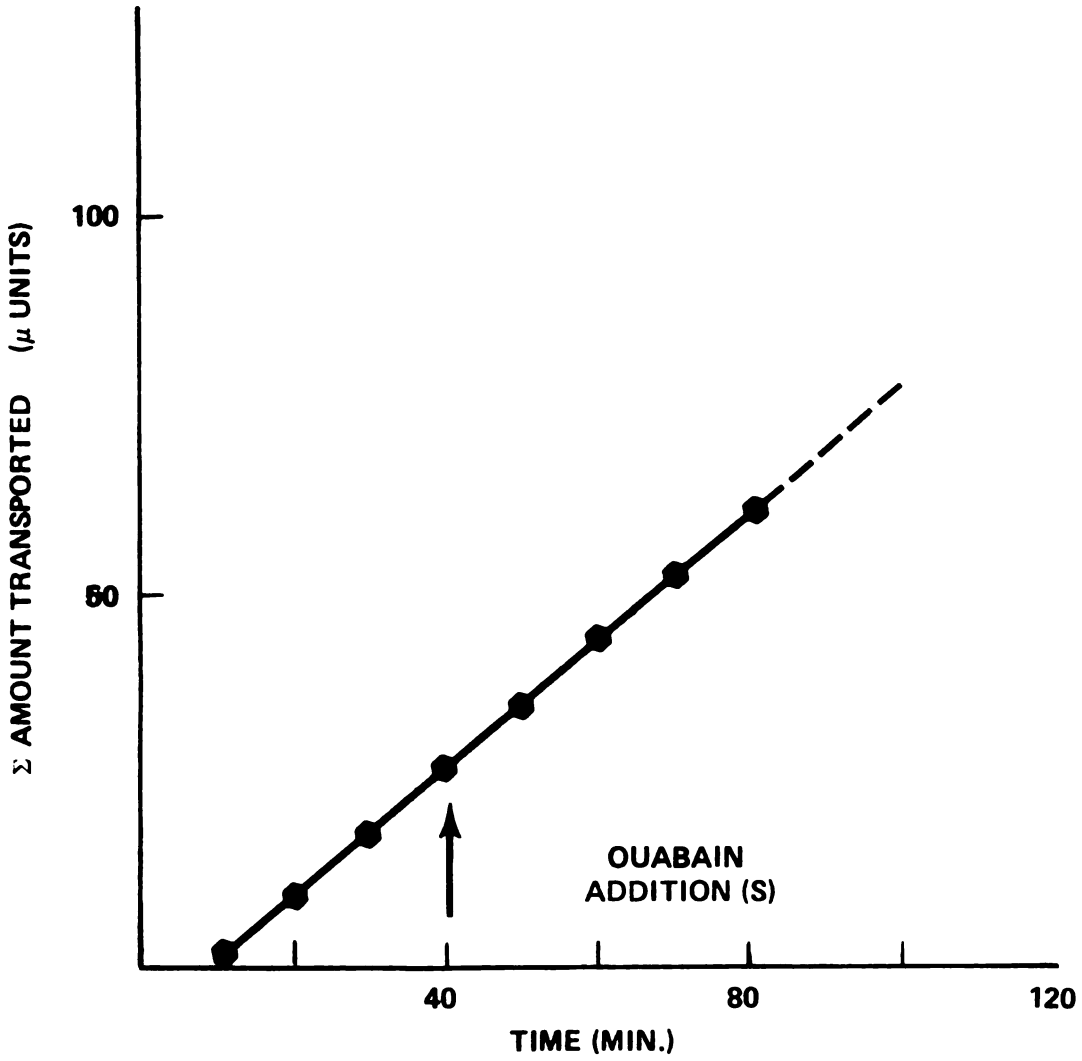

Figure 21. Effect of serosal ouabain addition on ^{14}C-salicylate flux in sodium-free buffer. The results of a typical experiment. At the arrow ouabain (1 x 10^{-3}M) was added to the serosal solution.

Table XII

Effect of Serosal Ouabain Addition on ^{14}C-Salicylate Flux in Sodium-Free Buffer

$J_{\overline{a}}$	47.8* ± 1.4 (SEM)	$p < 0.001$ by paired t-test
$J_{\overline{p}}$	52.2 ± 1.3	
% change of J	9.8% ± 5.6%	$p < 0.001$

n = 15 tissues (four animals)

* $\frac{\mu \text{ units}}{\text{hr. cm}^2}$ (where the mucosal concentration = 1000 μ units/ml)

chloride ion since the S-to-M flux of chloride ion was unaffected. The membrane is less permeable to choline than to sodium according to Barry and Eggenton (113). However, Nellans et al. (72) state that the marked decline in tissue conductance observed when sodium is replaced with choline is almost certainly attributable to the fact that the shunt pathway, which accounts for more than 80% of the total conductance, is relatively impermeable to choline.

Glucose Addition

A study was made on the effect of added d-glucose on the transmural ^{14}C-salicylate flux and the electrical parameters of the tissue. Glucose was added to both mucosal and serosal solutions (to maintain iso-osmolarity) to a concentration of 25 mM after a stable salicylate flux developed during the control period. It can be seen in Table XIII that there was essentially no change in ^{14}C-salicylate transport before and after the glucose addition. (Six tissues from two animals were used.) Marked electrical changes were noted, however. The transmural PD increased by an average of 3.5 mv after the addition of glucose. The increase in I_{sc} was even more spectacular, with a greater than 300 μA average increase. The I_{sc} for two of the tissues went off scale (greater than 500 μA) and, therefore, had to be estimated. Figure 22 illustrates the effect of glucose on the transmural electrical parameters. The transmural resistance was not altered by the addition of glucose to the perfusing buffer, as observed in Figure 22 as well as in Table XIV.

The fact that addition of glucose stimulates active sodium-transport and increases transmural PD and I_{sc} is well established

Table XIII

Effect of Glucose Addition on ^{14}C-Salicylate Flux at I_{sc}

$J_{\overline{a}}$	120.4* ± 4.6 (SEM)	Not significant at $p < 0.2$
$J_{\overline{p}}$	117.1 ± 7.0	
% change of J	-2.9% ± 3.5%	

n = 6 tissues (two animals)

* $\frac{\mu \text{ units}}{\text{hr. cm}^2}$ (where the mucosal concentration = 1000 μ units/ml)

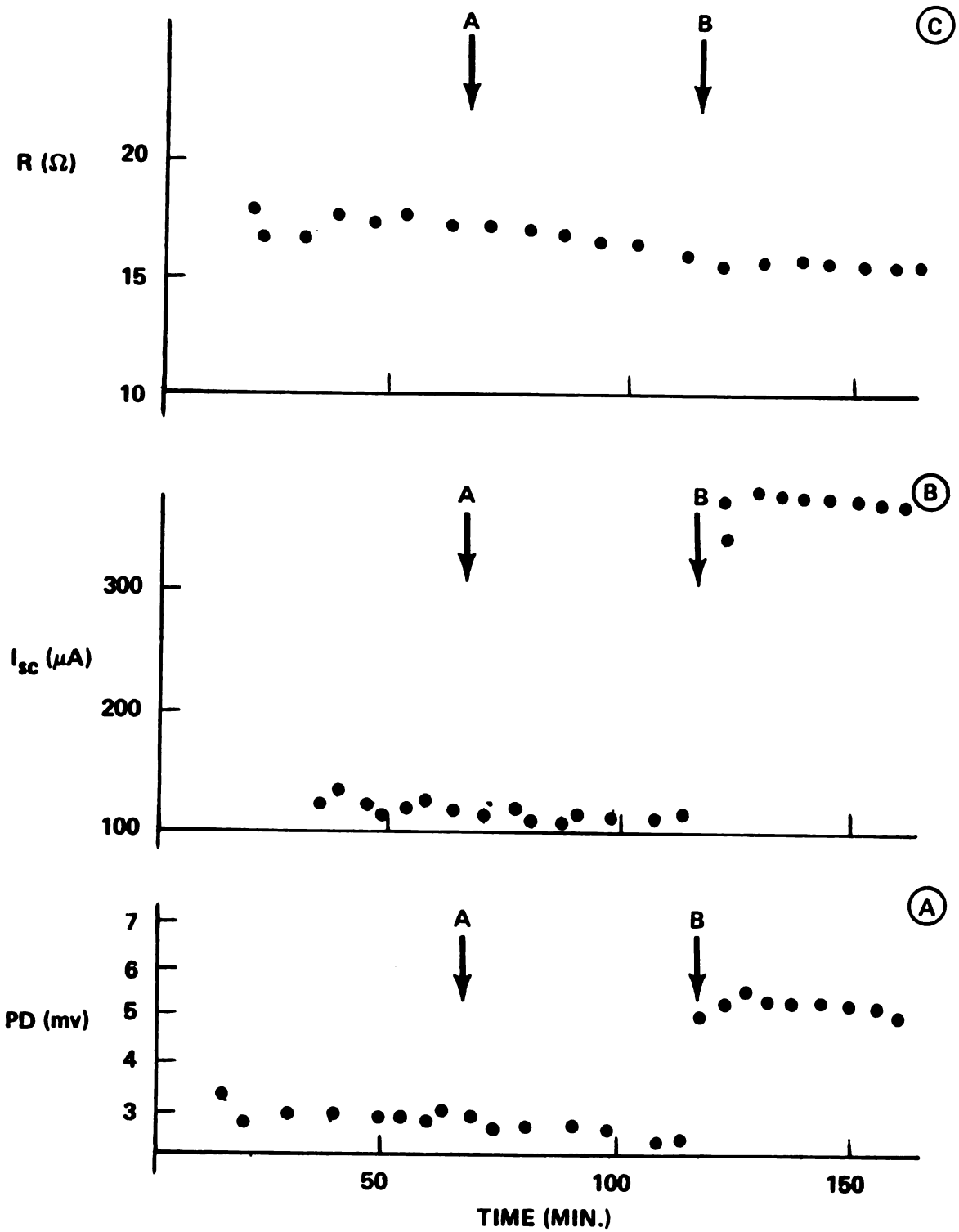

Figure 22. Effect of glucose addition on the transmural electrical parameters. The three parameters were monitored in the same tissue. At arrow A ^{14}C-salicylate was added to the mucosal solution. At arrow B 25 mM d-glucose was added to the mucosal and serosal solutions.

A: transmural PD
B: transmural I_{sc}
C: transmural R

Table XIV

Effect of Glucose Addition on Transmural Electrical Parameters

Resistance

$\overline{R}_a$	12.9 Ω	±	0.5 Ω (SEM)	$0.2 > p > 0.1$ by paired t-test
$\overline{R}_p$	12.2 Ω	±	0.4 Ω	

$\overline{R}_a$ = average calculated resistance before addition of glucose

$\overline{R}_p$ = average calculated resistance after addition of glucose

n = 5 tissues

Potential Difference

$\overline{PD}_a$	1.58 mv	±	0.26 mv	$p < .001$ by paired t-test
$\overline{PD}_p$	5.03 mv	±	0.44 mv	

$\overline{PD}_a$ = average potential difference before addition of glucose

$\overline{PD}_p$ = average potential difference after addition of glucose

n = 6 tissues

Table XIV (continued)

Short-Circuit Current

$\bar{I}_{sc_{\bar{a}}}$	121 μA	±	24 μA	.002 > p > .001 by paired t-test
$\bar{I}_{sc_{\bar{p}}}$	436 μA	±	62 μA	

$\bar{I}_{sc_{\bar{a}}}$ = average short-circuit current before addition of glucose

$\bar{I}_{sc_{\bar{p}}}$ = average short-circuit current after addition of glucose

n = 5 tissues

(19, 114-116). In this present study, no change in the flux of ^{14}C-salicylate was observed after the addition of 25 mM d-glucose even though the I_{sc} was greatly increased. There was no noticeable change in the transmural resistance due to glucose addition either. A decrease in the fluxes of riboflavin, sulfanilamide, and salicylate across the in vitro everted rat intestine was found by Mayersohn and Gibaldi (70). In their salicylate flux studies, they used a concentration of 219 mM glucose where the sugar quantitatively replaced NaCl, in terms of osmotic equivalents, in the control buffer. Thus, there was very little sodium ion remaining in the perfusing buffer. What they actually measured then was the flux of salicylate in the presence of very low concentrations of sodium ion rather than measuring the effect of glucose on salicylate flux. Jackson et al. (42) found a very large increase in the M-to-S flux of benzoic acid in the presence of 10 mM glucose in their in vitro rat preparation. The M-to-S transport of benzoic acid was decreased in the same preparation in the presence of 10 mM galactose. Both sugars are actively transported and both increase transmural PD and I_{sc}; however, only glucose is metabolized. Why these hexoses produced opposite effects on the in vitro intestinal flux of benzoic acid is not known nor was an explanation offered by these authors (42).

Salicylate Addition

The electrical properties of the stripped rat jejunum were affected by the addition of sodium salicylate to the mucosal perfusion solution. Figure 23 illustrates this effect on the transmural PD. There is normally a slight decline in PD with

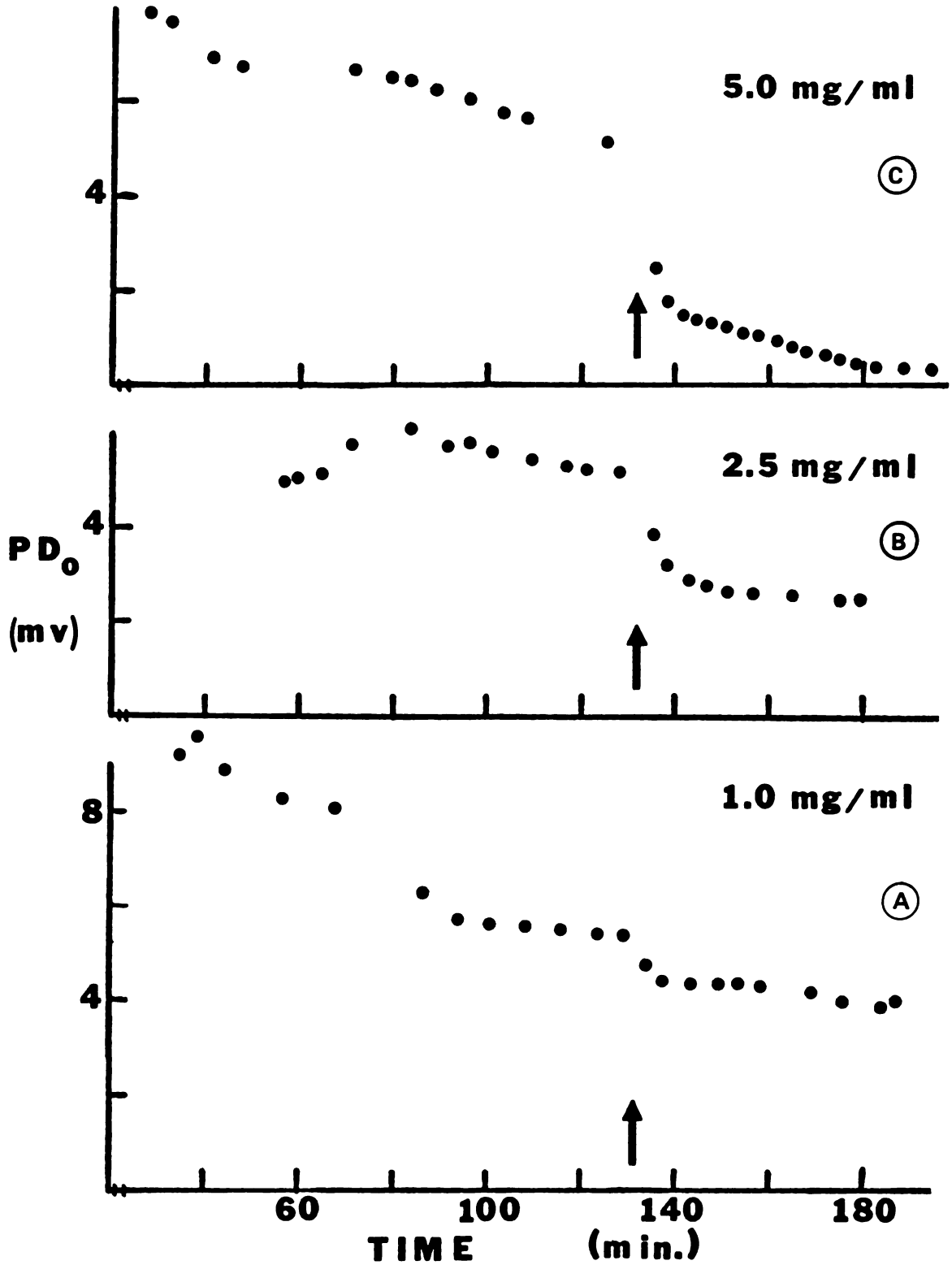

Figure 23. Effect of mucosal salicylate addition on transmural PD at concentrations of 1.0, 2.5 and 5.0 mg/ml (graphs A, B and C, respectively). A different tissue was used at each concentration.

time, but after the addition of the unlabelled salicylate, as signified by the arrow, there is a definite decrease in the PD. This decrease starts immediately, but it takes 20 to 40 minutes to reach a steady state level. In this figure, the results are shown for three different tissues to which different concentrations of salicylate were added. The decrease in PD appears related to the mucosal salicylate concentration present.

Figure 24 shows another electrical parameter, I_{sc}, plotted vs time. Similar results are seen in this plot as that seen with PD. There is a decline in the current after salicylate addition, and, again, in these tissues the change seemed related to the mucosal salicylate concentration. The transmural resistance is plotted in Figure 25 and an effect due to salicylate addition is also seen. This parameter, however, increased in value, whereas PD and I_{sc} decreased. The changes in resistance again seem to reflect the concentrations of mucosal salicylate present. In Figure 25, the tissue to which 1 mg/ml salicylate was added shows a small increase in resistance; however, some tissues showed no change in resistance at this concentration.

Table XV summarizes the changes seen in the electrical parameters after the addition of the three different concentrations of salicylate. The change and percent change for each parameter are given. There were between 17 and 19 tissues from five animals run at each concentration of added salicylate. The numbers shown are the averages and standard errors. As salicylate concentration increased, larger decreases in PD were noted. Short-circuit current also decreased after salicylate addition, but there was little difference in the decreases at

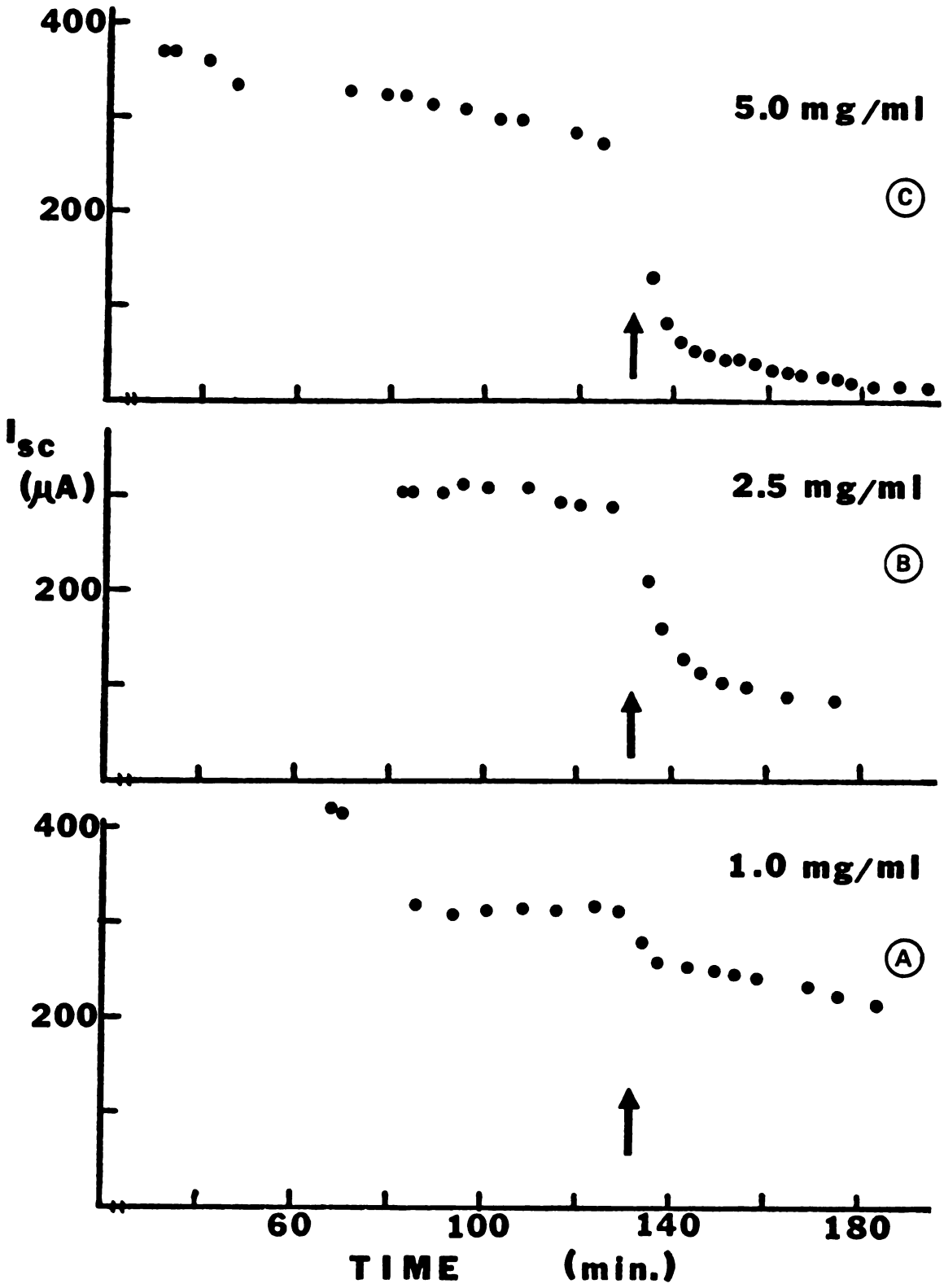

Figure 24. Effect of mucosal salicylate addition on transmural I_{sc} at concentrations of 1.0, 2.5 and 5.0 mg/ml (graphs A, B and C, respectively). A different tissue was used at each concentration.

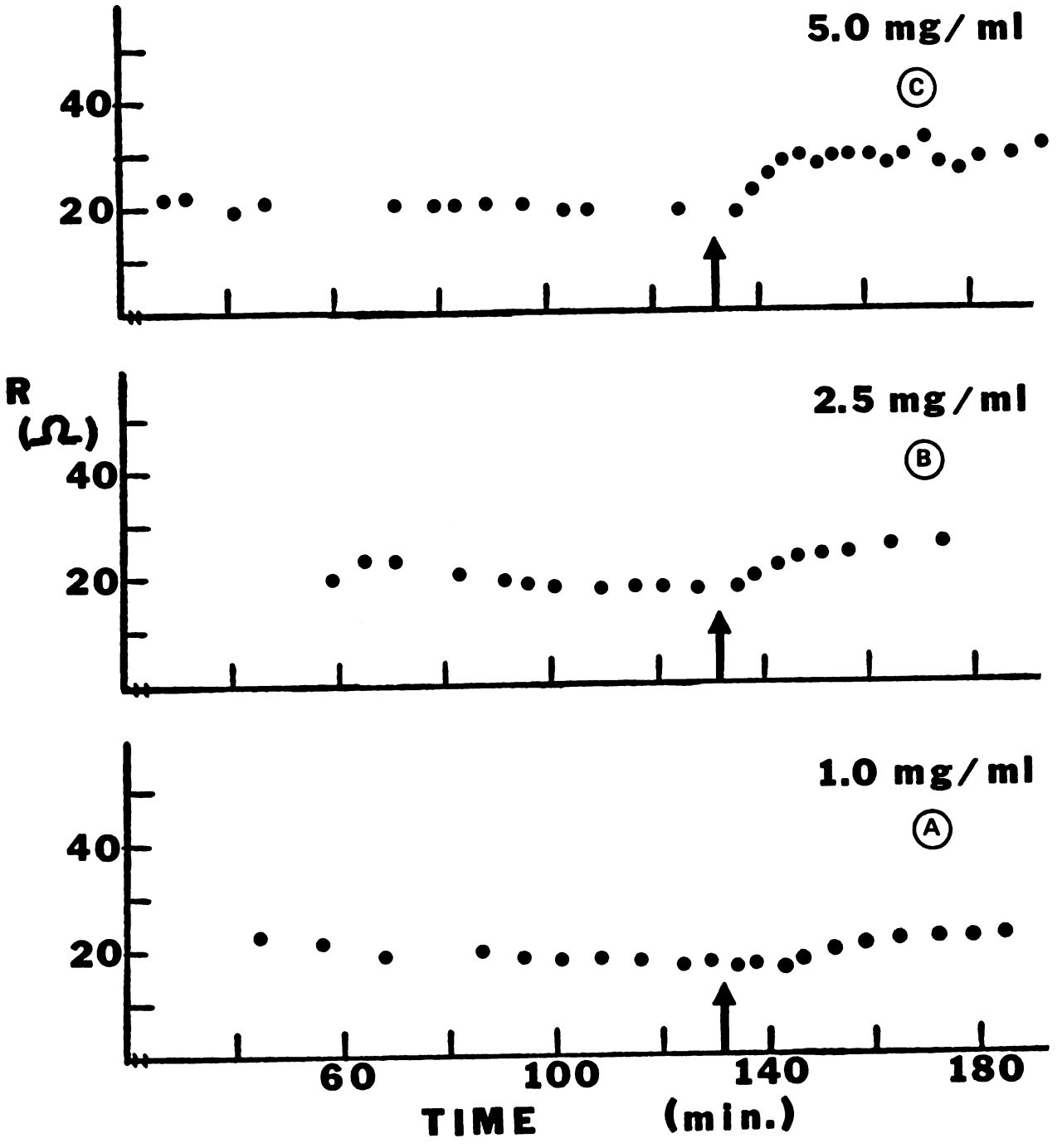

Figure 25. Effect of mucosal salicylate addition on transmural R at concentrations of 1.0, 2.5 and 5.0 mg/ml (graphs A, B and C, respectively). A different tissue was used at each concentration.

Table XV

Changes in Membrane Electrical Parameters with Addition of Mucosal Salicylate

SA conc. (mg/ml)	ΔPD_0 (mv)	$\% \Delta PD_0$	ΔI_{sc} (μA)	$\% \Delta I_{sc}$	ΔR_{peak} (Ω)	$\% \Delta R_{peak}$
1.0 n = 19	-1.9 ± 0.2*	-32.2 ± 2.7	-109 ± 7	-40.5 ± 3.4	+ 5.0 ± 0.8	+21.5 ± 3.0
2.5 n = 17	-3.1 ± 0.2	-60.5 ± 3.3	-191 ± 13	-72.4 ± 2.1	+10.5 ± 0.7	+52.0 ± 3.4
5.0 n = 17	-3.6 ± 0.2	-80.9 ± 1.7	-184 ± 12	-85.4 ± 1.9	+ 8.8 ± 0.9	+42.0 ± 3.8

*average ± SEM

2.5 mg/ml and 5.0 mg/ml. There was a significant increase in transmural resistance, and again no significant difference is seen between the effects at 2.5 mg/ml and at 5.0 mg/ml.

Washout experiments were run after the addition of salicylate, as they had been done with ouabain. Figure 26 records the results of a typical experiment showing how the I_{sc} is affected in this study. When salicylate was added to the perfusing solution, the I_{sc} started to decrease immediately and continued to do so until salicylate was removed. Following the washout of salicylate (as indicated by the arrow in Figure 26), the I_{sc} increased to a peak and then resumed the slow decline in this parameter normally seen with aging of the tissue preparation (as seen in Figure 10, B). The peak value attained after the washout appears to be consistent with the value which would have been expected at that time, based on the level of I_{sc} previous to the salicylate addition and also on the slope of the normal time-dependent portion of the curve. This indicated that the effect of added salicylate was reversible for the conditions of the study.

In the present work, it has been shown that the addition of mucosal salicylate (at different concentrations) affected the electrical parameters of the tissue. Other workers had observed the effect of salicylate on various tissues. Barker and Levitan (89, 96-99) found an increase in the permeability of a molluscan neuron to potassium ion and a decrease in the permeability of the neuron to chloride ion in the presence of salicylate. Salicylate caused the permeability of the neuron to change in a reversible, dose-dependent manner, producing a concomitant increase in membrane potential and a decrease in

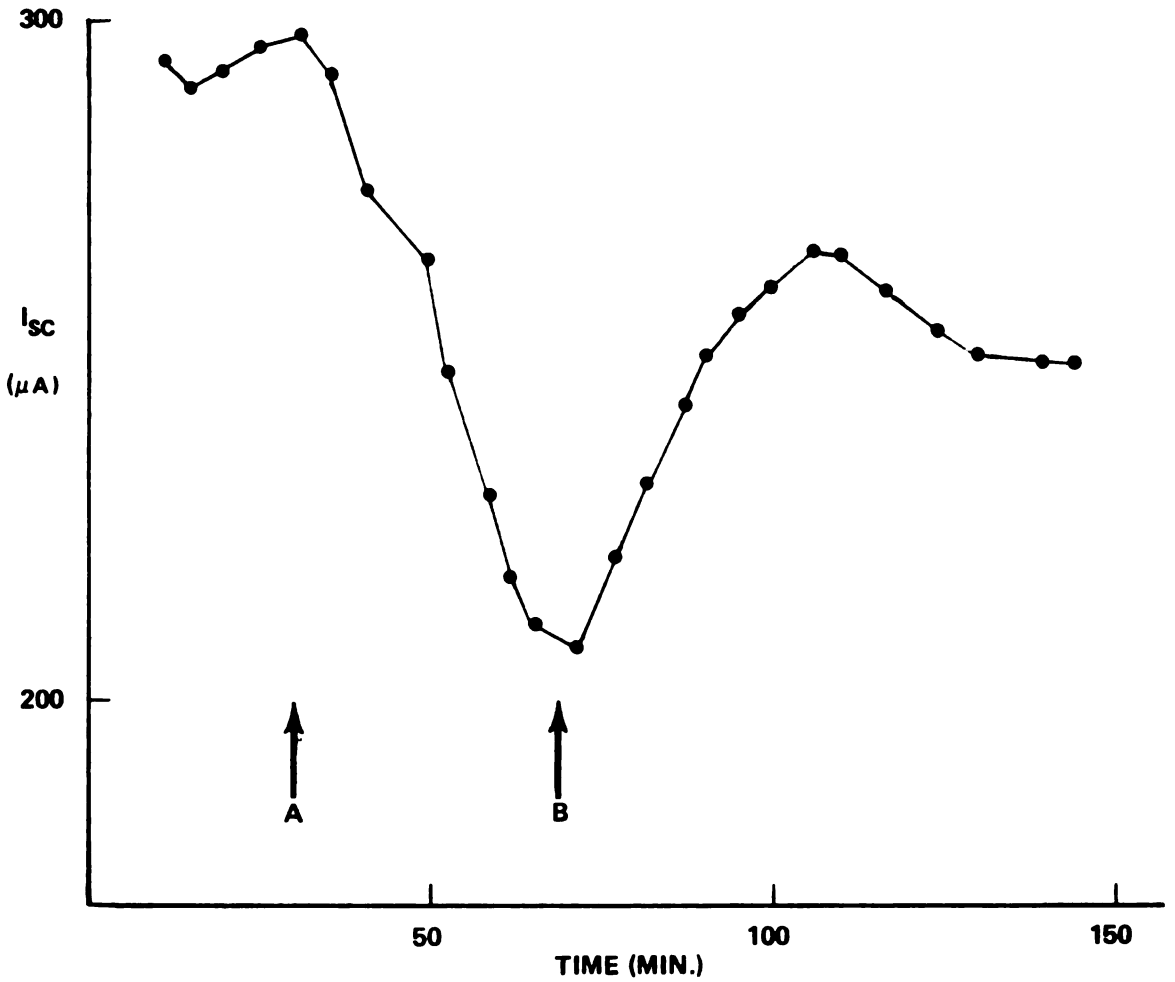

Figure 26. Effect of mucosal salicylate addition and washout on transmural I_{SC}. The results of a typical experiment. At arrow A salicylate was added and at arrow B the mucosal solution was drained, the tissue rinsed and the mucosal solution replaced with K-H buffer.

membrane resistance (96). A similar effect was found with artificial membranes and salicylate (100). A decrease in transmural PD and increase in tissue resistance was observed when salicylate was added to the serosal solution perfusing isolated bullfrog gastric mucosa (84). These parameters showed near-complete reversal following salicylate washout, as was also witnessed in the present study. The addition of salicylate to the mucosal bathing solution caused a decrease in both the transmural PD and transmural resistance. If the results of this present study are compared with those of the previous studies, an interesting correlation can be made. In the present study, the transmural PD was decreased as it was in the bullfrog stomach. The membrane PDs of the mollusk neuron and artifical membrane were increased. These PDs are negative numbers and were made more negative (a larger negative number) after the addition of salicylate. Therefore, in all cases the transmural PD was made more negative, and the normal function of the membrane was interferred with. These changes were dose-dependent for all cases.

The flux of ^{14}C-salicylate from a typical experiment is shown in Figure 27. Unlabelled sodium salicylate was added after the 50 minute sample was taken, as indicated by the arrow. There is a definite change in the slope of the amount transported vs time plot, and it achieves a new steady state approximately 20 to 30 minutes after the mucosal salicylate introduction. Control experiments again showed no change in the flux of ^{14}C-salicylate in the absence of added mucosal salicylate, and the flux followed the dotted line as indicated in Figure 27.

The relationship of the fluxes of ^{14}C-salicylate and the various concentrations of added salicylate are shown in Table

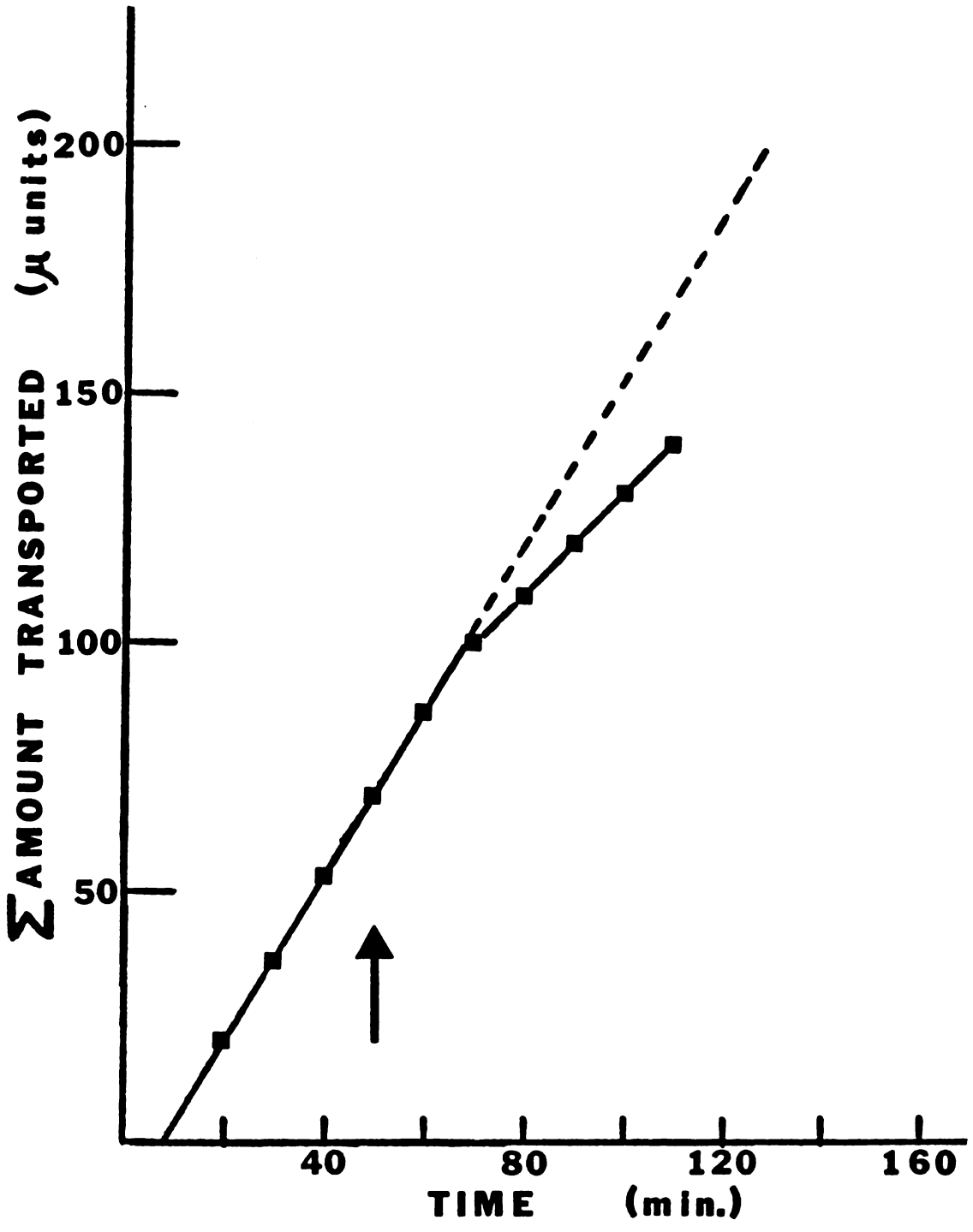

Figure 27. Effect of mucosal salicylate addition on ^{14}C-salicylate flux at I_{sc}. The results of a typical experiment. At the arrow salicylate was added to the mucosal solution.

XVI. There were from 16 to 19 tissues run at each concentration, and the values listed are the averages and standard errors. $J_{\overline{a}}$ is the flux of ^{14}C-salicylate before the mucosal salicylate addition and $J_{\overline{p}}$ is the flux after salicylate addition. A paired t-test showed that there was a significant difference between $J_{\overline{a}}$ and $J_{\overline{p}}$ at all three concentrations. But, the decrease in flux due to 2.5 mg/ml of added mucosal salicylate was not significantly different than the decrease caused by 5.0 mg/ml.

Figure 28 is a composite showing the percent changes in the ^{14}C-salicylate flux and the three transmural electrical parameters (PD, I_{sc}, and R) plotted vs the concentration of the added salicylate. As can be seen, the change is not linear with respect to salicylate concentration; but, instead, appears to show a saturation effect, although it is difficult to make any definite conclusion for only three salicylate concentrations.

Table XVI

Effect of Mucosal Salicylate Addition on ^{14}C-Salicylate Flux at I_{sc}

conc. (mg/ml)	$J_{\overline{a}}$	$J_{\overline{p}}$	ΔJ	$\% \Delta J$
1.0 n = 19	91.1* ± 7.6 (a)	74.8 ± 5.2	-16.3 ± 4.3	-15.1 ± 3.7
2.5 n = 16	84.5 ± 4.5	56.2 ± 2.8	-28.3 ± 4.7	-31.1 ± 4.9
5.0 n = 17	77.4 ± 5.6	54.7 ± 4.2	-22.6 ± 3.2	-28.4 ± 3.4

* $\frac{\mu \text{ units}}{\text{hr. cm}^2}$ (where mucosal concentration = 1000 μ units/ml)

(a) average ± SEM

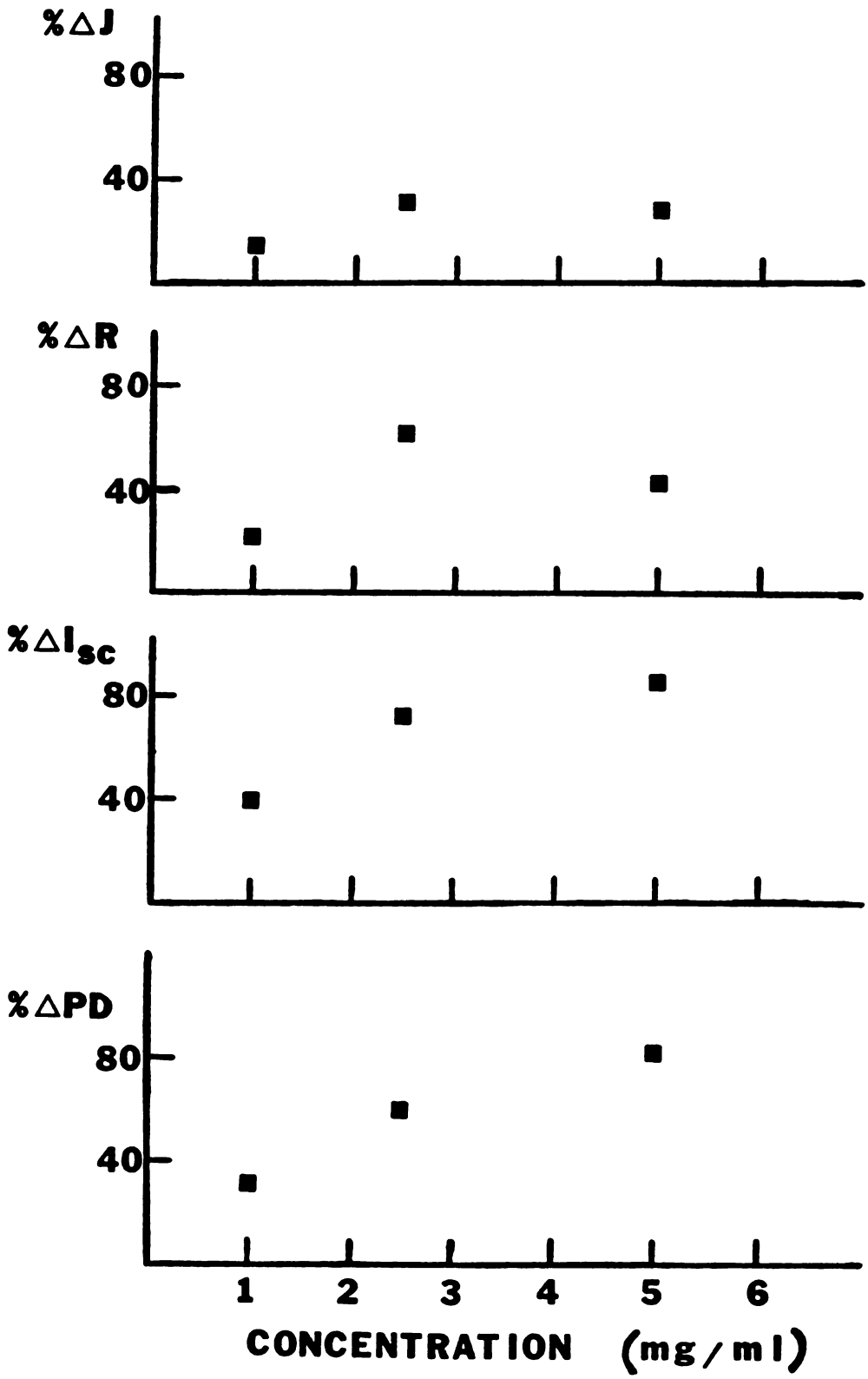

Figure 28. Composite graph of percent changes of ^{14}C-salicylate flux and transmural electrical parameters vs. concentration of mucosal salicylate. Each point is the average of 16 to 19 experiments. (Data in Tables XV and XVI.)

DISCUSSION

This investigation has shown that salicylate ions are indeed participating in salicylate intestinal transfer in this *in vitro* preparation. The simultaneous transfer of antipyrine with salicylate in this study showed the difference in absorption between a neutral and ionized compound.

The mucosal to serosal flux ($J_{m\rightarrow s}$) of an ion has been related to the transmural PD by Schultz and coworkers (43), as previously discussed in the Introduction. They have demonstrated that if the unidirectional flux of an ion is attributable to simple ionic diffusion and if the partial ionic conductance is independent of the imposed transmural PD, there should be a linear relation between that flux and $\xi^{-1/2}$ (a function of PD). A plot of $J_{m\rightarrow s}$ *vs* $\xi^{-1/2}$ will have an intercept related to the flux via the cell, J_m, and a slope equal to the flux via the tramsural shunt pathway at short-circuit current, ${}_oJ_d$. Figure 29 shows the ^{14}C-salicylate flux constant plotted *vs* $\xi^{-1/2}$. This graph contains data at 83 different PDs with 32 tissues from nine animals. The data was fit by a nonweighted least squares computer program. Treatment of this data showed that 51% of $J_{m\rightarrow s}$ occurred via the transmural shunt pathway for ^{14}C-salicylate under the conditions of this experiment. This value was calculated by the following equations:

$$\text{\% transfer via transmural shunt} = \frac{\text{slope}}{\text{intercept + slope}} \times 100\% \quad \text{(Eq. 21)}$$

or

$$\text{\% transfer via transmural shunt} = \frac{J_d}{J_m + J_d} \times 100\% \quad \text{(Eq. 22)}$$

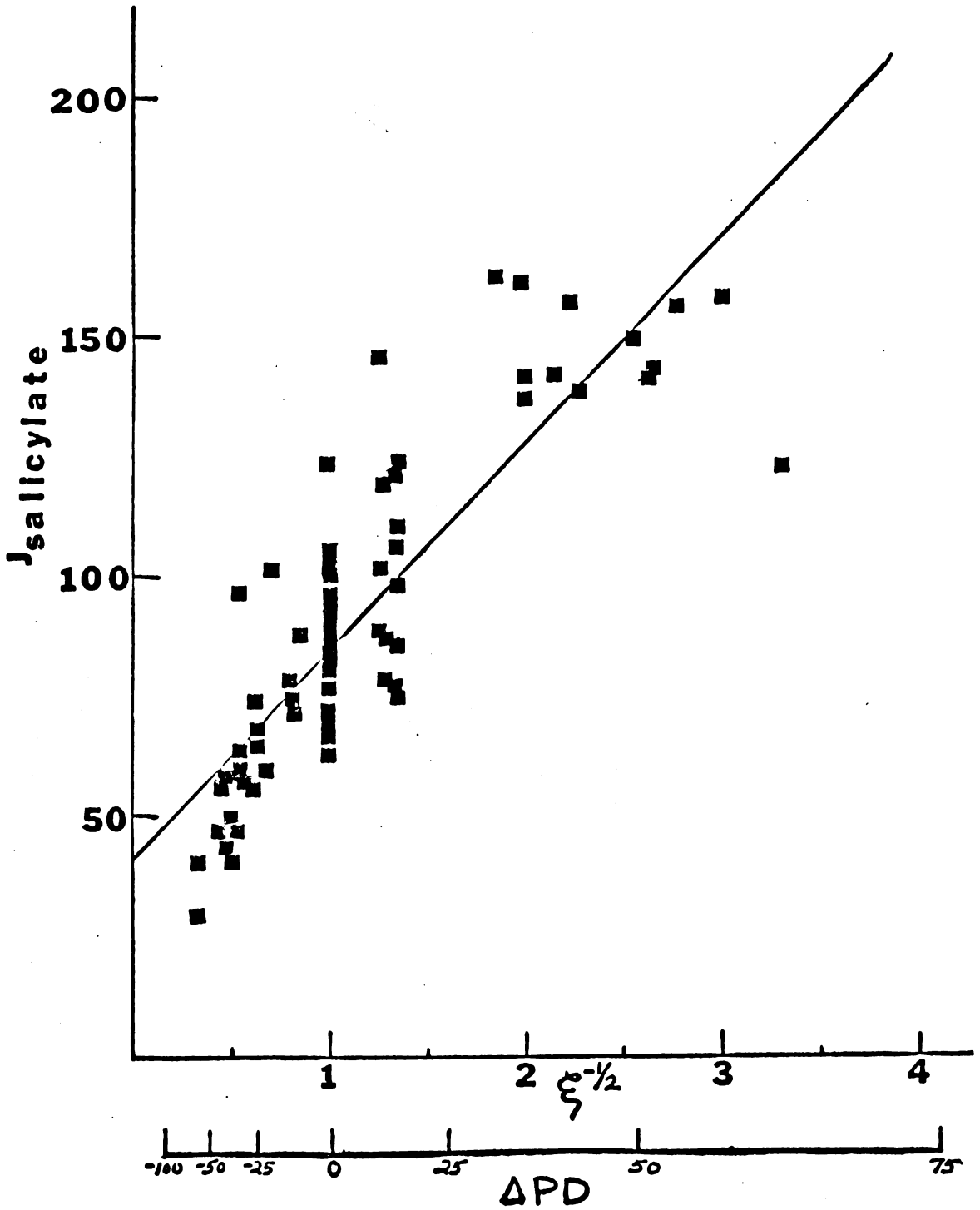

Figure 29. Effect of transmural PD (related to ξ function) on ^{14}C-salicylate flux. This graph contains data at 83 different PDs with 32 tissues from nine animals.

This same type of plot was also made using data collected from a single animal, as seen in Figure 30. This plot shows considerably less scatter of data over that observed in Figure 29. It is interesting to note that both of these plots appear to contain some suggestion of a hyperbolic shape, with the curve rising sharply at lower $\xi^{-1/2}$ values, then curving over as higher values of $\xi^{-1/2}$ are approached. Similar tendencies can be observed in the flux *vs* $\xi^{-1/2}$ plots for sodium, chloride, potassium and rubidium ions reported previously (43, 73) although this fact was not commented upon. Possibly this tendency to level out at a high potential difference (where the M→S potential difference is the opposite charge to the ion whose transport is being measured) may reflect a saturation mechanism. This would indicate that passive processes might not be operative under conditions of high potential difference due to some interaction of the charge and the diffusing substance. However, at the present time it cannot be positively concluded whether such an interaction does in fact take place. Therefore, further discussion will continue to be made with reference to the Frizzell and Schultz equations (43).

The ^{3}H-antipyrine data was plotted in a similar fashion, with the assumption that antipyrine might carry a positive charge. Therefore, z was given the value of +1. If the $J_{m\rightarrow s}$ of the radioisotope is not affected by a change in the transmural potential difference, then a straight line parallel to the x-axis would be expected. Figure 31 shows ^{3}H-antipyrine flux data plotted *vs* the potential difference function. The slope of the line is

13.42 μ units/cm^2 hr. and the intercept is 142.13. The correlation coefficient for the antipyrine flux data is only 0.31, whereas r = 0.83 for the salicylate flux data shown in Figure 29. This implies no correlation between the ^{3}H-antipyrine flux and the changes in transmural PD. This does not mean to say that antipyrine is transported only via the cell membrane and not by the transmural shunt pathway. The data only show that ^{3}H-antipyrine mucosal to serosal flux is not affected by a change in these imposed transmural PDs. Since antipyrine is an uncharged molecule, it is not expected to respond to a change in PD in the same manner that an ionized molecule would. Thus, no correlation would be anticipated between the flux of antipyrine and $\xi^{-1/2}$ (or PD).

A recent publication (72) proposed a possible error in the method of calculating the value for the imposed transmural PD (or E_{vc}). The standard method for correcting for fluid resistance consists of measuring the fluid resistance in the absence of tissue and using this value for all subsequent current adjustments in the presence of tissue. Nellans *et al.* (72) point out that insertion of tissue between the two half chambers displaces some of the fluid and, thus, the correction for fluid resistance determined in the absence of tissue should be decreased. The authors calculated that in their apparatus using stripped rabbit ileum this error would result in an underestimate of the tissue resistance by approximately 15%. This error would be negligible

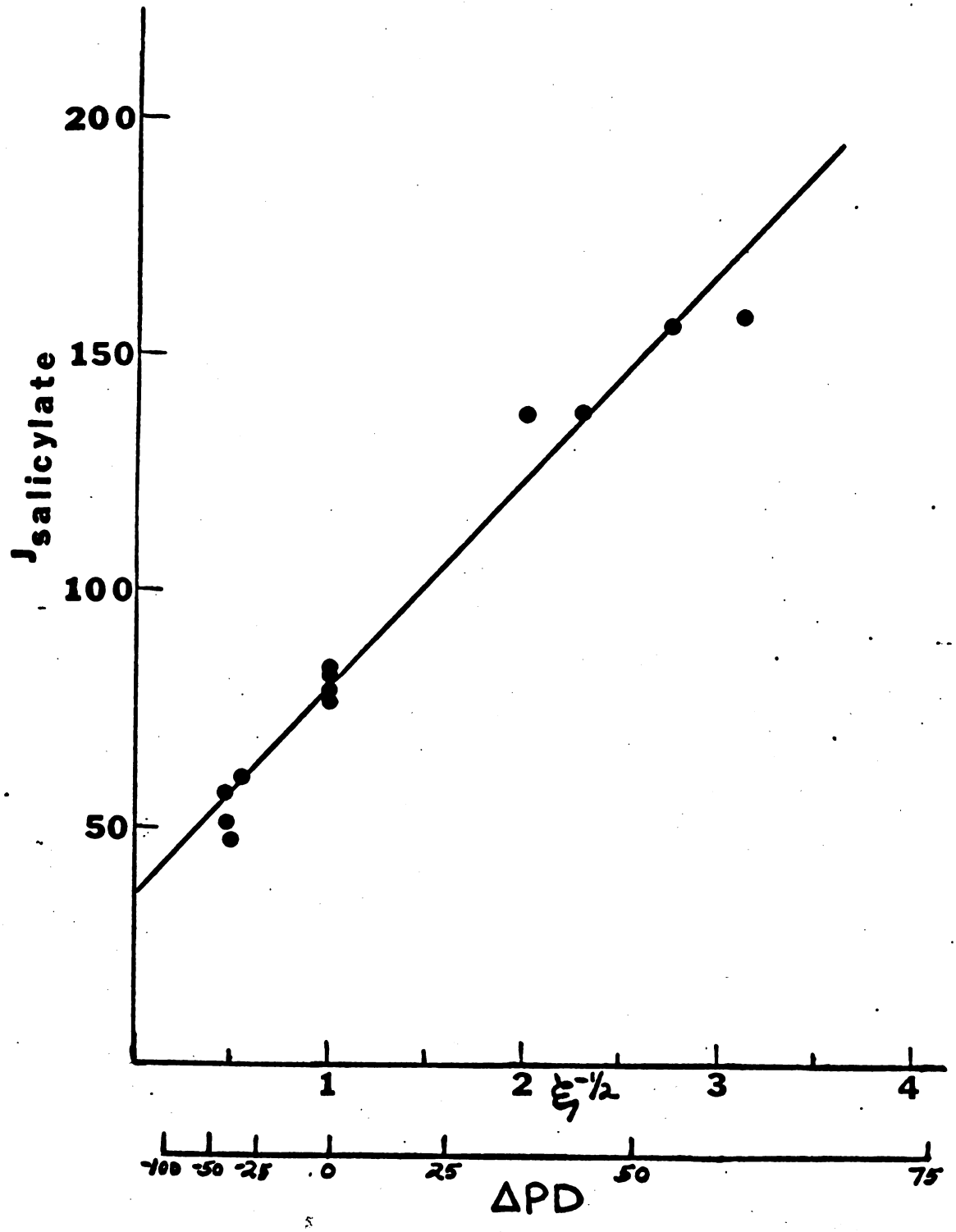

Figure 30. Effect of transmural PD (related to ξ function) on ^{14}C-salicylate flux (tissues from one animal only).

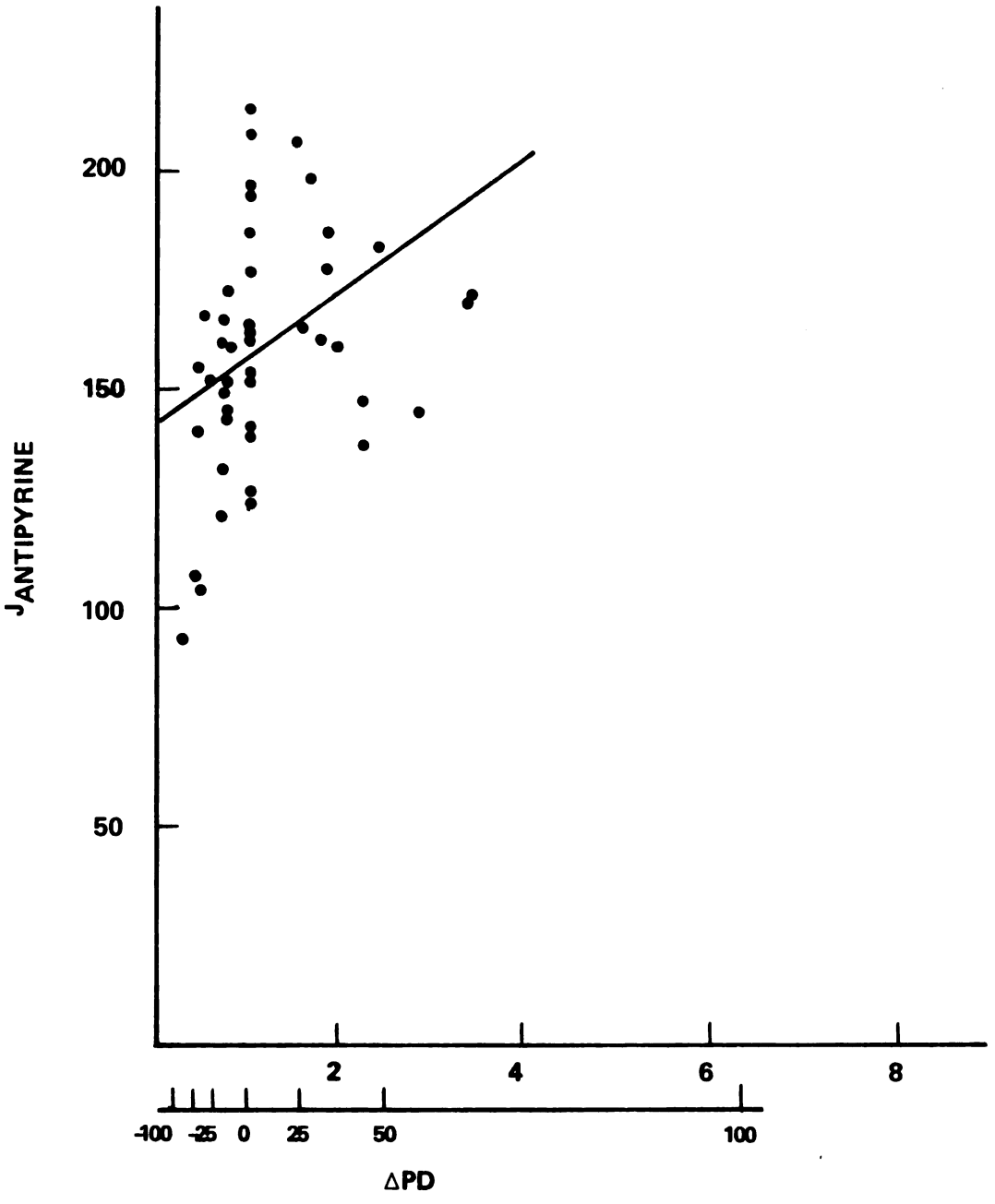

Figure 31. Effect of transmural PD (related to ξ function) on ^{3}H-antipyrine flux. This graph contains data on 45 different PDs with 13 tissues.

in the short circuited state because only relatively small currents are passed across the tissue. However, when the tissue is clamped at large positive or negative PDs, this error becomes more important. Thus, they corrected all of their data for this source of error by increasing the estimated tissue resistance by 15%. Following this suggestion, the data from Figure 29 using the 15% correction were recalculated, but the results were not greatly different. The new values for J_m and ${}_oJ_d$ are 49.57 and 34.58, μ units/cm^2 hr., respectively. With the recalculation salicylate transferred via the tight junctions is now 41% of the total $J_{m \rightarrow s}$ unidirectional flux.

This relationship between $J_{m \rightarrow s}$ and $\xi^{-1/2}$ has been shown for sodium ion under normal conditions and various experimental conditions. This relationship has also been demonstrated for chloride, potassium, and rubidium ions (43, 73). Ionic diffusion has thus been shown to be affected by a change in imposed PD. If salicylate were absorbed as nonionized salicylic acid, as suggested by the pH partition hypothesis, which states that the intestinal absorption of drugs occurs via the neutral species only, but a process of nonionic diffusion, then there should be no change in salicylate transport with a concurrent change in transmural PD. However, if salicylate were absorbed as the salicylate anion, then a change in the imposed transmural PD should cause a change in salicylate flux across the tissue.

These series of experiments demonstrated that salicylate flux was, indeed, influenced by the transmural PD, whereas the flux of antipyrine, a neutral compound, was essentially constant with varying transmural PD. Both fluxes were determined simultaneously in the same tissue.

The ^{14}C-butanol experiments were undertaken to determine if its transmural flux differed at maximum positive and negative transmural PDs, since the ^{3}H-antipyrine flux was somewhat altered at maximum positive transmural PDs. It appeared from the results of these experiments that the flux of butanol, a compound which is absorbed via the cell membrane and has low water solubility ($\sim$9%), was not affected by large changes in the imposed transmural PD. The permeability of the membrane relevant to butanol was, thus, not altered by the imposed PD. Antipyrine flux was altered somewhat by the maximum positive imposed transmural PDs, and the explanation for this phenomenon is unclear. Antipyrine is very water soluble, its reported water solubility is 100 gm/100 ml at 25° C (117). There is the possibility that the large positive imposed PD affected the permeability of the tissue relevant to antipyrine, such as constricting the aqueous channels in the tissue, to decrease the transmural shunt pathway. But, then, if the only effect of the imposed PD was to alter the route of transfer of the compound, one would assume that salicylate would also be similarly affected. This was not the case, for salicylate transport was changed in the opposite direction from that observed for antipyrine. Also, a change in the transmural shunt pathway would be reflected in a change in the electrical resistance of the tissue. As has been already mentioned, experiments were run to

determine the change in the transmural electrical resistance in the presence of maximum positive and negative imposed transmural PDs, and no change was observed. Another possible explanation for antipyrine flux showing a change due to a large imposed transmural PD might be that antipyrine is ionized to a very small degree and was affected by the imposed electric field, just as was the salicylate anion. The pK_a of antipyrine is 1.45 according to Bodforss and Guthe (118), and one would not normally expect antipyrine to be ionized at a pH of 7.4. A clear explanation of the changes of antipyrine flux due to the imposed transmural PD requires further study.

The intracellular pH of the jejunal tissue was determined to see if there was an effect on the tissue due to a change in the imposed transmural PDs. If the pH_i of the tissue changed with a change in the imposed transmural PD, then this might relate to the change in ^{14}C-salicylate flux observed during a change in the imposed PD across the tissue. If the pH_i were altered, this would, in turn, affect the percent of salicylate that would be nonionized, and thus would affect the rate of absorption of salicylate across the tissue. This might possibly be an explanation of the changes in absorption rate of ^{14}C-salicylate seen with changes in imposed transmural PD. The results of the pH_i experiments showed no statistical significant difference in the pH_i's calculated from tissues maintained at the different transmural PDs.

The values for pH_i of frog and mammalian muscle under normal conditions as measured by various workers with the CO_2 method have been reported in the range of 6.9 to 7.3 (106). The first application of the DMO technique to the measurement of pH_i was the study by Waddell and Butler (106) for dog

skeletal muscle. They found that the pH_i of normal, resting muscle averaged 7.04. Subsequently, a number of other workers have used DMO for the measurement of pH_i in various types of cells as reviewed by Butler *et al.* (119) and Waddell and Bates (120). Some of the tissues and cells that have been studied include the turtle heart with pH_i 7.57 (121), skeletal muscle from the human, dog, cat, dogfish, and rat with a pH_i range of 6.72 to 7.28 (106, 122-126), rat diaphragm with pH_i = 7.21 (127), brain tissue of dog, cat, and rat with a pH_i range of 7.0 to 7.2 (128-132), human erythrocytes with a pH_i range of 6.99 to 7.29 (see 120 for list of references), rat liver with pH_i = 7.23 (127) and various tumors, such as Ehrlich ascites and breast carcinoma, with a pH_i of about 7.2 (133-135). The pH of various cells, tissues, and cell fractions from the guinea pig, rat, rabbit, and mouse were estimated by visual observation of the dyes bromophenol red, bromothymol blue, and neutral red (136). Values between 6.2 and 7.3 were reported.

It has been reported that retina, fetal bone, and intestinal epithelium were among the tissues found to have apparently the highest pH_i values when determined by comparing the distribution of ^{14}C-DMO, ^{14}C-urea, and ^{14}C-carboxylinulin in whole-body sagittal sections of mice (120, 137). Withrow *et al.* (127) reported pH_i values of jejunal tissue of rats exposed to various acid-base distortions, and these values ranged from 6.77 to 7.34. However, they did not report a control pH_i value. While the bulk of the evidence indicates that the pH_i value of most animal tissues and cells is approximately 7 under normal conditions *in vivo*, a sufficiently large range of values have been reported and the value of 7.27 for the pH_i of stripped jejunal tissue maintained at I_{sc} found in this present study is reasonable.

Previous investigations have been undertaken to determine the effect of a change in membrane potential on pH_i. Caldwell (138) and Kostyuk and Sorokina (139) changed the external K^+ concentration over wide ranges and were able to decrease the potential to negligible values or even to reverse the potential with high concentrations of K^+ in the medium. However, neither of these groups found any effect of the change in membrane potential on pH_i. The frog sartorius muscle showed a stable pH_i over a several hour interval with a wide range of membrane potentials. The pH_i in the crab muscle and squid axon was influenced both by changes in the CO_2 tension of the medium and by changes in the external pH from certain salts. However, there was no correlation of the changes in the pH gradient with the changes in the membrane potential (120). In contrast to these studies Carter et al. (140-142), used various types of electrodes to determine pH_i and membrane potential. This group concluded that pH_i is directly related to the membrane potential and the extracellular pH. They found perfect agreement between calculations of pH_i from the membrane potential assuming Donnan equilibrium and the measurements made from three types of electrodes. These studies have been criticized because the pH electrodes were filled with distilled water for the internal reference solution (120). The pH of an unbuffered solution within the glass bulb is subject to continual change through leaching of alkaline constituents from the inner surface of the pH-sensitive glass membrane. The electrodes also had extremely high resistances. It's possible that the electrodes were responding to electrical potentials in the area unrelated to the pH of the cell water, thus, explaining why they found perfect agreement between their change in potential and the potentials

across the cell membrane (120). The findings in this present study of no change in pH_i values with change in imposed transmural PD is not unique. These results imply that the fraction of salicylate in the ionic form has not been altered by a change in the transmural PD, and, thus, this factor could not be an explanation for the observed change in the intestinal flux of ^{14}C-salicylate due to the change in the transmural PD.

Because most drugs can be considered to be weak electrolytes, this fact should be emphasized in studying the passage of drugs through membranes. Some investigators have said that the ionized form of the drug is very water soluble and is too large to permit diffusion through the pores of the plasma membrane (44, 45). Since the nonionized molecule is usually lipid soluble, this form of the drug permeates the membrane readily (44). These investigators then said that most drugs move through the small intestinal epithelia by passive diffusion of their nonionized forms, leading to the development of the theory of nonionic diffusion or the pH partition hypothesis. However, it was found that when steady state concentration ratios of drugs were determined between plasma and g.i. lumen, the ratios were not consistent with the pH of the bulk solutions (30). These scientists reconciled the differences of their theory and data by postulating the existence of a microenvironment at the surface of the small intestinal epithelia where the pH is maintained at a value different from the pH of the bulk solution within the intestinal lumen (30). A structural basis for maintaining the difference of pH between the microclimate and the bulk solution has yet to be identified. Also, as mentioned earlier, the concept of a calculated virtual pH at the mucosal border has been

criticized by Barry et al. (33), Benet (34, 35), and Smolen (37) as being thermodynamically unsound. The virtual pH hypothesis ignored the possibility of drug ion absorption and assumed instead that the ionized molecule did not pass membranes, but rather only the nonionized drug form was absorbed. More evidence is accumulating in the literature that supports the contention that drug ions are absorbed to an appreciable degree (1, 2, 9, 16, 37-41, 143).

A new theory has been developed by Jackson (42, 112, 144) similar to that of the previous theory by Hogben et al. (30). Jackson suggests that the mechanism for jejunal transport of weak electrolytes may be described in terms of a model system of three compartments in series, in which the pH of the intermediate compartment is greater than that of the bulk phases, rather than of lower pH as in the virtual pH theory. This theory was developed after experimentation showed no change in flux of benzoic acid and benzylamine at different transmural PDs (42). These workers checked the fluxes at open circuit (2.5 mv), at I_{sc} (0 mv), and at 25 mv. The equipment described appeared to be similar to that used in this present study; however, the procedures differed somewhat in that the tissue was not stripped of serosa and muscularis externa, and also the tissue was reported as being opened along the antimesenteric border rather than along the mesentery. The fluxes in these experiments were determined during the period 30 to 40 minutes after the addition of tracer. The electrical parameters observed in the experiments by Jackson et al. (42) were somewhat different than the values determined in this present study; they found a higher value for tissue resistance (also indicating that the tissue was unstripped) and a lower value for I_{sc}. Another important

difference in procedure concerned the amount of drug used in the flux studies. Jackson et al. (42) used 1 mM of drug in both the mucosal and serosal solutions, in addition to the radioactive tracer that was added to one compartment. This present study used only radioactive tracer, which was added to the mucosal perfusion fluid; no cold drug was added to either side. Other experiments in this present study have shown that different concentrations of added salicylate can affect the flux of ^{14}C-salicylate as well as the electrical parameters of the tissue. No mention was made by Jackson of running the flux studies with only tracer drug present, or comparing fluxes of tracer drug in the absence of unlabelled drug or in the presence of unlabelled drug on one side. These differences in techniques, as used in the Jackson study and compared to this present work, may account for the different results obtained. By taking only two samples to determine the fluxes (30-40 minute period) they could well have missed changes in the fluxes of the acid and base studied. Salicylic acid (used in this study) is similar enough in structure to benzoic acid (as used by Jackson) so that this should not be an explanation for this discrepancy. Jackson found no effect of PD changes on the fluxes of benzoic acid and benzylamine, whereas the results of this present study indicate that significant changes in the fluxes of these compounds should have occurred at the PD range used in their study. Preliminary work has shown changes in the flux of ^{14}C-amphetamine with changes in the transmural PD (145); and again amphetamine is structurally similar to benzylamine. The design of this present work is again emphasized, in that each tissue serves as its own control, and the fluxes in the same tissue are determined under both

control and experimental conditions. This procedure decreases the amount of variation often seen in biological preparations and allows a much smaller change to be observed and tested for significance.

Because Jackson found no effect of transmural PD on the fluxes of weak electrolytes, he assumed that the asymmetric patterns of weak electrolyte movement did not reflect the influence of transmural gradients of electrical potential. Jackson further assumed that one of the membrane barriers of his three compartment model (the mucosal side of the intestinal wall) is relatively impermeable to the ionized forms of the transported weak electrolytes while ions can permeate the serosal barrier. He felt this was consistent with his findings that alterations in the transmural PD did not change the flux of weak electrolytes. Using his derived equation for the three compartment model, Jackson calculated the pH of the intermediate compartment to be alkaline (range of pH 7.65 to 8.55, depending on the value of the permeability ratio used). Since past studies have shown that intracellular pH is lower than the pH of the bathing medium (120), Jackson proposed that his intermediate compartment, therefore, could not be the intracellular milieu but rather was the lateral intercellular channels. However, this new theory is really not very different than the previous virtual pH hypothesis. Jackson has now defined physiologically the region of the microenvironment and in Jackson's theory the intermediate pH is higher than the bulk pH's, rather than a lower pH as in the virtual pH hypothesis. But, the previous criticisms of Barry et al. (33), Benet (34, 35), and Smolen (37) of the virtual pH hypothesis should hold for this new theory as

well. This new proposal is just as thermodynamically untenable as the virtual pH hypothesis.

Passage of various compounds through tight junctions is now being accepted by many investigators. Fromter and Diamond (26) have proposed that a wide variety of molecules and ions are transferred across epithelial barriers via the paracellular route through the tight junctions. Other workers have found that replacing sodium ion with potassium ion in the perfusing buffer caused a decrease in the rate of absorption of various drugs, especially if they were ionized (16, 66). Since increased potassium ion concentration has been shown to cause swelling of intestinal epithelial tissue via water uptake (67), it has been proposed by Benet et al. (16) that the swelling caused by the increased potassium ion closed off the tight junctions between columnar cells in the mucosal epithelium. This phenomenon would affect transport of compounds that were absorbed via the paracellular route and shouldn't affect those compounds absorbed transcellularly.

Some investigators still do not accept the role of tight junctions in solute absorption and believe that the normal junctions between the cells are so tight that solutes crossing epithelia must pass through the plasma membranes of the individual cells (44-46). However, all cells in an animal are not alike; cells from one organ may be different than cells from another organ. Even a single organ is rarely made up of homogeneous cells. Therefore, there is no reason to assume that all cell membranes and tissue barriers throughout the body should function identically with respect to solute transfer. In fact, it has been noted that certain tissues, primarily from

the small intestine and the proximal tubule of the kidney, behave differently in terms of absorption and reabsorption of various compounds. Correlations have been made of the electrical resistance of various tissues and their permeabilities (26) and certain tissues, such as small intestine, gall bladder, and renal proximal tubule, which are more involved in the passage of various compounds, have a lower resistance and are termed "leakier" than other tissues, such as frog skin, toad bladder, and the loop of Henle, where transfer of various ions and compounds is somewhat more prohibited.

Passage across intestinal epithelia is depicted in Figure 32, which shows two intestinal cells and the tight junction between them. Transfer from mucosa to serosa is possible via the cell membrane, J_m, or via the tight junctions and the intercellular spaces, J_d. The total transfer would be a combination of the two with the physical-chemical characteristics of the compound and membrane determining the degree of importance of each pathway to the total transfer of the molecule.

An earlier theory by Burgen (146) discussed the active transport process as occurring via pores in cell membranes rather than via carrier molecules. Modifications in the shape of the pore in the cell membrane could alter the path a solute molecule might follow, thereby forcing the solute molecule to move against a concentration gradient, as shown in Figure 33. Certain positions of the pore would tend to make the solute more "comfortable" than other positions or configurations in which the molecule might be more "uncomfortable" (147). These pores could be visualized to undergo contraction and expansion, similar to an accordion-type movement, during the active transport

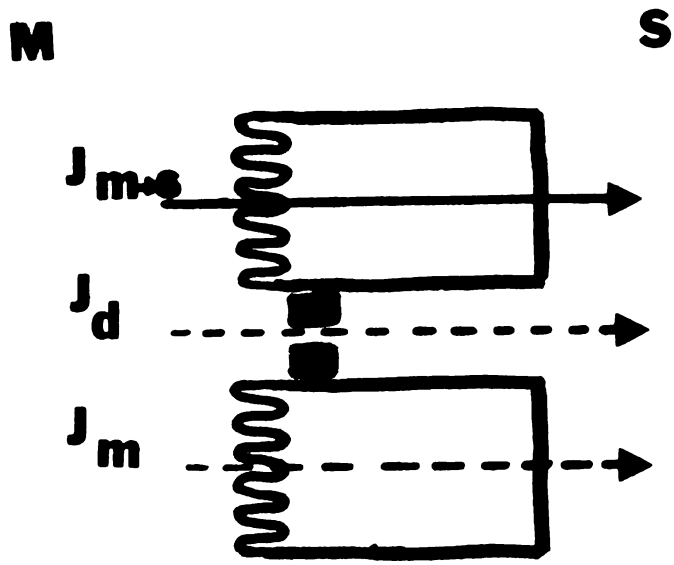

$$J_{m+d} = J_m + J_d$$

Figure 32. Diagrammatic representation of two intestinal cells illustrating transcellular pathway (J_m) and paracellular pathway (J_d).

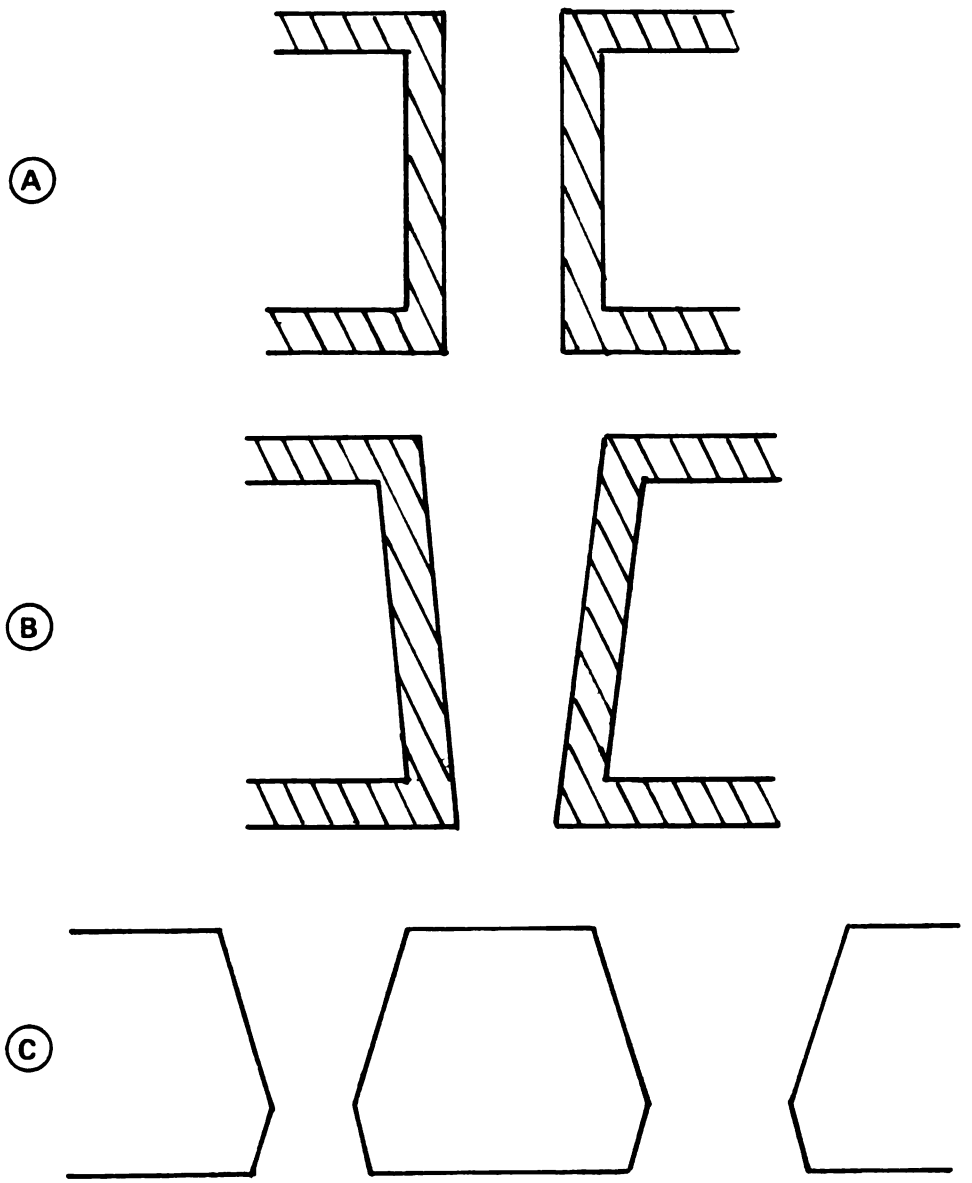

Figure 33. Diagrammatic representation of Bergen's theory of active transport. Graph A represents a pore in a cell membrane. Graph B shows the pore in different position or configuration. Graph C depicts the contraction and expansion of the pore, similar to accordion-type movement.

process, resulting in the propulsion of the solute molecule through the membrane. Portions of this theory could be extended to conceptualize the channel between two intestinal cells to be similar to the pore of a cell membrane. During active sodium-transport, an expansion of the transmural shunt pathway might be theorized, resulting in an increase of the overall flux of ^{14}C-salicylate. Conversely, inhibiting active sodium-transport may lead to a decrease in the transmural shunt pathway for ^{14}C-salicylate and, therefore, a reduction in M-to-S flux. This could be an explanation for the alteration of the ^{14}C-salicylate flux observed after the addition of agents which affect cellular metabolism. Thus, this study has shown that salicylate ions are indeed participating in salicylate intestinal transfer in this in vitro preparation. The simultaneous transfer of antipyrine with salicylate in this study showed the difference in absorption between a neutral and ionized compound. The salicylate anion is probably being absorbed via the tight junctions and intercellular spaces.

This study has shown that changes in the structure and function of the membrane, as reflected in the electrical parameters of the tissue, can be caused by various agents, and, in turn, can affect in vitro salicylate ion transport, probably via the transmural shunt pathway. The transmural flux of ^{14}C-salicylate across the epithelia of stripped rat jejunum at I_{sc} was studied in the presence of various agents affecting cellular metabolism. These were ouabain, a selective inhibitor of active sodium-transport; a choline-containing buffer devoid of sodium ion; glucose, an actively transported sugar which is also metabolized; and sodium salicylate, itself (a known uncoupler

of oxidative-phosphorylation). The common denominator in these studies appeared to be a change in transmural resistance. The M-to-S flux of ^{14}C-salicylate was decreased after the addition of serosal ouabain, mucosal salicylate, or in the presence of a sodium-free buffer. The transmural resistance was also increased due to these situations. However, the addition of glucose did not alter either the ^{14}C-salicylate flux or the transmural resistance. Thus, it is suggested that certain perturbing agents may lead to a change in the physical size of the pathway available for transport, e.g. the transmural shunt pathway. Figure 34 is a diagrammatic representation of two intestinal cells illustrating the tight junction and intercellular space before and after the addition of an inhibitor, such as ouabain or salicylate.

As seen in Figure 16, the addition of ouabain to the buffer solution perfusing the serosal side of the tissue causes a profound change in the electrical parameters of the tissue. It is apparent from this and other studies (19, 148) that the I_{sc} is greatly and immediately decreased upon the addition of ouabain. The work of Skou (149) has shown that the membrane bound Na^{+} and K^{+} activated Mg^{+2} dependent adenosine triphosphatase (NaK-ATPase) is the biochemical expression of the sodium-pump. Ouabain, a cardiac glycoside, is a specific inhibitor of NaK-ATPase and, hence, inhibits active sodium-transport. Since the transepithelial I_{sc} is a measure of active ion transport across the tissue, an inhibition of active sodium-transport would be reflected by a decrease in the I_{sc}. The enzyme NaK-ATPase has been localized on the basolateral membrane of the epithelial cells by autoradiographic studies (150) and studies on fractionated small intestinal cells (151-153). Serosal ouabain

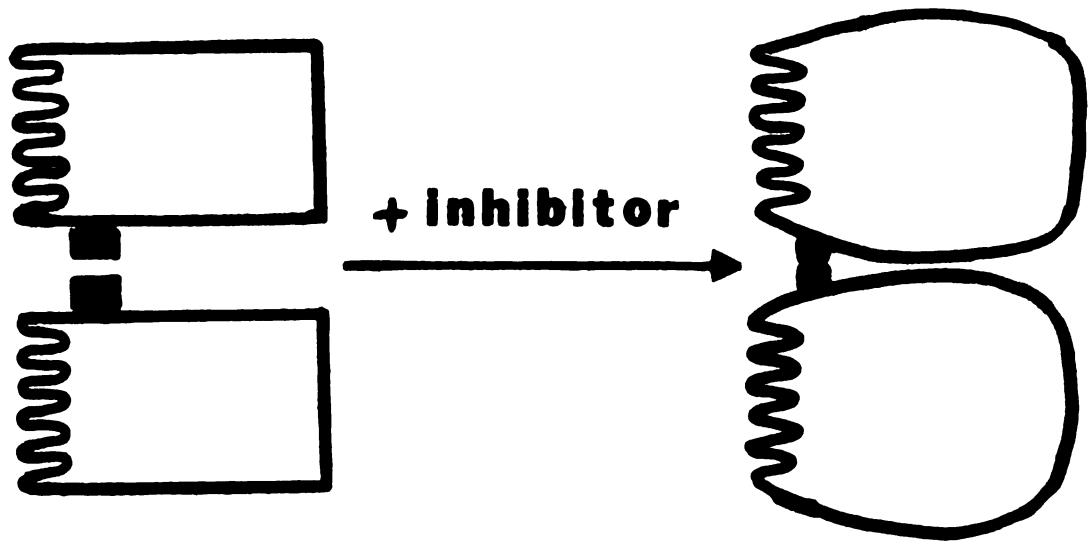

Figure 34. Diagrammatic representation of two intestinal cells illustrating tight junction, intercellular space and effect of addition of inhibitor.

caused an increase in tissue resistance (see Graph C in Figure 16) that has also been found by other workers (154). In fact, transmural tissue resistance has been observed to increase in the presence of other metabolic inhibitors, such as KCN and iodoacetate (63), cyanide (154), and amiloride (154). Rose and Schultz (63) noted a significant increase in transepithelial resistance within three to eight minutes after introduction of an inhibitor and that this increase lasted for the remainder of their experiment, i.e., at least 60 minutes. In the present studies the change in resistance is apparent shortly after the addition of ouabain; however, the peak of the resistance change is not achieved until 20 to 30 minutes after serosal ouabain introduction. The mucosal to serosal flux of ^{14}C-salicylate is also inhibited by the addition of serosal ouabain. However, there is a delay of 20 to 30 minutes before this change is apparent. A strong similarity is seen between the delay times for both the transepithelial resistance increase and the decrease in the intestinal flux of salicylate in the presence of serosal ouabain. This facet of the study, the characterization of the resistance influence on drug transport, has been pursued further by D. Adair and coworkers (155).

Mayersohn and Gibaldi (66) in their studies of <u>in vitro</u> intestinal absorption of riboflavin, salicylate and sulfanilamide, found that ouabain did not affect the transfer of any of these compounds. Ouabain was present in the buffer solutions (mucosal and serosal) initially and, thus, the rate of transfer of the drugs (with and without ouabain) were compared in different tissues rather than in the same tissue as in this present investigation. Another very important difference in methods of

experimentation included the fact that salicylate was present in the mucosal medium at a concentration of 2 mg/ml in the studies by Mayersohn and Gibaldi. The present studies indicated that the addition of mucosal salicylate at concentrations similar to that used by Mayersohn and Gibaldi caused a significant inhibition of the ^{14}C-salicylate flux. The in vitro inhibition of tracer salicylate flux by concentrations of salicylate of 1 mg/ml and higher are capable of producing an inhibition similar to that found for serosal ouabain. Thus, in those tissues studied by Mayersohn and Gibaldi in their investigation of the possible effect of ouabain on in vitro salicylate absorption the study would appear to have been invalidated by the concentrations of salicylate utilized. Also, in the investigations run by Mayersohn and Gibaldi, the buffer solutions used to perfuse the tissue did not contain calcium ions, an important component necessary for the structural integrity of the tissue. The functions of calcium ion include its influence on cellular adhesiveness, neuromuscular excitability, and maintenance and function of cell membranes (156). An agent which binds calcium ions and removes them from the tissue, edetic acid (EDTA), will alter the permeability of the intestinal tissue as shown by the change in transfer rates for various drugs (157-159). The tissue will not maintain its structural integrity for as long a period in the absence of calcium ions in the perfusing solution as it would in the presence of calcium ions. Another problem with the tissue preparation used by Mayersohn and Gibaldi was that only the mucosal side of the tissue was oxygenated, and not the serosal side. Also, the tissue was not stripped and therefore the full

thickness of tissue must be traversed for oxygen to reach the serosal side. The sodium-pump sites have been shown to be located on the basolateral surfaces of the epithelial cells (150) and thus these energy-utilizing sites were probably partially anoxic in the Mayersohn and Gibaldi preparations and would have been somewhat inhibited initially, so that the addition of ouabain may not have had much effect since these sites were already depressed. It has recently been demonstrated in rabbit ileum (72) and rat small intestine (160) that oxygen consumption and bicarbonate production by stripped mucosal preparations are more than twice that observed for the unstripped, whole tissue.

A plausible explanation for the decrease in salicylate flux observed after the addition of ouabain involves ouabain's inhibition of active sodium-transport. Inhibition of the sodium-pump, as in the presence of ouabain, leads to a cellular accumulation of sodium ions and, concomitantly, chloride ions and water. Since there is no active efflux of sodium ions there is a resultant swelling of the cell (59). This swelling causes a decrease in the transmural shunt pathway, which is thought to function via the tight junctions (26). Therefore, the change of salicylate flux after ouabain addition appears to occur via a physical disruption rather than a direct energy disruption; that is, a change in the structure of the tissue (the semi-permeable barrier) has occurred. The mucosal to serosal flux of benzoic acid across the <u>in vitro</u> rat jejunum was found to decrease in the presence of the metabolic inhibitors, 2,4-dinitrophenol, sodium fluoroacetate, and iodoacetamide (112). These results appear related to the present findings and could be used to

postulate a similar explanation.

The results of the glucose addition experiments showed no alteration in the ^{14}C-salicylate flux or transmural resistance. The transmural PD and I_{sc} were profoundly increased. Mayersohn and Gibaldi (70) found a decrease in salicylate flux in the presence of glucose, while Jackson *et al.* (42) found a large increase in benzoic acid flux in the presence of glucose, as previously discussed in the Results section.

Other contradictory work in this area appears in the literature. Esposito and Csaky (161) measured the extracellular space (ECS) in the epithelium of rat small intestine under various conditions. They incubated the intestine in Ringer-bicarbonate buffer containing 14 mM glucose which produced a swelling of the tissue (162). They explained this result as due to the accumulation of sugar in the intracellular compartment and a stimulation of intestinal water transport by glucose, resulting in a swelling of the cells with a reduction of the ECS. These findings are at least in the same direction as those of Mayersohn and Gibaldi (70), but since Mayersohn and Gibaldi's methods are questionable, the results of Esposito and Csaky can't be called a corroboration of their data.

Munck and Schultz (73) measured the unidirectional influx of sodium ion across the epithelium of *in vitro* rat jejunum as a function of the transepithelial electrical potential difference using the technique described by Frizzell and Schultz (43). The unidirectional influx of sodium ion in the presence and absence of 28 mM glucose was plotted as a function of $\xi^{-1/2}$, which in turn is a function of the transmural PD, as was discussed in the Introduction. Their results showed two parallel

lines in the flux vs $\xi^{-1/2}$ plot. This indicated that the slope in both conditions was the same ($_oJ_d$) and only the intercept (J_m) was changed. The presence of glucose markedly enhanced the influx component that is independent of PD, the J_m or the flux via the cell membrane, but did not affect the flux via the transmural shunt pathway, J_d. These results suggest that the enhancement of sodium ion influx by glucose is not due to a change in the permeability of the extracellular diffusional pathway; but, rather, add to the evidence that the increase in sodium ion influx in the presence of actively transported sugars is the result of a carrier-mediated co-transport process located at the brush border of the villus absorptive cells (163). The results of the studies reported here are entirely consistent with those found by Munck and Schultz (73). No change was observed in the resistance of the tissue due to the addition of glucose to the perfusion medium. This corresponds to their findings of parallel lines in the J vs $\xi^{-1/2}$ plot which implies no change in the flux of sodium ion via the transmural shunt pathway. Also, the addition of glucose did not affect the M-to-S flux of ^{14}C-salicylate. This is in keeping with the suggestion that glucose does not affect the permeability of the membrane, at least not to sodium ions, but, rather is involved with a carrier mechanism that leads to an increase in active sodium-transport. The transport of salicylate has been assumed to occur passively in the g.i. tract, though an active or facilitated transport process for salicylate has been suggested for other sites, such as kidney and brain. The observations of this study suggest that the transport of salicylate is not affected by a change in cellular energy utilization that does

not affect the transmural resistance at the same time. (Ouabain represents an agent where a change in cellular energy utilization is observed to cause a change in transmural resistance and, concomitantly, a change in transmural flux of ^{14}C-salicylate.) It appears that a change in the transmural shunt pathway is the prime factor causing a change in the M-to-S transport of ^{14}C-salicylate. On the basis of their influx studies, Munck and Schultz (73) also suggested that,

> ". . .ionic diffusion takes place predominately via aqueous, extracellular pathways. These observations also suggest that, as for rabbit ileum and rabbit gall bladder, the diffusional pathway is electrically neutral and that cation selectivity is a consequence of the fact that the pathway is lined with either fixed dipolar molecules or fixed zwitterions (i.e., dissociated anions and cations in approximately equivalent amounts) aligned so that the electonegative group restricts the partition coefficient and/or mobility of anions [(43, 56, 164, 165)]. However, additional study is necessary to verify this notion."

The M-to-S flux of ^{14}C-salicylate was inhibited by the addition of salicylate to the mucosal bathing solution. Much work has been done in other laboratories on the absorption rates of salicylate under various conditions. For instance, salicylate flux has been measured by Mayersohn and Gibaldi (66, 68, 71) in the presence of various additives, such as different ions, drugs, or metabolic inhibitors. Salicylate flux was also determined in diseased and fasted animals (166-168). The various additives often showed negligible effects on the absorption rates. However, in these previous experiments salicylate was present at 1 mg/ml, or 2 mg/ml concentrations, and sometimes even higher. The activity of salicylate alone at these concentrations might be sufficient to mask the effect

of the other compounds. Also, the action of this concentration of salicylate on the normal intestinal mucosa may be different than that which may occur in diseased or fasted mucosa. Thus, it would be best to run tracer fluxes only, to determine the true effects of the additives or the condition of the intestinal mucosa.

This study also demonstrated an inhibition in the transmural I_{sc} of the stripped rat jejunum after the addition of mucosal salicylate. Similar results were shown with ouabain, which inhibits the sodium pump. Salicylate is known to be an uncoupler of oxidative phosphorylation and thus affects the active transport of ions across the tissue, which is reflected by the transmural I_{sc}. As hypothesized for ouabain, disruption of this active transport process may lead to a cellular accumulation of sodium ion, and, concomitantly, chloride ion and water, resulting in cell swelling. This swelling could cause a decrease in the extracellular space and thus a decrease in the transmural shunt pathway, corresponding to an increase in the transmural resistance. Thus, it is thought that the inhibition of the flux of ^{14}C-salicylate due to salicylate addition appears to occur via a physical disruption rather than a general energy disruption.

REFERENCES

1. Pyorala, K., J. Jussila, O. Mustala, and M. Siurala. Absorption of Warfarin from the Stomach and Small Intestine. Scand. J. Gastroenterol. (suppl.), 9, 95-103 (1970).

2. Siurala, M., O. Mustala, K. Pyorala, M. Kekki, M. Airaksinen, J. Jussila, H. Salmi, and R. Jalkunen. Studies on Gastrointestinal Absorption of Drugs. Acta Hepato-Gastroenterol., 19, 190-198 (1972).

3. Holdworth, C.D. and A.M. Dawson. The Absorption of Monosaccharides in Man. Clin. Sci., 27, 371-379 (1964).

4. Sladen, G.E. and A.M. Dawson. Further Studies on the Perfusion Method for Measuring Intestinal Absorption in Man: The Effects of a Proximal Occlusive Balloon and a Mixing Segment. Gut, 11, 947-954 (1970).

5. Rohde, J.E. and L.C. Chen. Permeability and Selectivity of Canine and Human Jejunum During Cholera. Gut, 13, 191-196 (1972).

6. Nayak, R.K. and L.Z. Benet. The Use of the Unanesthetized Rhesus Monkey as a Model for Studying the Gastrointestinal Absorption of Drugs. J. Pharmacokinet. Biopharm., 2, 417-431 (1974).

7. Nayak, R.K. Gastrointestinal Absorption Studies in Unanesthetized Rhesus Monkeys. A dissertation submitted in partial fulfillment of the requirements for the degree of Doctor of Philosophy (Pharmaceutical Chemistry) to the Graduate Division, University of California, San Francisco, 1973.

8. Levine, R.R. and E.W. Pelikan. The Influence of Experimental Procedures and Dose on the Intestinal Absorption of an Onium Compound, Benzomethamine. J. Pharmacol. Exp. Ther., 131, 319-327 (1961).

9. Doluisio, J.T., N.F. Billups, L.W. Dittert, E.T. Sugita, and J.V. Swintosky. Drug Absorption I: An In Situ Rat Gut Technique Yielding Realistic Absorption Rates. J. Pharm. Sci., 58, 1196-1200 (1969).

10. Schanker, L.S., D.J. Tocco, B.B. Brodie, and C.A.M. Hogben. Absorption of Drugs from the Rat Small Intestine. J. Pharmacol. Exp. Ther., 123, 81-88 (1958).

11. Wilson, T.H. and G. Wiseman. The Use of Sacs of Inverted Small Intestine for the Study of the Transference of Substances from the Mucosal to the Serosal Surface. J. Physiol. (London), 123, 116-125 (1954).

12. Crane, R.K. and T.H. Wilson. In Vitro Method for the Study of the Rate of Intestinal Absorption of Sugars. J. Appl. Physiol., 12, 145-146 (1958).

13. Dietschy, J.M., H.S. Salomon, and M.D. Siperstein. Bile Acid Metabolism.I. Studies on the Mechanisms of Intestinal Transport. J. Clin. Invest., 45, 832-846 (1966).

14. Bates, T.R. and M. Gibaldi. "Gastrointestinal Absorption of Drugs," in Current Concepts in the Pharmaceutical Sciences: Biopharmaceutics. J. Swarbrick, ed., Lea and Febiger, Philadephia, 1970, Chapter 2, pp. 57-99.

15. Parsons, D.S. "Methods for Investigation of Intestinal Absorption," in Handbook of Physiology. Sec. 6: Alimentary Canal, Vol. III, Am. Physiol. Society, Washington, D.C., 1968, Chapter 64, pp. 1177-1216.

16. Benet, L.Z., J.M. Orr, R.H. Turner, and H.S. Webb. Effect of Buffer Constituents and Time on Drug Transfer Across In Vitro Rat Intestine. J. Pharm. Sci., 60, 234-238 (1971).

17. Turner, R.H., C.S. Mehta, and L.Z. Benet. Apparent Directional Permeability Coefficients for Drug Ions: In Vitro Intestinal Perfusion Studies. J. Pharm. Sci., 59, 590-595 (1970).

18. Ussing, H.H. and K. Zerahn. Active Transport of Sodium as the Source of Electric Current in the Short-Circuited Isolated Frog Skin. Acta Physiol. Scand., 23, 110-127 (1951).

19. Schultz, S.G. and R. Zalusky. Ion Transport in Isolated Rabbit Ileum .I. Short-Circuit Current and Na Fluxes. J. Gen. Physiol., 47, 567-584 (1964).

20. Field, M., D. Fromm, and I. McColl. Ion Transport in Rabbit Ileal Mucosa. I. Na and Cl Fluxes and Short-Circut Current. Am. J. Physiol., 220, 1388-1396 (1971).

21. Schultz, S.G. and R.A. Frizzell. An Overview of Intestinal Absorptive and Secretory Processes. Gastroenterology, 63, 161-170 (1972).

22. Hogben, C.A.M. Active Transport of Chloride by Isolated Frog Gastric Epithelium: Origin of the Gastric Mucosal Potential. Am. J. Physiol., 180, 641-649 (1955).

23. Knauf, H. and E. Fromter. Elektrische Untersuchungen am Hauptausfuhrungsgang der Speicheldrusen des Menschen. II. Bestimmung des Kurzschlusstromes. Pfluegers Arch., 316, 259-274 (1970).

24. Leaf, A., J. Anderson, and L.B. Page. Active Sodium Transport by the Isolated Toad Bladder. J. Gen. Physiol., 41, 657-668 (1958).

25. Ussing, H.H., P. Kruhoffor, J. Hess-Thaysen, and N.A. Thorn. The Alkali Metal Ions in Biology, Springer, Berlin, 1960.

26. Fromter, E. and J. Diamond. Route of Passive Ion Permeation in Epithelia. Nature (London), New Biol., 235, 9-13 (1972).

27. Fromter, E. The Route of Passive Ion Movement through the Epithelium of Necturus Gallbladder. J. Membr. Biol., 8, 259-301 (1972).

28. Davson, H. and J.F. Danielli. Permeability of Natural Membranes, Cambridge University Press, New York, 1952.

29. Schanker, L.S., P.A. Shore, B.B. Brodie, and C.A.M. Hogben. Absorption of Drugs from the Stomach. I. The Rat. J. Pharmacol. Exp. Ther., 120, 528-538 (1957).

30. Hogben, C.A.M., D.J. Tocco, B.B. Brodie, and L.S. Schanker. On the Mechanism of Intestinal Absorption of Drugs. J. Pharmacol. Exp. Ther., 125, 275-282 (1959).

31. Schanker, L.S. Absorption of Drugs from the Rat Colon. J. Pharmacol. Exp. Ther., 126, 283-290 (1959).

32. Shore, P.A., B.B. Brodie, and C.A.M. Hogben. The Gastric Secretion of Drugs: A pH Partition Hypothesis. J. Pharmacol. Exp. Ther., 119, 361-369 (1957).

33. Barry, R.J.C., M.J. Jackson, and D.H. Smyth. Transfer of Propionate by Rat Small Intestine In Vitro. J. Physiol. (London), 182, 150-163 (1966).

34. Benet, L.Z. Intestinal pH and its Effect on Drug Absorption. I. An examination of the Virtual pH Hypothesis, presented to the A.Ph.A. Academy of Pharmaceutical Sciences, 114th Annual Meeting of the American Pharmaceutical Association, Las Vegas, April, 1967.

35. Benet, L.Z. "Biopharmaceutics as a Basis for the Design of Drug Products," in Drug Design. Vol. 4. E. Ariens, ed., Chapter 1, pp. 1-35.

36. Wagner, J.G. Biopharmaceutics: 5. Mechanisms of Gastrointestinal Absorption of Drugs. Drug Intell., 2, 244-248 (1968).

37. Smolen, V.F. Misconceptions and Thermodynamic Untenability of Deviations from pH-Partition Hypothesis. J. Pharm. Sci., 62, 77-79 (1973).

38. Smyth, D.H. and R. Whittam. Membrane Transport and Intestinal Absorption. Br. Med. Bull., 23, 231-235 (1967).

39. Lanman, R.C., C.E. Stremsterfer, and L.S. Schanker. Absorption of Organic Ions from the Rat Small Intestine. Xenobiotica, 1, 613-619 (1971).

40. Nogami, H. and T. Matsuzawa. Studies on the Absorption and Excretion of Drugs. I. Kinetics of Penetration of Acidic Drug, Salicylic Acid, through the Intestinal Barrier In Vitro. Chem. Pharm. Bull., 9, 532-540 (1961).

41. Nogami, H. and T. Matsuzawa. Studies on the Absorption and Excretion of Drugs. II. Kinetics of Penetration of Basic Drug, Aminopyrine, through the Intestinal Barrier In Vitro. Chem. Pharm. Bull., 10, 1055-1060 (1962).

42. Jackson, M.J., Y. Shiau, S. Bane, and M. Fox. Intestinal Transport of Weak Electrolytes: Evidence in Favor of a Three-Compartment System. J. Gen. Physiol., 63, 187-213 (1974).

43. Frizzell, R.A. and S.G. Schultz. Ionic Conductances of Extracellular Shunt Pathway in Rabbit Ileum: Influence of Shunt on Transmural Sodium Transport and Electrical Potential Differences. J. Gen. Physiol., 59, 318-346 (1972).

44. Hogben, C.A.M. "Routes of Drug Administration: Biological Membranes and Their Passage by Drugs," in Handbook of Experimental Pharmacology. Vol. 28, Part 1, Springer Verlag, 1971, Chapter 1.

45. Schanker, L.S. "Absorption of Drugs from the Gastrointestinal Tract," in Handbook of Experimental Pharmacology. Vol. 28, Part 1, Springer Verlag, 1971, Chapter 2.

46. Cohn, V.H. "Transmembrane Movement of Drug Molecules," in Fundamentals of Drug Metabolism and Drug Disposition. B.N. LaDu, H.G. Mandel, E.L. Way, eds., Waverly Press, Baltimore, 1971, Chapter 1.

47. Grantham, J.J., C.E. Ganote, M.B. Burg, and J. Orloff. Paths of Transtubular Water Flow in Isolated Renal Collecting Tubules. J. Cell Biol., 41, 562-576 (1969).

48. Schmidt-Nielsen, B. and L.E. Davis. Fluid Transport and Tubular Intercellular Spaces in Reptilian Kidneys. Science, 159, 1105-1108 (1968).

49. Claude, P. and D.A. Goodenough. Fracture Faces of Zonula Occludentes from "Tight" and "Leaky" Epithelia. J. Cell Biol., 58, 390-400 (1973).

50. Moreno, J.H. and J.M. Diamond. "Cation Permeation Mechanisms and Cation Selectivity in 'Tight Junctions' of Gallbladder Epithelium" in Membranes. Vol. 3. G. Eisenman, ed., Marcel Dekker, Inc., New York, 1975, pp. 383-497.

51. Wade, J.B. and M.J. Karnovsky. The Structure of the Zonula Occludens: A Single Fibril Model Based on Freeze-Fracture. J. Cell Biol., 60, 168-180 (1974).

52. Weinstein, R.S. and N.S. McNutt. Cell Junctions. N. Engl. J. Med., 286, 521-524 (1972).

53. Diamond, J.M. Tight and Leaky Junctions of Epithelia: A Perspective on Kisses in the Dark. Fed. Proc., 33, 2220-2224 (1974).

54. Barry, P.H. and J.M. Diamond. A Theory of Ion Permeation through Membranes with Fixed Neutral Sites. J. Membr. Biol., 4, 295-330 (1971).

55. Wright, E.M., P.H. Barry, and J.M. Diamond. The Mechanism of Cation Permeation in Rabbit Gallbladder. Conductances, the Current-Voltage Relation, the Concentration Dependence of Anion-Cation Discrimination, and the Calcium Competition Effect. J. Membr. Biol., 4, 331-357 (1971).

56. Barry, P.H., J.M. Diamond, and E.M. Wright. The Mechanism of Cation Permeation in Rabbit Gallbladder. Dilution Potentials and Biionic Potentials. J. Membr. Biol., 4, 358-394 (1971).

57. Machen, T.E., D. Erlij, and F.B.P. Wooding. Permeable Junctional Complexes: The Movement of Lanthanum Across Rabbit Gallbladder and Intestine. J. Cell Biol., 54, 302-312 (1972).

58. Whittembury, G. and F.A. Rawlins. Evidence of a Paracellular Pathway for Ion Flow in the Kidney Proximal Tubule: Electromicroscopic Demonstration of Lanthanum Precipitate in the Tight Junction. Pfluegers Arch., 330, 302-309 (1971).

59. Ussing, H.H., D. Erlij, and U. Lassen. Transport Pathways in Biological Membranes. Annu. Rev. Physiol., 36, 17-49 (1974).

60. Schultz, S.G., R.A. Frizzell, and H.N. Nellans. Ion Transport by Mammalian Small Intestine. Annu. Rev. Physiol., 36, 51-91 (1974).

61. Windhager, E.E., E.L. Boulpaep, and G. Giebisch. Electrophysiological Studies on Single Nephrons. Proc. Int. Congr. Nephrol., 3, 35-47 (1966).

62. Ussing, H.H. and E.E. Windhager. Nature of Shunt Path and Active Transport Path through Frog Skin Epithelium. Acta Physiol. Scand., 61, 484-504 (1964).

63. Rose, R.C. and S.G. Schultz. Studies on the Electrical Potential Profile Across Rabbit Ileum: Effects of Sugars and Amino Acids on Transmural and Transmucosal Electrical Potential Differences. J. Gen. Physiol., 57, 639-663 (1971).

64. Diamond, J.M. and W.H. Bossert. Standing-Gradient Osmotic Flow: A Mechanism for Coupling of Water and Solute Transport in Epithelia. J. Gen. Physiol., 50, 2061-2083 (1967).

65. Edmonds, C.J. "Salts and Water," in Intestinal Absorption, Biomembranes. 4B. D.H. Smyth, ed., Plenum Press, New York, 1974, Chapter 14, pp. 711-759.

66. Mayersohn, M. and M. Gibaldi. Drug Transport. II. The Effect of Various Cations on the Passive Transfer of Drugs Across the Everted Rat Intestine. Biochim. Biophys. Acta, 196, 296-304 (1970).

67. Bosackova, J. and R.K. Crane. Cation Inhibition of Active Sugar Transport and Na-22 Influx into Hamster Small Intestine, In Vitro. Biochim. Biophys. Acta, 102, 423-435 (1965).

68. Mayersohn, M., M. Gibaldi, and B. Grundhofer. Drug Transport. V: Mechanism of Potassium Ion Inhibition of Passive Transfer of Solutes Across Everted Rat Intestine. J. Pharm. Sci., 60, 1813-1817 (1971).

69. Mayersohn, M. and M. Gibaldi. Drug Transport. I: Effect of Potassium Ion on the In Vitro Transfer of Serosal Drugs Across the Rat Intestine: Preliminary Observations. J. Pharm. Sci., 58, 1429-1430 (1969).

70. Mayersohn, M. and M. Gibaldi. Drug Transport. III: Influence of Various Sugars on Passive Transfer of Several Drugs Across the Everted Rat Intestine. J. Pharm. Sci., 60, 225-230 (1971).

71. Mayersohn, M. and M. Gibaldi. Drug Transport. IV: Influence of Hypotonic and Hypertonic Solutions on Passive Drug Transfer Across the Everted Rat Intestine. J. Pharm. Sci., 60, 326-327 (1971).

72. Nellans, H.N., R.A. Frizzell, and S.G. Schultz. Brush-Border Processes and Transepithelial Na and Cl Transport by Rabbit Ileum. Am. J. Physiol., 226, 1131-1141 (1974).

73. Munck, B.G. and S.G. Schultz. Properties of the Passive Conductance Pathway Across In Vitro Rat Jejunum. J. Membr. Biol., 16, 163-174 (1974).

74. Clarkson, T.W. and S.R. Toole. Measurement of Short-Circuit Current and Ion Transport Across the Ileum. Am. J. Physiol., 206, 658-668 (1964).

75. Mullins, L.J. Penetration of Anions through Frog Skin. Am. J. Physiol., 194, 369-372 (1958).

76. Menninger, J.R., F.M. Snell, and R.A. Spangler. Voltage Clamp for Biological Investigations. Rev. Sci. Instrum., 31, 519-521 (1960).

77. Wright, G.H. A Simple Device for Electronic Measurement of Short-Circuit Current. J. Physiol. (London), 178, 1P-2P (1965).

78. LaForce, R.C. Device to Measure the Voltage-Current Relations in Biological Membranes. Rev. Sci. Instrum., 38, 1225-1228 (1967).

79. Barry, W., H.E.F. Davies, and M.J. Wooster. Apparatus for Automatic Short-Circuiting of Frog Skin In Vitro. J. Physiol. (London), 213, 13P (1971).

80. Isaacson, L.C., R.J. Douglas, and J. Pepler. Automatic Measurement of Voltage and Short-Circuit Current Across Amphibian Epithelia. J. Applied Physiol., 31, 298-299 (1971).

81. Candia, O.A. An Automatic Voltage Clamp Recorder for Inexcitable Membranes. IEEE Trans. Biomed. Eng., 13, 189-194 (1966).

82. Quay, J.F., C.F. Rothe, and W. McD. Armstrong. An Automatic Voltage Clamp Device with Solution Resistance Compensation for Measuring Transepithelial Electrical Parameters. Biophys. J., 8, A-45 (1968).

83. Rothe, C.F., J.F. Quay, and W.M. Armstrong. Measurement of Epithelial Characteristics with an Automatic Voltage Clamp Device with Compensation for Solution Resistance. IEEE Trans. Biomed. Eng., 16, 160-164 (1969).

84. Kasbekar, D.K. Effects of Salicylate and Related Compounds on Gastric HCl Secretion. Am. J. Physiol., 225, 521-527 (1973).

85. Pierson, R.N., P.R. Holt, and R.M. Watson. Aspirin and Gastrointestinal Bleeding: Chromate Blood Loss Studies. Am. J. Med., 31, 259-265 (1961).

86. Roth, J.L., A. Valdes-Dapena, and P. Pieses. Topical Action of Salicylates in Gastrointestinal Erosions and Hemorrhage. Gastroenterology, 44, 146-158 (1964).

87. Thorsen, W.B., Jr., D. Western, and Y. Tanaka. Aspirin Injury to the Gastric Mucosa: Gastrocamera Observations of the Effect of pH. Arch. Intern. Med., 121, 499-506 (1968).

88. Hingson, D.J. and S. Ito. Effect of Aspirin and Related Compounds on the Fine Structure of Mouse Gastric Mucosa. Gastroenterology, 61, 156-177 (1971).

89. Levitan, H. and J.L. Barker. Effect of Non-Narcotic Analgesics on Membrane Permeability of Molluscan Neurones. Nature (London), New Biol., 239, 55-57 (1972).

90. Randall, L.O. "Non-Narcotic Analgesics," in Physiological Pharmacology, Vol. 1, W.S. Root and F.G. Hofmann, eds., Academic Press, New York, 1963, pp. 313-416.

91. Lim, R.K.S. Pain. Annu. Rev. Physiol., 32, 269-288 (1970).

92. Collier, H.O.J. A Pharmacological Analysis of Aspirin. Adv. Pharmacol. Chemother., 7, 333-405 (1969).

93. Woodbury, D.M. "Analgesics and Antipyretics," in The Pharmacological Basis of Therapeutics. L.S. Goodman and A. Gilman, eds., MacMillan, New York, 1965, Chapter 17, pp. 312-344.

94. Ferreira, S.H. Prostaglandins, Aspirin-Like Drugs and Analgesia. Nature (London), New Biol., 240, 200-203 (1972).

95. Hamberg, M. Inhibition of Prostaglandin Synthesis in Man. Biochem. Biophys. Res. Commun., 49, 720-726 (1972).

96. Barker, J.L. and H. Levitan. Salicylate: Effect on Membrane Permeability of Molluscan Neurons. Science, 172, 1245-1247 (1971).

97. Barker, J.L. and H. Levitan. The Antagonism between Salicylate-Induced and pH-Induced Changes in the Membrane Conductance of Molluscan Neurons. Biochim. Biophys. Acta, 274, 638-643 (1972).

98. Levitan, H. and J.L. Barker. Salicylate: A Structure-Activity Study of Its Effects on Membrane Permeability. Science, 176, 1423-1425 (1972).

99. Levitan, H. and J.L. Barker. Membrane Permeability: Cation Selectivity Reversibly Altered by Salicylate. Science, 178, 63-64 (1972).

100. McLaughlin, S. Salicylates and Phospholipid Bilayer Membranes. Nature (London), 243, 234-236 (1973).

101. McLaughlin, S. The Mechanism of Action of DNP on Phospholipid Bilayer Membranes. J. Membr. Biol., 9, 361-372 (1972).

102. McLaughlin, S.G.A., G. Szabo, and G. Eisenman. Divalent Ions and the Surface Potential of Charged Phospholipid Membranes. J. Gen. Physiol., 58, 667-687 (1971).

103. Krebs, H.A. and K. Henseleit. Untersuchungen Uber die Harnstoffbildung im Tier Korper. Hoppe-Seylers Z. Physiol. Chem., 210, 33-66 (1932).

104. Asano, Y., U.A. Liberman, and I.S. Edelman. Thyroid Thermogenesis: Relationships between Na^+-Dependent Respiration and Na^+-K^+-Adenosine Triphosphatase Activity in the Rat Skeletal Muscle. J. Clin. Invest., Feb. 1976, in press.

105. Wolfe, D.L., S.C. Forland, and L.Z. Benet. Drug Transfer Across Intact Rat Intestinal Mucosa Following Surgical Removal of Serosa and Muscularis Externa. J. Pharm. Sci., 62, 200-205 (1973).

106. Waddell, W.J. and T.C. Butler. Calculation of Intracellular pH from the Distribution of 5-5-Dimethyl-2, 4-oxazolidinedione (DMO). Application to Skeletal Muscle of the Dog. J. Clin. Invest., 38, 720-729 (1959).

107. Irvine, R.O.H., S.J. Saunders, M.D. Milne, and M.A. Crawford. Gradients of Potassium and Hydrogen Ion in Potassium-Deficient Voluntary Muscle. Clin. Sci., 20, 1-18 (1960).

108. Waddell, W.J. "Intracellular pH," in Alfred Benzon Symposium III, Ion Homeostasis of the Brain, B.K. Siesjo and S.C. Sorensen, eds., Academic Press, New York, 1971.

109. Gulyassy, P.F. Intracellular H^+ Concentration of the Isolated Urinary Bladder of the Toad. Nature (London), 206, 511-512 (1965).

110. Civan, M.M. Effects of Active Sodium Transport on Current Voltage Relationship of Toad Bladder. Am. J. Physiol., 219, 234-245 (1970).

111. Mandel, L.J. and P.F. Curran. Response of the Frog Skin to Steady-State Voltage Clamping. I. The Shunt Pathway. J. Gen. Physiol., 59, 503-518 (1972).

112. Jackson, M.J. and B.N. Morgan. Relations of Weak-Electrolyte Transport and Acid-Base Metabolism in Rat Small Intestine In Vitro. Am. J. Physiol., 228, 482-487 (1975).

113. Barry, R.J.C. and J. Eggenton. "Electrical Activity of the Intestine," in Biomembranes, Intestinal Absorption, Vol. 4B, D.H. Smyth, ed., Plenum Press, New York, 1974, Chapter 18, pp. 917-960.

114. Clarkson, T.W., A.C. Cross, and S.R. Toole. Dependence on Substrate of the Electrical Potential Across the Isolated Gut. Nature (London), 191, 501-502 (1961).

115. Clarkson, T.W., A.C. Cross, and S.R. Toole. Electrical Potentials Across Isolated Small Intestine of the Rat. Am. J. Physiol., 200, 1233-1235 (1961).

116. Barry, R.J.C., S. Dikstein, J. Matthews, and D.H. Smyth. Electrical Potentials in the Isolated Intestine. J. Physiol. (London), 155, 17P-18P (1961).

117. Hodgman, C.D., Ed.-in-Chief, Handbook of Chemistry and Physics. The Chemical Rubber Publishing Co., Cleveland, 1960.

118. Bodforss, S. and A. Guthe. Constitution of Salipyrine. Ber., 57B, 842-846 (1924).

119. Butler, T.C., W.J. Waddell, and D.T. Poole. The pH of Intracellular Water. Ann. N.Y. Acad. Sci., 133, 73-77 (1966).

120. Waddell, W.J. and R.G. Bates. Intracellular pH. Physiol. Rev., 49, 285-329 (1969).

121. Waddell, W.J. and H.F. Hardman. Intracellular pH of Isolated Perfused Turtle Heart. Am. J. Physiol., 199, 1112-1114 (1960).

122. Tobin, R.B. Plasma, Extracellular and Muscle Electrolyte Responses to Acute Metabolic Acidosis. Am. J. Physiol., 186, 131-138 (1956).

123. Robin, E.D., H.V. Murdaugh, Jr., and E. Weiss. Acid-Base, Fluid and Electrolyte Metabolism in the Elasmobranch. I. Ionic Composition of Erythrocytes, Muscle and Brain. J. Cell. Comp. Physiol., 64, 409-418 (1964).

124. Grantham, J.J. and P.R. Schloerb. Measurement of Intracellular Hydrogen Ion Concentration in Patients. Surg. Forum, 15, 81-82 (1964).

125. Bittar, E.E., M.F. Watt, V.R. Pateras, and A.E. Parrish. The pH of Muscle in Laennec's Cirrhosis and Uremia. Clin. Sci., 23, 265-276 (1962).

126. Irvine, R.O.H., R.O. Farrelly, and S. Fraser. Studies on the Effect of Glycerophosphate and Phosphatidyl Ethanolamine on Intracellular pH and Electrolyte Content of Voluntary Muscle. Clin. Sci., 27, 1-7 (1964).

127. Withrow, C.D., T. Elsmore, J.A. Williams, and D.M. Woodbury. "Hydrogen Ion Distribution and Regulation in Various Rat Tissues," in Alfred Benzon Symposium III, Ion Homeostasis of the Brain, B.K. Siesjo and S.C. Sorensen, eds., Academic Press, New York, 1970, pp. 341-351.

128. Robin, E.D. "Intra- and Subcellular Aspects of the Chemical Control of Ventilation," in The Regulation of Human Respiration. D.J.C. Cunningham and B.B. Lloyd, eds., Blackwell, Oxford, 1963, pp. 223-233.

129. Roos, A. Intracellular pH and Intracellular Buffering Power of the Cat Brain. Am. J. Physiol., 209, 1233-1246 (1965).

130. Brodie, D.A. and D.M. Woodbury. Acid-Base Changes in Brain and Blood of Rats Exposed to High Concentrations of Carbon Dioxide. Am. J. Physiol., 192, 91-94 (1958).

131. Koch, A. and D.M. Woodbury. Carbonic Anhydrase Inhibition and Brain Electrolyte Composition. Am. J. Physiol., 198, 434-440 (1960).

132. Ponten, U. The CO_2-Binding Capacity of Rat Brain Tissue In Vivo. Experientia, 20, 287-290 (1964).

133. Poole, D.T. Intracellular pH of the Ehrlich Ascites Tumor Cell as It Is Affected by Sugars and Sugar Derivatives. J. Biol. Chem., 242, 3731-3736 (1967).

134. Poole, D.T., T.C. Butler, and W.J. Waddell. Intracellular pH of the Ehrlich Ascites Tumor Cell. J. Natl. Cancer Inst., 32, 939-946 (1964).

135. Schloerb, P.R., G.L. Blackburn, J.J. Grantham, D.S. Mallard, and G.K. Cage. Intracellular pH and Buffering Capacity of the Walker-256 Carcinoma. Surgery, 58, 5-11 (1965).

136. Novelli, A., G. Nanni, and I. Baldini. The pH as Controlling Factor of Shape and Function of Mitochondria. Experientia, 18, 558-559 (1962).

137. Waddell, W.J. and G.C. Marlowe. "The Tissue Distribution of 2-C^{14}-5,5-Dimethyl-2,4-oxazolidinedione (C^{14}-DMO), C^{14}-Inulin, and C^{14}-Urea Studied with Whole Body Autoradiography," IIIrd Intern. Congr. Nephrol., Vol. 2, Washington, D.C., 1966, p. 292.

138. Caldwell, P.C. Studies on the Internal pH of Large Muscle and Nerve Fibres. J. Physiol. (London), 142, 22-62 (1958).

139. Kostyuk, P.G. and Z.A. Sorokina. "On the Mechanism of Hydrogen Ion Distribution Between Cell Protoplasm and the Medium," in Membrane Transport and Metabolism. A. Kleinzeller and A. Kotyk, eds., Academic Press, New York, 1960, pp. 193-203.

140. Carter, N.W. Direct Measurement of Intracellular pH with Glass Microelectrodes. Clin. Res., 9, 177 (1961).

141. Carter, N.W., F.C. Rector, Jr., D.S. Campion, and D.W. Seldin. Measurement of Intracellular pH with Glass Microelectrodes. Fed. Proc., 26, 1322-1326 (1967).

142. Carter, N.W., F.C. Rector, Jr., D.S. Campion, and D.W. Seldin. Measurement of Intracellular pH of Skeletal Muscle with pH-Sensitive Glass Microelectrodes. J. Clin. Invest., 46, 920-933 (1967).

143. Ochsenfahrt, H. and D. Winne. Der Einfluss der Durchblutung auf die Resorption von Arzneimitteln aus dem Jejunum der Ratte. Naunyn Schmiederbergs Arch. Pharmakol., 264, 55-75 (1969).

144. Jackson, M.J. "Transport of Short Chain Fatty Acids," in Biomembranes, Intestinal Absorption. Vol. 4B, D.H. Smyth, ed., Plenum Press, New York, 1974, Chapter 13, pp. 673-709.

145. Adair, D.W., S.F. Adair, and L.Z. Benet. Manuscript in Preparation.

146. Burgen, A.S.V. The Physiological Ultrastructure of Cell Membranes. Canad. J. Biochem. Physiol., 35, 569-578 (1957).

147. Davson, H. "Ionic Equilibria, Bioelectric Potentials, and Active Transport," in A Textbook of General Physiology, Vol. 1, 4th ed., Williams and Wilkins Co., Baltimore, 1970, Chapter 10, pp. 548-713.

148. Lyon, I. and R.K. Crane. Studies on Transmural Potentials In Vitro in Relation to Intestinal Absorption. II. An Effect of Ouabain on Glucose-Dependent Increment of Transmural Potential of Rat Small Intestine. Biochim. Biophys. Acta, 126, 146-153 (1966).

149. Skou, J.C. The Influence of Some Cations on an Adenosine Triphosphate from Peripheral Nerves. Biochim. Biophys. Acta, 23, 394-401 (1957).

150. Stirling, C.E. Radioautographic Localization of Sodium Pump Sites in Rabbit Intestine. J. Cell Biol., 53, 704-714 (1972).

151. Fujita, M., H. Matsui, K. Nagano, and M. Nakao. Asymmetric Distribution of Ouabain-Sensitive ATPase Activity in Rat Intestinal Mucosa. Biochim. Biophys. Acta, 233, 404-408 (1971).

152. Fujita, M., H. Ohta, K. Kawai, H. Matsui, and M. Nakao. Differential Isolation of Microvillus and Baso-Lateral Plasma Membranes from Intestinal Mucosa: Mutually Exclusive Distribution of Digestive Enzymes and Ouabain-Sensitive ATPase. Biochim. Biophys. Acta, 274, 336-347 (1972).

153. Quigley, J.P. and G.S. Gotterer. Distribution of (Na+ K)-Stimulated ATPase Activity in Rat Intestinal Mucosa. Biochim. Biophys. Acta, 173, 456-468 (1969).

154. Larsen, E.H. "Effect of Amiloride, Cyanide, and Ouabain on the Active Transport Pathway in the Toad Skin," in Alfred Benzon Symposium V, Transport Mechanisms in Epithelia H.H. Ussing and N.A. Thorn, eds., Academic Press, New York, 1972, pp. 131-147.

155. Adair, D.W., S.F. Adair, and L.Z. Benet. Correlation of In Vitro Intestinal Flux of Salicylate and Antipyrine with Transmural Resistance, presented to the A.Ph.A. Academy of Pharmaceutical Sciences, Chicago, August, 1974.

156. Avidi, L.V. Intestinal Absorption of Calcium. Arch. Intern. Med., 129, 345-355 (1972).

157. Nayak, R.K. and L.Z. Benet. Drug Transfer Across Rat Intestinal Musculature After Edetic Acid Treatment. J. Pharm. Sci., 60, 1508-1511, (1971).

158. Feldman, S. and M. Gibaldi. Physiologic Surface-Active Agents and Drug Absorption. II. Comparison of the Effect of Sodium Taurodeoxycholate and Ethylenediaminetetra acetic Acid on Salicylamide and Salicylate Transfer Across the Everted Rat Small Intestine. J. Pharm. Sci., 58, 967-970 (1969).

159. Tidball, C.S. Magnesium and Calcium as Regulators of Intestinal Permeability. Am. J. Physiol., 206, 243-246 (1964).

160. Bronk, J.R. and D.S. Parsons. The Polarographic Determination of the Respiration of the Small Intestine of the Rat. Biochim. Biophys. Acta, 107, 397-404 (1965).

161. Esposito, G. and T.Z. Csaky. Extracellular Space in the Epithelium of Rats' Small Intestine. Am. J. Physiol., 226, 50-55 (1974).

162. Csaky, T.Z. and G. Esposito. Osmotic Swelling of Intestinal Epithelial Cells During Active Sugar Transport. Am. J. Physiol., 217, 753-755 (1969).

163. Kinter, W.B. and T.H. Wilson. Autoradiographic Study of Sugar and Amino Acid Absorption by Everted Sacs of Hamster Intestine. J. Cell Biol., 25, 19-40 (1965).

164. Sandblom, J.P., and G. Eisenman. Membrane Potentials at Zero Current: The Significance of a Constant Ionic Permeability Ratio. Biophys. J., 7, 217-242 (1967).

165. Schultz, S.G. "Principles of Electrophysiology and Their Application to Epithelial Tissues," in Gastrointestinal Physiology. E.D. Jacobson, ed., Butterworth, London (in press.

166. Diamond, L., J.T. Doluisio, and W.G. Crouthamel. Physiological Factors Affecting Intestinal Drug Absorption. Eur. J. Pharmacol., 11, 109-114 (1970).

167. Orr, J.M. and L.Z. Benet. The Effect of Fasting on the Rate of Intestinal Drug Absorption in Rats: Preliminary Studies. Am. J. Dig. Dis., 20, 858-865 (1975).

168. Orr, J.M. Factors Affecting the Absorption of Drug Across the In Vivo Rat Intestine. A dissertation submitted in partial fulfillment of the requirements for the degree of Doctor of Philosophy (Pharmaceutical Chemistry) to the Graduate Division, University of California, San Francisco, 1974.

APPENDIX

BUFFER KH ε glu

RAT WT. 390

5/14/73

ouabain addition

9.05 Ω CHANNEL 3

9.675 Ω CHANNEL 4

TIME	Pd_o	I_o	Pd_{sc}	I_{sc}	Ω		TIME	Pd_o	I_o	Pd_{sc}	I_{sc}	Ω
19	4.3						19	5.3				
23	4.05						23.5	4.8				
29	4.2						29.5	4.95				
31.6	4.37	140			22.2		32	5.08	154			23.3
38.3	4.70	162			20.0		39	5.5	190			19.3
46	5.0	190	2.7	294	17.1							
48	auto		2.7	294			48.3	5.45	186	(2.7	280)	19.4
52.7	4.95		2.75	291	17.4		50	auto		2.75	280	
56	4.9		2.85	300	16.8		53.5	5.3		2.65	279	18.8
73	4.8		2.83	305	16.0		57	5.35		2.65	282	18.7
							74.5	5.3		2.57	276	18.8
81.0							81.5					
83.5	4.5		2.4	270	16.5		84	5.1		2.45	267	18.6
92.5	4.5		2.53	270	17		93	5.08		2.43	264	18.8
104.2	4.75		2.95	325	14.6		105	5.3		2.7	295	18.4
116	4.65		2.85	320	14.4		116.5	5.25		2.7	295	18.2
121.5	4.62		2.9	320	14.5		122	5.13		2.75	295	17.0
124.5	4.03		2.24	240	17.1		125	4.46		1.96	222	19.2
127.5	3.52		1.92	210	16.9		128	4.0		1.67	196	19.3
133	2.98		1.65	178	17.0		134.5	3.4		1.35	160	23.8
141	2.53		1.36	150	16.9		141.7	2.98		1.13	118	25.2
145.8	2.36		1.24	136	17.4		146.5	2.70		0.96	120	20.8
154.7	2.13		1.14	120	18.2		155.3	2.34		0.78	100	21.5
164	1.77		0.92	102	17.3		165	2.06		0.67	89	21.0
176	1.5		0.86	91	16.9		176.5	1.78		0.60	79	20.5
185	1.36		0.80	85	16.4		185.5	1.61		0.55	73	19.9
195	1.20		0.71	76	16.1		195.5	1.47		0.53	69	18.3

Figure A-1. Example of Worksheet for Monitoring Tissue Electrical Parameters

DMO 0.1 ml
Inulin 0.1 ml.

Date 10/4/73
channel 2
I_{sc}
Intracellular pH 7.39

Scint Sample T

Blank 41
Tissue 25853 25812

2-1 37
2-2 37 → 37
2-3 59925
2-4 63443
2-5 59741
2-6 64742 → 61926

$[In]$ = 619.26 cpm/μl.

Tare = 16.5261
Wet = 16.6100 → 0.0839
Dry = 16.5346 0.0085
Total H_2O = 75.4 μl

(extra) V_E = 41.68 μl.
(intra) V_I = 33.72 μl.

Scint C

207
97901 97694

248
291 → 270

124509
130415
131406
140217 → 131367

$[DMO]$ = 1313.67 cpm/μl.

V_E = 25812/61926 = 41.68 μl.
DMO_E = (1313.67)(41.68) = 54753.77 cpm
DMO_I = 97694 - 54754 = 42940 cpm
$[DMO_I]$ = 42940/33.72 = 1273.51 cpm/μl

$pH = pK_a + \log \frac{[salt]}{[acid]}$ $\left.\begin{matrix} pH = 7.4 \\ pK_a = 6.13 \end{matrix}\right\} \Rightarrow \frac{S}{a} = 18.62$

salt + acid = $[DMO_I]$ = 1273.51 cpm/μl
$[acid] = [DMO]/19.62$ = 66.96 cpm/μl
$[salt] = [DMO_I] - [acid]$ = 120.51 cpm/μl.

$pH_i = pK_a + \log \frac{[salt]}{[acid]}$
$pH_i = 6.13 + \log 1205.51/66.96$
$pH_i = 6.13 + \log 18.02$
$pH_i = 6.13 + 1.26$
$pH_i = 7.39$

Figure A-2. Example of Worksheet for Intracellular pH Calcuations

antipyrine (^3H) salicylate (^{14}C) S 126/73

M → S

ΔPD

t_o = 61 (^3H)

t_o = 66 (^{14}C) CHANNEL 3

t_o = 61.5 (^3H)

t_o = 66.5 (^{14}C) CHANNEL 4

SCINT	SAMPLE	VOL	M/S	T_{tran}	T_{death}	SCINT	SAMPLE	VOL	M/S	T_{tran}	T_{death}
50	3-1	0.1	M		52	65	4-1	0.1	M		52
51	3-2	1	S		55	66	4-2	1	S		55
52	3-3	0.1	M		64.5	67	4-3	0.1	M		65
41	3-4	1	S	10	71	45	4-4	1	S	10	71.5
53	3-5	0.1	M		75.9	68	4-5	0.1	M		76.2
42	3-6	1	S	20	81	46	4-6	1	S	20	81.5
43	3-7	1	S	30	91	47	4-7	1	S	30	91.5
44	3-8	1	S	40	101	48	4-8	1	S	40	101.5
54	3-9	1	S	50	111	69	4-9	1	S	50	111.5
55	3-10	1	S	60	121	70	4-10	1	S	60	121.5
56	3-11	1	S	70	131	71	4-11	1	S	70	131.5
57	3-12	1	S	80	141	72	4-12	1	S	80	141.5
58	3-13	0.1	M		144	73	4-13	0.1	M		144.2
59	3-14	1	S	90	151	74	4-14	1	S	90	151.5
60	3-15	1	S	100	161	75	4-15	1	S	100	161.5
61	3-16	1	S	110	171	76	4-16	1	S	110	171.5
62	3-17	1	S	120	181	77	4-17	1	S	120	181.5
63	3-18	1	S	130	191	78	4-18	1	S	130	191.5
64	3-19	0.1	M		193.6	79	4-19	0.1	M		193.9

Figure A-3. Example of Worksheet for Monitoring Serosal and Mucosal Samples

antipyrine (^{3}H) salicylate (^{14}C)

M → S ^{14}C (^{3}H) channel

5/26/73

APD

CHANNEL 3

SCINT	SAMPLE	CPM	NET CPM	CONC	AMT TRANSP	Σ AMT. TRANSP	TIME
50	3-1	30					
52	3-3	33					
53	3-5	41737	41707		44134	7 cpm	
58	3-13	46185	46155		1000	μ units/ml.	
64	3-19	44572	44542				
51	3-2	28	-				
41	3-4	100	72	0.163	0.163	0.163	5
42	3-6	753	725	1.643	1.496	1.659	15
43	3-7	1550	1522	3.449	1.970	3.629	25
44	3-8	2228	2200	4.985	1.881	5.510	35
54	3-9	2994	2966	6.720	2.234	7.744	45
55	3-10	3747	3719	8.427	2.379	10.123	55
56	3-11	4431	4403	9.976	2.392	12.515	65
57	3-12	4933	4905	11.114	2.136	14.651	75
59	3-14	5515	5487	12.432	2.429	17.080	85
60	3-15	5757	5729	12.981	1.792	18.872	95
61	3-16	5715	5687	12.886	1.203	20.075	105
62	3-17	5673	5645	12.790	1.193	21.268	115
63	3-18	5793	5705	12.926	1.415	22.683	125

Figure A-4. Example of Worksheet for Flux Calculations (Single Isotope or ^{14}C-Isotope in the Presence of ^{3}H-Isotope)

antipyrine (^{3}H) salicylate (^{14}C) — 5 126 173

M → S — ^{3}H (^{14}C) channel — ΔPD

R = 0.7021 — CHANNEL 3

SCINT	SAMPLE	TOTAL CPM H	NET CPM H	NET CPM ^{14}C	NET CPM ^{3}H	Conc.	AMT. TRANSP.	ΣAMT. TRANSP.		TIME
50	3-1	67								
52	3-3	56681	56614		56614					
53	3-5	80465	80398	41707	51116					
58	3-13	88410	88343	44155	55933		54/682.5 cpm			
64	3-19	85545	85478	44542	54205		1000 μ units/ml.			
51	3-2	71								
41	3-4	1182	1111	72	1060	1.946	1.946	1.946		10
42	3-6	3315	3244	725	2735	5.021	3.270	5.216		20
43	3-7	5461	5390	1522	4321	7.933	3.414	8.630		30
44	3-8	7325	7254	2200	5709	10.481	3.341	11.971		40
54	3-9	8908	8837	2966	6755	12.402	2.969	14.940		50
55	3-10	10601	10530	3719	7919	14.539	3.377	18.317		60
56	3-11	11949	11878	4403	8787	16.132	3.047	21.364		70
57	3-12	13180	13109	4905	9665	17.744	3.225	24.589		80
59	3-14	14244	14173	5487	10321	18.949	2.979	27.568		90
60	3-15	15459	15388	5729	11366	20.867	3.813	31.381		100
61	3-16	16083	16012	5687	12019	22.066	3.286	34.667		110
62	3-17	16926	16855	5645	12892	23.669	3.810	38.477		120
63	3-18	17883	17812	5705	13807	25.349	4.047	42.524		130

Figure A-5. Example of Worksheet for Flux Calculations (Double Isotope -- for ^{3}H-Isotope in the Presence of ^{14}C-Isotope)

SUMMARY

A sensitive method of studying *in vitro* drug absorption has been developed, utilizing the short-circuit technique of Ussing with modifications by Schultz and Zalusky for use with mammalian small intestine. The method allows the continuous monitoring of the electrical properties of the tissue during drug absorption and also permits the adjustment of some of these properties. Thus, it is possible to observe the effect of the drug on the electrical parameters of the tissue as well as the effect of the electrical properties on the intestinal absorption of the drug.

The transmural flux of ^{14}C-salicylate across the epithelia of stripped rat jejunum was studied initially to demonstrate the contribution of the ionized species of drugs to the intestinal absorption process. The transmural potential difference (PD) was varied using the experimental instrumentation designed for this purpose. Salicylate responded to this change in potential in a similar manner as sodium and chloride ions, rather than as a neutral compound such as antipyrine. Double isotope techniques were employed in this study, with ^{14}C-salicylate and ^{3}H-antipyrine fluxes being determined simultaneously across the same tissue. Mathematical expressions were employed which related the transmural PD with transcellular absorption routes (via the cell membrane) and paracellular absorption routes (via the transmural shunt pathway). These experiments demonstrated that salicylate flux was, indeed,

influenced by the transmural PD, whereas, the flux of antipyrine, a neutral compound, was essentially constant under various transmural PDs.

The transmural flux of ^{14}C-salicylate at short-circuit current (I_{sc}) was studied before and after the addition of agents affecting cellular metabolism to further elucidate the mechanisms responsible for intestinal drug absorption. Each tissue segment served as its own control, and absorption rates were measured under both control and experimental conditions.

The addition of 1 mM ouabain, a selective inhibitor of active sodium-transport, to the buffer solution perfusing the serosal side of the tissue profoundly changed the electrical parameters of the tissue. The mucosal to serosal (M-to-S) flux of ^{14}C-salicylate was inhibited following serosal ouabain addition, and this change was apparent after a twenty-to-thirty minute interval. A similar delay was seen for the increase in transepithelial resistance (R). Ouabain was also added in the absence of sodium ions, insuring that the previous observations were due to the inhibition of sodium-transport rather than to other ouabain activities. Under these conditions, ouabain caused only a small change in the salicylate absorption rate; however, the initial ^{14}C-salicylate transport rate was much lower in the sodium-free choline buffer.

The addition of 25 mM glucose increased the transmural PD and I_{sc}, but no change in the ^{14}C-salicylate flux or transmural R was observed. This suggests that the transport of salicylate is not

affected by a change in cellular metabolism which does not also affect the transmural R.

The addition of various concentrations of mucosal salicylate (a known uncoupler of oxidative-phosphorylation) decreased the transmural PD and I_{sc} while increasing the transmural R. The changes in these parameters appeared to show a saturable effect with respect to salicylate concentration. The M-to-S flux of ^{14}C-salicylate was also inhibited by the addition of mucosal salicylate. The decrease in the flux varied with the salicylate concentration, but not in a linear fashion. This indicated a dose-dependent absorption of *in vitro* ^{14}C-salicylate.

This study has shown that changes in the permeability of the membrane (i.e., functional state), as reflected in the electrical parameters of the tissue, can be caused by various agents and, in turn, can affect *in vitro* salicylate ion transport, probably via the transmural shunt pathway.